

**STUDY OF AN UNMANNED LUNAR
MISSION FOR VOLATILE GAS RECOVERY
(PHASE 1 – FINAL REPORT)**

WCSAR-TR-AR3-9309-1

Technical Report



**Wisconsin Center for
Space Automation and Robotics**



**A NASA supported Center for
the Commercial Development of Space**

**STUDY OF AN UNMANNED LUNAR
MISSION FOR VOLATILE GAS RECOVERY
(PHASE 1 – FINAL REPORT)**

WCSAR-TR-AR3-9309-1

N. Duffie, G. Kulcinski, I. Sviatoslavsky, B. Bartos, S.
Rutledge, L. Wittenberg, T. Ylikorpi, E. Mogahed

Wisconsin Center for Space Automation and Robotics
University of Wisconsin
1500 Johnson Drive
Madison WI 53706

September 1993

Internal Rpt. Number: WCSAR-TR-AR1-9309-1

and: WCSAR-TR-AR3-9309-1

NATIONAL AERONAUTICS AND SPACE ADMINISTRATION

JOHNSON SPACE CENTER CONTRACT NUMBER: NAG 9-615, Basic

STUDY OF AN UNMANNED LUNAR MISSION
FOR VOLATILE GAS RECOVERY
(PHASE 1- FINAL REPORT)

SEPTEMBER 30, 1993

AUTHORS: N.Duffie, G. Kulcinski, I.Sviatoslavsky, B. Bartos, S. Rutledge,
L.Wittenberg,, T. Ylikorpi and E. Mogahed

WISCONSIN CENTER FOR SPACE AUTOMATION AND ROBOTICS
(WCSAR)

1500 JOHNSON DRIVE, MADISON, WI 53706-1687

PHONE: (608) 262-5524

FAX: (608) 262-9458

TABLE OF CONTENTS

EXECUTIVE SUMMARY.....	1
I. INTRODUCTION.....	5
A. Purpose of Study	5
B. Background.....	7
C. Site Selection and Sample Selection.....	13
D. Description of Analytical Techniques Selected	15
E. Scope of Study	15
II.A. INSTRUMENTATION REQUIREMENTS	16
A. Description of Scientific Equipment.....	16
B. Sample Acquisition and Analysis.....	21
C. Mass and Power Requirement.....	39
II.B SELECTING A SOIL SAMPLE COLLECTING INSTRUMENT FOR AN AUTOMATED LUNAR ROVER.....	45
A. Introduction.....	45
B. Sample Acquisition Concepts.....	46
C. Concept Analysis	48
II.C. A PRELIMINARY DESIGN OF A SAMPLE HANDLING APPARATUS AND A SAMPLE ACQUISITION DEVICE FOR AN AUTOMATED LUNAR ROVER.....	52
A. Introduction.....	52
B. Sample Manipulating Arrangement.....	52
C. Installing the Flip Scoop on the Rover	57
D. A Preliminary Design of the Flip Scoop	59
III. MISSION AND SYSTEMS DESIGN	63
A. Mission Study Overview:.....	63
B. Ground Rules.....	65

C. Mission Objectives and Requirements:	66
D. Rover Design.....	71
E. Transportation: Lander and Launch Vehicles:.....	82
F. Cost Estimation:	91
G. Recommendations:.....	99
IV. SUMMARY AND CONCLUSIONS	104
V. REFERENCES	107
APPENDICES	
A. Sampling Concept Data Sheets	
B. Sample Manipulating Arrangement; Proposal I	
C. Sample Manipulating Arrangement; Proposal II	

Study of Unmanned Lunar Mission for Volatile Gas Recovery

EXECUTIVE SUMMARY

This report summarizes a one-year study of a proposed robotic mission to assay the volatiles which can be recovered by heating the lunar maria regolith. These gases include H₂, He, N₂, CO₂, and CO. The H₂ could be reacted with the mineral ilmenite (FeTiO₃) to form H₂O which along with the gases N₂ and CO₂ would be useful for human life-support. The He is of interest because it contains a high abundance of the ³He isotope which has been identified as a potential fuel for nuclear fusion power plants sited on the earth.

The study provides an initial mission plan and can be utilized for follow-on assay missions which would quantify the abundance, location, and recovery technology required to exploit these lunar resources. This information would be communicated to earth stations so that a mission to the moon to extract significant quantities of these volatiles could be initiated after the year 2000.

The study consisted of five tasks, namely: Task 1.0 Mission Requirement, Task 2.0 Science Instrumentation, Task 3.0 Rover Design, Task 4.0 Converge on Optimal System Design, and Task 5.0 Launch Vehicle.

Site Selection

This mission for volatile gas assay would prefer a site with high volatiles content but also, with some diversity. The relationship between the retained solar wind implanted He and the TiO₂ content of the soil was utilized to select a landing site at 9°N and 20°E on the Mare Tranquillitatis which is reasonably level for up to 100 km to the southeast. The proposed sampling protocol would be to collect two samples, nearly adjacent. If their results agreed within the experimental deviation, the rover would proceed 0.5 km along the planned route and select two new samples.

Assay of Regolith:

The assay of the regolith samples would be accomplished by the scientific equipment in the following sequence : 1) retrieve the sample of regolith from the lunar surface; 2) reduce the sample to ~ 1.0 gram of particles < 200 μm ; 3) weigh the sample; 4) characterize the mineral content (TiO_2); 5) heat the sample to 1200° in a vacuum oven; 6) collect the volatile products; 7) characterize the volatile products qualitatively and quantitatively; 8) transmit the data.

An important component of the instrument package is the mass spectrometer which will be utilized to characterize the mineral content of the soil, especially Ti, and the volatile gases. A Fourier Transformer Mass Spectrometer (FTMS) was identified to be particularly useful with high resolution for ions in the 1 to 72 AMU range. Although a miniaturized FTMS was not available at this time, it was assumed that one could be constructed similar to the mass spectrometer developed for the Mars - MESUR program, which has an earth mass of 12 kg and requires 25 watts of power. Such an instrument should be able to detect ^3He in the evolved gases; however, quantitative measurements of the He isotopic ratio in the presence of other gases requires experimental verification.

Parametric studies indicated that a one gram sample of high-Ti maria regolith released sufficient gases to create a pressure of ~70 Pa (0.56 torr) in a one liter container at 30°C , which is a sufficient sample for the mass spectrometer. A one-gram sample of surface regolith would occupy a volume of 0.8 cm and could be contained in a ferritic steel crucible 0.8 cm OD x 1.57 cm high.

This sample and container would be placed in a coiled electrical heater inside of an evacuated one-liter container. The heater was well-insulated to prevent heat losses. Heat transfer calculations indicate that the sample would attain 1200°C in 6 minutes with a 50 W heater and 14 minutes with a 25 W heater. Before the sample is heated, a laser beam delivers 0.45 to 2.0 J per pulse at a wavelength of $1\mu\text{m}$ to the surface of the

sample. This absorption of the laser energy vaporizes some of the minerals in the soil. These vaporized ions are quantitatively determined by the mass spectrometer.

A lunar rover platform with the sampler equipment attached has been conceptually designed. A scoop from this platform is lowered and filled with a surface layer of soil as the rover slowly moves forward. The scoop is rotated upwards and the sample passes through two vibrating screens and into the sample container. The sample and container are weighed on an automated scale which is calibrated before each sample. The sample container of ferritic steel is handled by magnetic chucks and placed in the heating chamber. The total mass on the platform is 17.9 kg. A sequential time program for one sample analysis indicates that from the start of the sample collection, through the analysis to transmitting the data requires 1100 s (18.3 min). With a 25 W heater 73 % of the time is used heating the sample.

Mission Systems and Design:

An iterative design procedure was utilized in which the mass, size and power requirements for the instrument package were imposed upon a rover design. The rover design was, then, input to the lander design which subsequently formed the requirements to the launch vehicle and upper stage design. From these iterations two solutions emerged: one based on the Delta launch vehicle and the other on the Atlas launch vehicle.

Several ground rules were assumed, namely: (1) only one lunar mission would be planned; consequently, Research and Development costs for new hardware should be avoided; (2) flight qualified hardware should be utilized whenever possible; and (3) maximize the science data as long as a medium class launch vehicle could be used.

Although few rover designs exist an algorithm was developed to trade rover mass, rover power and science instrument mass. This analysis indicated that an "average" rover subsystems which includes communication, thermal, manipulation, computation, control chassis and structure have a mass fraction of 0.72. Power

subsystem mass was calculated assuming General Purpose Heat Source, RTG's with a specific power of 5W/kg and a power management battery of 30 W-hr/kg.

Two existing rover designs were found to be compatible with this study, namely; (1) the 75 kg Small Marsokhod with a 100 km range for a Delta class mission; and (2) the JPL 290 kg Lunar Site Characterization Rover with range up to 1000 km for an Atlas class mission.

The Small Marsokhod (SMR) which was extensively displayed in the USA during 1992-93 was selected for this study. Its principal advantage is high probability in heterogeneous terrain; however, it has articulated motions with increased complexity which would probably not be needed on smooth areas of Mare Tranquillitatis, especially if it had telerobotic ability to avoid craters.

Various Artemis lander designs with lunar descent stages appropriate for medium class launch vehicles were evaluated for this study. A low earth parking orbit of 185 km x 185 km x 28.5° was assumed. Three lander options were examined: (1) a Bipropellant Lander, BL; (2) a Bipropellant Lander upper stage and a Solid Propellant Lower Stage (BL & SLS); and (3) a Bipropellant Lander upper stage and a Bipropellant Lower Stage (BL & BLS). An algorithm was developed showing Landed Payload Fracture as a Function of Dry Landed mass for the three architectures.

An estimated SMR mission cost was estimated based upon the USAF Unmanned Spacecraft Model, 5th Edition, with all costs normalized to \$1990. the estimated Space Segment costs were close to the goal of \$200 M. When costs were added for Launch Segment, Ground Segment and Operations and Maintenance the total Life Cycle Costs over the life of the mission were \$357 M.

I. INTRODUCTION

A. Purpose of Study

The purpose of this study was to prepare a near-term mission plan which would lead to a systematic assay of the volatile gases retained in the lunar soil particles. This report summarizes a one-year study of such a proposed unmanned mission. This study provides an initial step in the mission plan and can be used as a basis for further programs, culminating in a mission to the moon to extract significant quantities of lunar volatiles after the year 2000. This latter mission would test key technologies for the recovery processes and establish the overall feasibility of further large scale volatile recovery missions.

Further unmanned exploration of the moon and other planets require that indigenous resources be utilized. Volatile gases derived from the lunar soil have been shown to be valuable resources for life-support and energy systems.

The following scenarios or a combination of them were suggested in the original proposal:

Scenario 1: Regolith would be sampled and concentrations of lunar volatiles measured at various locations on the moon for the purpose of determining sites for future resource operations. A robotic vehicle would collect and heat samples of lunar regolith to obtain the volatiles. These volatiles would be analyzed, and the results of the analysis would be communicated to earth.

Scenario 2: Regolith would be collected on a continuous basis and concentrations of the lunar volatiles would be determined at a localized area on the moon. A robotic vehicle would collect the regolith, extract the volatiles, and compress and store the volatiles in an appropriate container. The concentrations of the volatiles would be identified communicated to earth, and the container holding the volatiles would be returned to earth and analyzed.

Scenario 3: Regolith would be collected on a continuous basis and concentrations of the lunar volatiles would be determined at a localized area on the moon. A robotic vehicle would collect the regolith, extract the volatiles, separate out He-3, and compress and store the He-3 in an appropriate container. The container holding the volatiles would be returned to earth and analyzed.

Scenario 1 was developed in this report because of its basic importance to the whole program and a desire to keep the direct mission cost below 200 M\$ for the R D & T and first production unit for the science package, rover and lunar lander.

A program flow is given in Figure I.1. The first task (Task 1.0) of this study

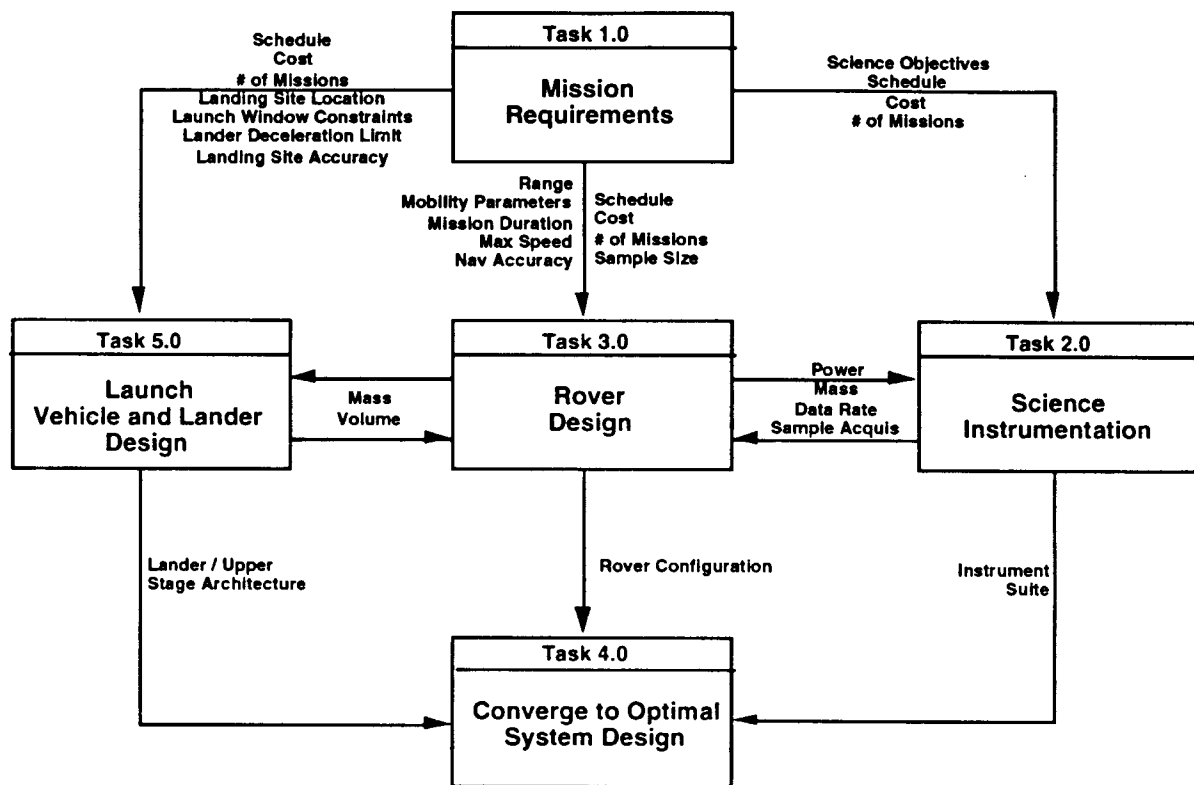


Figure I.1 Mission Study Overview.

was to establish the mission requirements and objectives of the mission. The second task (Task 2.0) involved the definition of various systems for recovery and analysis of the lunar volatiles. Task 3.0 involved definition of the various robotic vehicular systems required for the volatile recovery. Task 4.0 involved the integration of the robotic vehicle mission transportation requirements. Task 5.0 considered the launch vehicle and lander design options.

B. Background

1. Occurrence of Volatiles on the Moon

Further manned exploration of the moon and other planets and bodies within the solar system requires that indigenous resources be utilized in order to decrease the supply requirements from earth. Studies of the lunar soil samples, acquired by the Apollo and Lunar missions, indicate that upon heating in a vacuum these soils evolve the volatile gases H_2 , He, N_2 , CO_2 , CO and SO_2 . The H_2 would be valuable as a rocket fuel or it could be reacted with the mineral ilmenite to form water, while the N_2 , CO_2 and the H_2O would be useful for the life-support of space-travelers. The element He is of interest because it contains a high abundance of the rare isotope 3He , which has been identified as a potentially valuable fuel material for the nuclear fusion/electrical generating power plants being developed for use on earth [1].

In order to assess the feasibility and economic potential in exploiting these lunar volatiles, we must be able to assess the total quantity of these volatiles and identify the most abundant sites. The delineation of the most abundant sites may require the analyses of a large number of soil samples because the sites visited by the Apollo astronauts were only a small fraction of the lunar surface. It is not known if the volatile gases in the soil vary widely over a distance of a few meters or several kilometers. Also, analyses of the samples in the pristine lunar environment is highly desirable because of the contamination of terrestrial air and water which occurred for some of the Apollo

samples. For these reasons, the mission plan embraced a science package capable of quantitative measurements of the gases. This analytical equipment would be mounted on an unmanned rover, equipped with a sample retriever, and have the ability to travel 10's of kilometers.

2. Relationship of Lunar Volatiles to Other Soil Constituents:

The occurrence of most of these volatile gases in the lunar soil is related to the solar wind ions which travel outward from the sun. The composition of the solar wind ions is >90% H⁺, 4 -5% He⁺ plus other light ions. The He has an unusually high ³He/⁴He ratio of ~480 ppm (atomic) indicating that some of the ³He escapes from the sun's interior without undergoing nuclear fusion. These solar wind ions travel at a velocity of ~450 km/s with a flux of $\sim 6 \times 10^{10}$ ions/m²·s. Because the moon is not protected by a magnetosphere or an atmosphere, such as occurs on earth, these ions bombard the lunar surface and become embedded in the exposed rocks to depths of <1 μm. Several factors have been identified which can be used as guidelines to indicate the abundance of the solar wind ions in the exposed lunar surface.

3. Size Effects

The lunar regolith is a surficial layer of fragmented rock, which overlies the lunar bedrock. The regolith has been produced by the impact of innumerable meteorites, both large and very small, that have bombarded the moon for the past 4.5 billion years. This bombardment pulverizes the rock into particles which range in size from millimeters to <20 μm. The particles of this regolith <1 mm dia. are known as "lunar soil". The impact of the meteorites often eject regolith from below the surface to the exposed surface. By such a continuous process, called "gardening", the regolith has been mixed to a depth of several meters. The highland regoliths, 10-15 m thick, cover

the bright mountainous areas of the moon, while the darker maria regoliths are 4-5 m thick.

The soil particles at the lunar surface are exposed to the solar wind ions whenever they face the sun. Because the ions penetrate only $<1\text{ }\mu\text{m}$ into the particles; these ions essentially form only a surface layer on a particle. Consequently, it has been observed that the smaller particles with a high surface to volume ratio have the highest concentration of solar wind ions per weight of particles [2].

4. Chemical Effects of the Soil

The composition of the lunar rocks include the silicate suite plus oxide and sulfide minerals. Analyses of Apollo 11 lunar solid samples indicated [3] that the He atoms were especially well retained in soil particles which bore fragments of the mineral ilmenite, FeTiO_3 . As shown in Figure 1.2, the relationship between He content and TiO_2 in the regolith is approximately linear [4] between 2 and 8 wt % TiO_2 . Above 8 wt %, the He content remains high; however, the scatter in the He content increases and has not been adequately explained for these Apollo 17 samples. The scatter may reflect the fact that the samples are mixtures of highland and maria regoliths in the Taurus-Littrow valley. Recently, experimental evidence has shown that poor He retention of silicate materials is due to the fact that continued solar wind bombardment of the surface forms amorphous coatings which release the trapped He. Conversely, the ilmenite particles are much less susceptible to such radiation damage and, consequently, provide better retention of the He. This information indicates that the surface of the moon which contains high concentrates of the element Ti in the mineral ilmenite should be an indication of high He content. This mineral occurs principally in certain maria but not in the highlands.

5. Soil Maturity

Soil maturation [5] occurs when the regolith on the lunar surface is bombarded by micrometeorites which often cause melting of the soil particles followed by the solidification of glassy particles called "agglutinates". It has been shown that higher agglutinate fraction of the soil correlates with high exposure rates. Often associated with the phenomenon of agglutinate formation is a chemical reaction due to the fact that H^+ ions have been implanted in the exposed soil; consequently, when the soil particles are melted an atmosphere of hydrogen is formed which reduces FeO in the soil to metallic Fe^0 . The dark shading of the lunar maria has been attributed to the accumulation of these fine Fe^0 particles. The amount of these fine metallic Fe particles in the soil can be determined by ferromagnetic resonances, I_s . Consequently, soils exhibiting high ratios of I_s/FeO can be used as an indicator of high maturity and long exposure to the solar wind.

6. Remote Sensing Information

As previously mentioned, the He concentration in the maria regolith appears to be a monotonic function of the ilmenite content of the soils, Figure I.2. Such a correlation makes it possible, therefore, to estimate the 3He content of unexplored areas of the moon based upon the TiO_2 content because TiO_2 can be determined by remote sensing techniques.

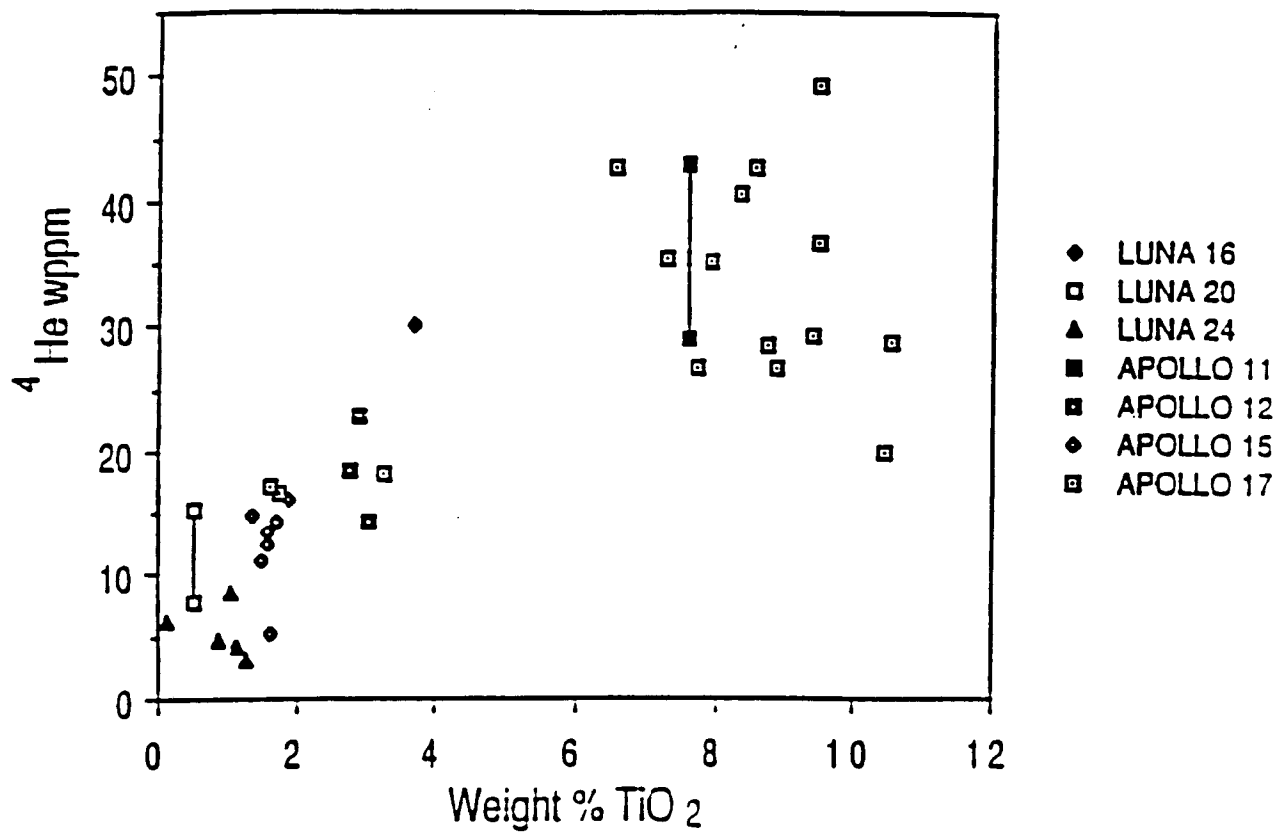


Figure I.2 Relationship between helium and titania in lunar regolith. The He-3 concentration is 0.0003 times the He-4 wppm [4].

Gamma ray spectroscopy of Ti, which made use of the radiation produced from cosmic ray bombardment of the lunar regolith, was recorded by the Apollo 15 and 16 orbiters as they encircled the moon near the equator [6]. Resolution of these data was poor and varied from 60 to 320 km; however, two maria of high-Ti regoliths were detected on the moon's near-side, Mare Tranquillitatis on the eastern side and the other in part of Oceanus Procellarium near the far-western side.

Optical spectroscopy techniques of reflected sunlight, as observed at earth-based observatories and by satellites, have provided high resolution of the TiO₂ contents of the moon's near-side. This technique makes use of ultraviolet negatives (0.40 μm) superimposed upon infrared negatives (0.56 μm) of the same area. These ratios are compared with similar color ratios determined from a reference area. The resulting ratios show consistency between 3 to 10 wt % TiO₂. The initial spectral ratio map by T.V. Johnson [7] indicated an area of high TiO₂, (<7% wt) along the eastern side of Mare Tranquillitatis. Later work by J.R. Johnson [8] produced enlarged maps of the west central region of Mare Tranquillitatis with a pixel-size resolution of 1.2 km. These maps indicated a region of greater than 7% TiO₂ and the terrain in this area may be more easily traversed than along the eastern side.

The 1990 Galileo spacecraft fly-by of the moon [9] using spectral reflectance spectroscopy indicated new regions of high TiO₂ within Oceanus Procellarium, especially near the Flamsteed region. The 1992 encounter of the same spacecraft with the moon [10] revealed another area of high TiO₂ content in the maria near the North Pole of the near-side.

C. Site Selection and Sample Selection

The landing and sampling site for the mission should be well-characterized and be located on the near-side for continuous communications. In addition, it should have the following desirable characteristics: (a) reasonably high He content in the regolith but with some diversity. (b) terrain must be reasonably level for up to 50 km, with no large craters. Such sites have been identified by remote-sensing with TiO content in the range of 5 to 10 wt % in both the northeastern and northwestern sides of Mare Tranquillitatis. Photographs indicate, however, that the proposed sites in the northeast are rippled with small hills which may be difficult for the rover to climb; however, the northwestern sites have a less hostile terrain.

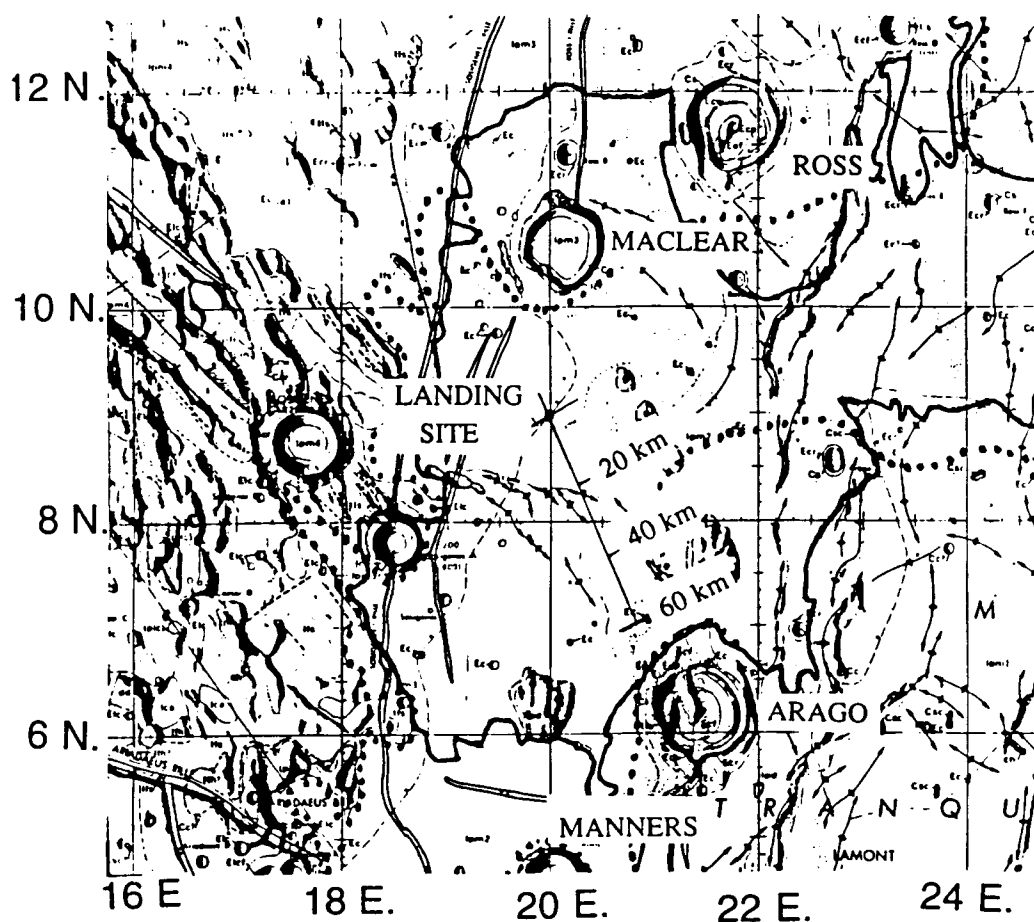


Figure I.3 Proposed lunar landing site.

For these reasons, therefore, the landing site selected [11] is at 9°N and 20°E. As shown in Figure I.3 this site would be located south of the craters Ross (26 km dia.) and Maclean (20 km dia), but north of the craters Arago (26 km dia) and Manners (15 km dia). Approximately 100 km of fairly unobstructed terrain exists south of Maclean.

The remote-sensing maps of J.R. Johnson were utilized in order to select a route for the rover which would sample a variety of regolith. This data suggested that from the landing site the rover could proceed in a southeasterly direction for ~60 km, as noted on Figure I.3, and sample regolith with contents of 6 to >10 wt % TiO₂. Such regolith would have average He concentrations of 35-45 wppm (0.014 - 0.018 wppm ³He).

The selection of a sampling strategy for the rover requires several considerations. Initially, as shown in Figure I.2, for Apollo 11 samples at 8 wt % TiO₂, the He analyses varied by ±20% about the median of 35.5 wt ppm He. Insufficient information is available to determine if this is due to the inherent statistical variation between the two samples, or if this variation is due to some external effect such as the depth of the sample in the regolith or the way the samples were retrieved and, subsequently, handled in the laboratory before the volatiles were evolved. A large number of samples in a small target area of the lunar regolith would need to be analyzed in order to define the statistical magnitude of the variation.

On the other-hand, much wider sampling ranges extending up to 10's of km would reveal broader, more regional variations of importance to resource assessment. Such sampling would provide calibration for the remote-sensing orbital missions.

For the first Lunar Prospectus mission the sampling protocol should probably be a compromise between the two strategies. For instance, two independently gathered samples adjacent to each other would be analyzed. If their He analyses were within, perhaps ±10%, the rover could proceed to a new site. The pixel sizes of the Johnson spectral photographs of Mare Tranquillitatis were 1.2 km and spectrographic reflection of data often showed changes between two adjacent areas. Consequently, the rover

could be moved up to 0.5 km between sampling sites to determine if the soil samples varied gradually or abruptly. If the rover transited the 60 km route previously described, a total of 120 sites would be surveyed and 240 samples would be analyzed.

D. Description of Analytical Techniques Selected

The primary focus of this lunar surface mission would be the quantitative analysis of volatiles derived from heating pristine lunar regolith samples which were never contaminated by the earth's atmospheric constituents. These gases would be contained in a vacuum chamber so that PVT measurements could be employed to determine the quantity of the gases. The chemical constituents of the gases would be determined by mass spectrometry. Several types of small mass spectrometers were surveyed for this application such as: time-of-flight, Fourier transform - ion cyclotron resonance and quadropole mass spectrometers. During this evaluation the common magnetic-deflection mass spectrometer was omitted because of the weight of the permanent magnet. A small quadropole mass spectrometer, similar to that design for the Mars MESUR mission [12] was selected, as described in Section II.

In order to further characterize each regolith sample, its Ti content would be determined. This determination would be accomplished when an intense, small laser beam would impinge upon the sample in the furnace prior to the heating of the sample. The absorption in the regolith of this laser energy would vaporize some of the sample as Ti ions and perhaps TiO ions. The identification and quantity of these ions would be determined by the same mass spectrometer used to analyze the evolved volatiles.

E. Scope of Study

1. Introduction

Task 1.0 - Mission Requirements

This study proposed a near-term unmanned mission plan to assay the volatile content of the lunar soil over a route of 10's of km on Mare Tranquillitatis. Requirements and equipment were evaluated or designed for the science package, the

sample retriever system and the rover. Several lunar lander and existing launch vehicles were considered. Several iterations were made with a costing-code to constrain the total mission cost.

The purpose of this study was to prepare a pre-conceptual design of an unmanned, lunar rover which would be landed by an early-return transportation vehicle on the lunar near-side with the capability to analyze the volatiles in the soil.

Task 2.0 - Science Instrumentation

The rover deploys a retriever apparatus which obtains a sample of the regolith and places it in a vacuum chamber for heating to liberate the volatile gases and measures the Ti content of the soil. A description of this instrumentation is given in Section II.

Task 3.0 - Rover Design

A rover design is presented in Section III which meets the requirements of the Science Instrumentation, and the vehicular mobility.

Task 4.0 - Converge to an Optimal System Design

Several types of lunar lander vehicles which would transport the rover to the lunar surface are discussed in Section III together with the power package.

Task 5.0 - Launch Vehicle

Several currently available U.S. launch vehicles are compared in Section III. Additional total life cycle cost of the mission, based on several different configurations, are delineated.

II.A. INSTRUMENTATION REQUIREMENTS

A. Description of Scientific Equipment

The primary mission of this experiment is to attempt to correlate the He content in lunar regolith to the mineral composition. All indications from the samples brought from the moon point to the affinity of implanted He species to regolith samples which

are high in ilmenite (FeTiO_3). This experiment will attempt to verify this conclusion by making a large number of measurements over an area in which, it is hoped, there will be variation in the mineral content of the regolith.

The functions which will be performed by the scientific equipment are the following:

- Pick up a sample of regolith from the lunar surface.
- Reduce the sample to ~ 1.0 gm of particles $< 200 \mu$.
- Weigh the sample.
- Characterize the mineral content in particular, the quantity of TiO_2
- Heat the sample to 1200°C in a vacuum oven.
- Collect the solar wind products.
- Characterize the solar wind products qualitatively and quantitatively.
- Transmit data.

1. Mass Spectrometry

The most important component of the instrumentation package is the mass spectrometer. This instrument is the heart of the system and will be needed to characterize the mineral content of the samples as well as identify and quantify the released solar wind products. To be able to do this, the mass spectrometer must be able to identify particles from 1 to 56 AMU, where Ti is 47.9 AMU. More than 60% of lunar surface materials consists of oxygen, all tightly bound chemically to other elements. The next most abundant element is Si at 16 - 17%, followed by Al at 4.5 - 10%, Ca and Mg at 5% each, and Fe at 2.5 - 6%. Ti and Na make up the remaining 1% [13]. These are the major elements, however, there are other elements of much lower concentrations.

There are many different kinds of mass spectrometers. The one being considered here is the FTMS (Fourier Transform) mass spectrometer. The FTMS, also sometimes called FT-ICR (Fourier Transform Ion Cyclotron Resonance), was invented in 1973 and

has undergone many improvements and innovations since then [14]. It relies on a fixed magnetic field \vec{B} to deflect an ion of charge, q , moving at velocity \vec{v} according to the Lorentz force $\vec{F} = q\vec{v} \times \vec{B}$. For spatially uniform \vec{B} a moving ion of mass m will be bent into a circular path in a plane perpendicular to the magnetic field with a natural angular frequency ω_0 ($\omega_0 = q B/m$ (mks units)). Thus if the magnetic field strength is known, measurements of the ion cyclotron frequency suffices to determine the ionic charge to mass ratio q/m . Thus a static magnetic field converts ionic mass into frequency. In order to detect the ions it is necessary to move them "off center" by applying an electric field oscillating at ω_0 . The electric field pushes the ions continuously forward in their orbits and the original ion packet spirals outward. The FT-ICR mass spectrometer thus can excite a whole spectrum at once and can detect a whole spectrum at once. The oscillating voltages induced by excited ions of different mass to charge ratios add together to give a time-domain digitized envelope, where a slowly oscillating signal comes from ions of higher mass while the rapidly oscillating signal from ions of lower mass. A discrete Fourier transform of the digitized time-domain data gives the frequency-domain spectrum which can be rescaled into a mass-domain spectrum. The relative intensities of the pulses in the mass-domain spectrum indicate the relative abundance of the species in the sample.

The proposed FTMS on which we base our assumption utilizes a permanent magnet of 0.1 T and can detect up to 72 AMU with resolving power of 200 and a mass accuracy of 400 ppm at 43 AMU. This instrument can be constructed with a lighter electromagnet. For this study we have adopted the mass spectrometer used by the MARS rover sample return science working group for evolved gas analysis. This instrument has an earth mass of 12 kg, requires 25 W of power and is 25 cm \times 25 cm \times 20 cm in overall dimensions [12].

2. Quantification of TiO_2

Sputtering secondary ions from lunar samples and measuring the count rate can establish the elemental concentration of Ti. An experiment conducted at LANL [15] demonstrates how this can be done. Three lunar simulants were used varying in TiO_2 content. The simulants were replications of an Apollo 11 high-Ti mare basalt soil, an Apollo 15 low-Ti mare basalt soil and an Apollo 16 aluminous highland soil. The simulants were sputtered by Ar^+ ions at 5 keV and the Ti^+ ion count rates measured. In Figure II.1, the Ti^+ fluxes from the three simulants are plotted against the weight percent of TiO_2 as determined by an electron microprobe. The observed secondary ion fluxes correspond to the true composition of TiO_2 to better than 10% for the high-Ti basalt and 20% for the low-Ti simulant. In this experiment we propose to use a laser beam for

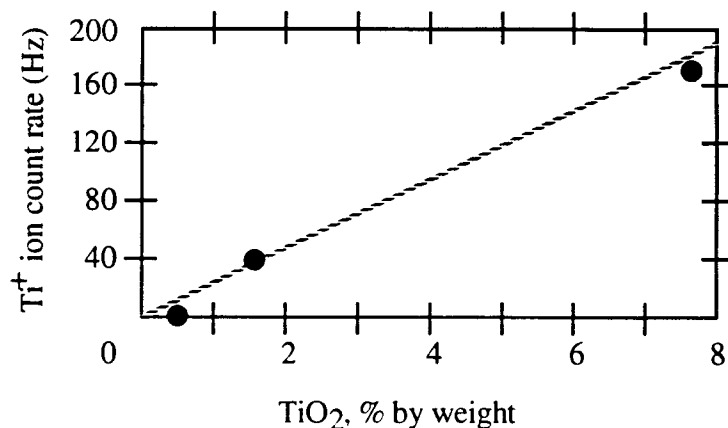


Figure II.1 Intensity of Ti^+ ions sputtered from lunar regolith simulants with varying TiO_2 content

sputtering the secondary ions and determining the TiO_2 weight percent. The analysis of the solar wind product composition can then be correlated to the TiO_2 content, satisfying the original mission of the experiment.

3. Quantifying He-3

For determining the amount of He in a sample, several methods can be used. First, it has been determined fairly reliably that the He³/He⁴ ratio in most lunar regolith samples is constant at ~1/2500. Thus by measuring the He⁴ concentration, the He³ concentration can be deduced. Secondly, mass-spectrometric methods have been used to show He³ concentration down to ~1 ppb in 1.0 torr gas samples [16]. Figure II.2 is a mass spectrometric scan of processed He⁴ in which all traces of He³ have been removed, and along side of it a scan in which there is 1.02 ppb of He³. The He³ pulse is quite prominent even at the 1 ppb concentration, and furthermore, it is clearly distinguishable from the HD peak.

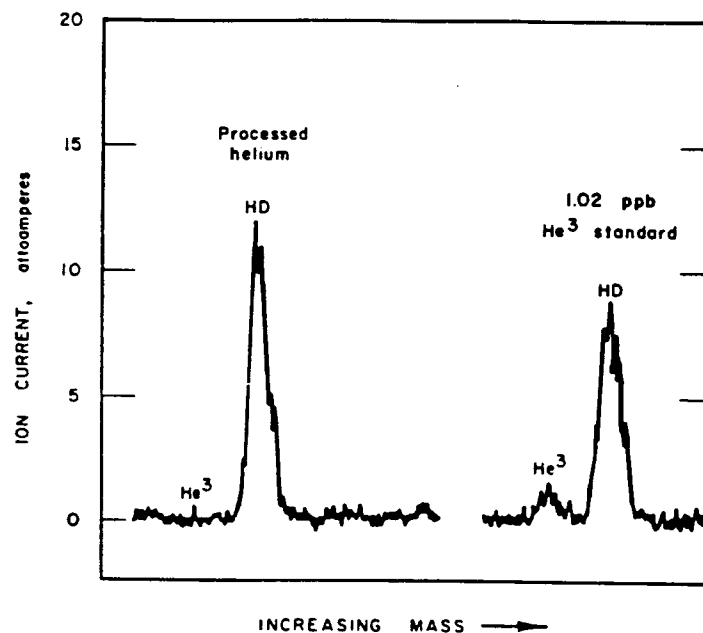


Figure II.2 Mass spectrometric scan of processed He⁴ (zero He³) and He⁴ with 1.02 ppb of He³

Although qualitatively the He³ peak is evident, the question still remains as to whether an instrument can be designed to give accurate quantitative measurements relative to the complete spectrum of the evolved gases. After all, the quantity of He³ evolved constitutes only 37 wppm of the total solar wind products obtained by heating a

representative sample to 1200°C. Thus, it would seem that a more accurate quantitative assessment of He-3 can be obtained by relying in the He3/He4 ratio.

B. Sample Acquisition and Analysis

In this section a description is given of the scheme for obtaining lunar regolith samples and the processes needed to analyze and characterize them.

1. Determining Sample Size

Figure II.3 shows the cumulative pressure of all the solar wind products obtained from heating one gram of lunar regolith to 1200°C and collecting the released gases in a

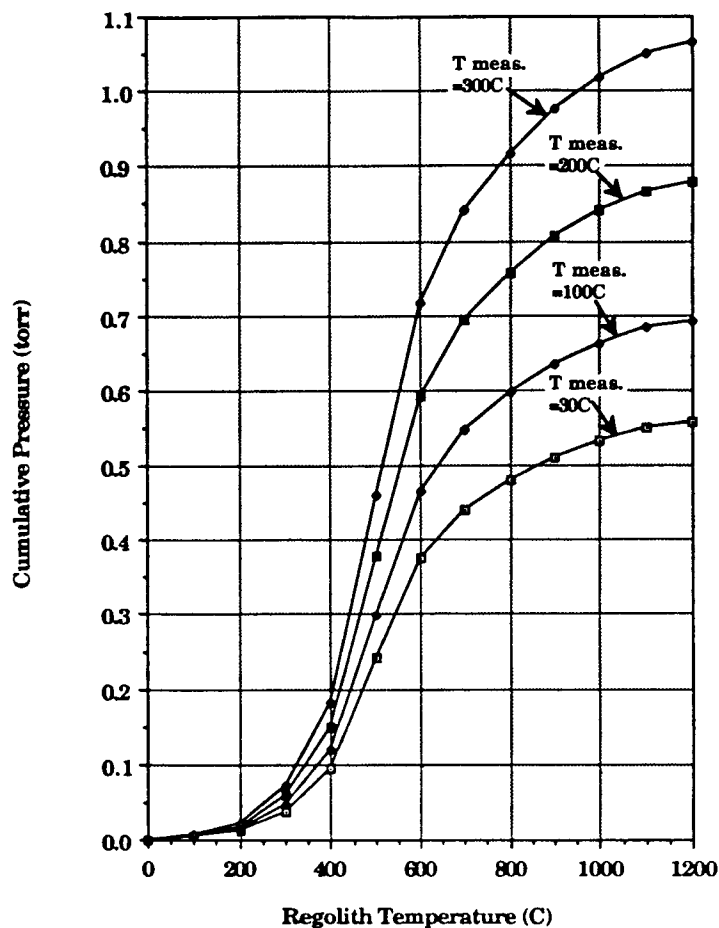


Figure II.3 Cumulative pressure of all solar wind products from one gram of regolith as a function of heating temperature collected in a 1000 cc container at different measuring temperatures

one liter (1000 cm^3) container. The sample used is that of a high-Ti mare regolith similar to those collected at the Apollo 11 and Apollo 17 sites [17, 18, 19]. The pressure in torr is plotted against the heating temperature from 0°C to 1200°C for gas temperatures of 30°C , 100°C , 200°C and 300°C . It can be seen that at 30°C , the cumulative pressure is ~ 0.56 torr, more than adequate to be the input to a mass spectrometer. Figure II.4 shows the pressures again at 30°C with the $\text{He}_4 + \text{He}_3$ partial pressures shown separately. Again this pressure is ~ 0.13 torr. In the low-Ti mare basalts, the He pressure will be down around .05 torr, again more than adequate for input into a mass spectrometer. We conclude from this that a sample of one gram is all that will be needed to obtain adequate characterization of the solar wind products. At a density of 1.265 g/cm^3 , this is a volume of 0.8 cm^3 . Table II.1 shows a tabulation of the expected solar wind product releases from one gram of the described sample. Listed are the molecular weight, the mass of released gases in μg , the % by weight and the partial pressure in torr for a volume of one liter at 30°C .

2. Optimizing Sample Container Dimensions

It has been determined that a one gram sample having a volume of 0.8 cm^3 will be used in each heating sequence. To minimize heating time we optimize the sample container dimensions. Assuming a cylindrical geometry heater made from coiled heating elements, we vary the sample contained diameter from 0.5 cm to 1.0 cm and thus the height of the container varies from 4 cm at OD of 0.5 to 1.0 cm at OD of 1.0.

A sealed heater is used to minimize the possibility of shorts and increase reliability. Figure II.5 shows a coiled heater on top and a heater cross section on the bottom.

The heater consists of a 1 mm NiCr wire, surrounded by BeO insulation and sheathed with a TZM (Molybdenum alloy) sheath to give an overall diameter of 3 mm. This heater is coiled such that its 1D is 2 mm larger than the OD of the sample container. The number of coils needed depends on the OD of the container and varies

from 13 coils at 0.5 cm OD to 3.4 coils at 1.0 cm OD. Details of the heater will be described in a later section; here we only give the energy needed to heat the elements of the heater, the parts surrounding the heater, the sample container and the sample itself.

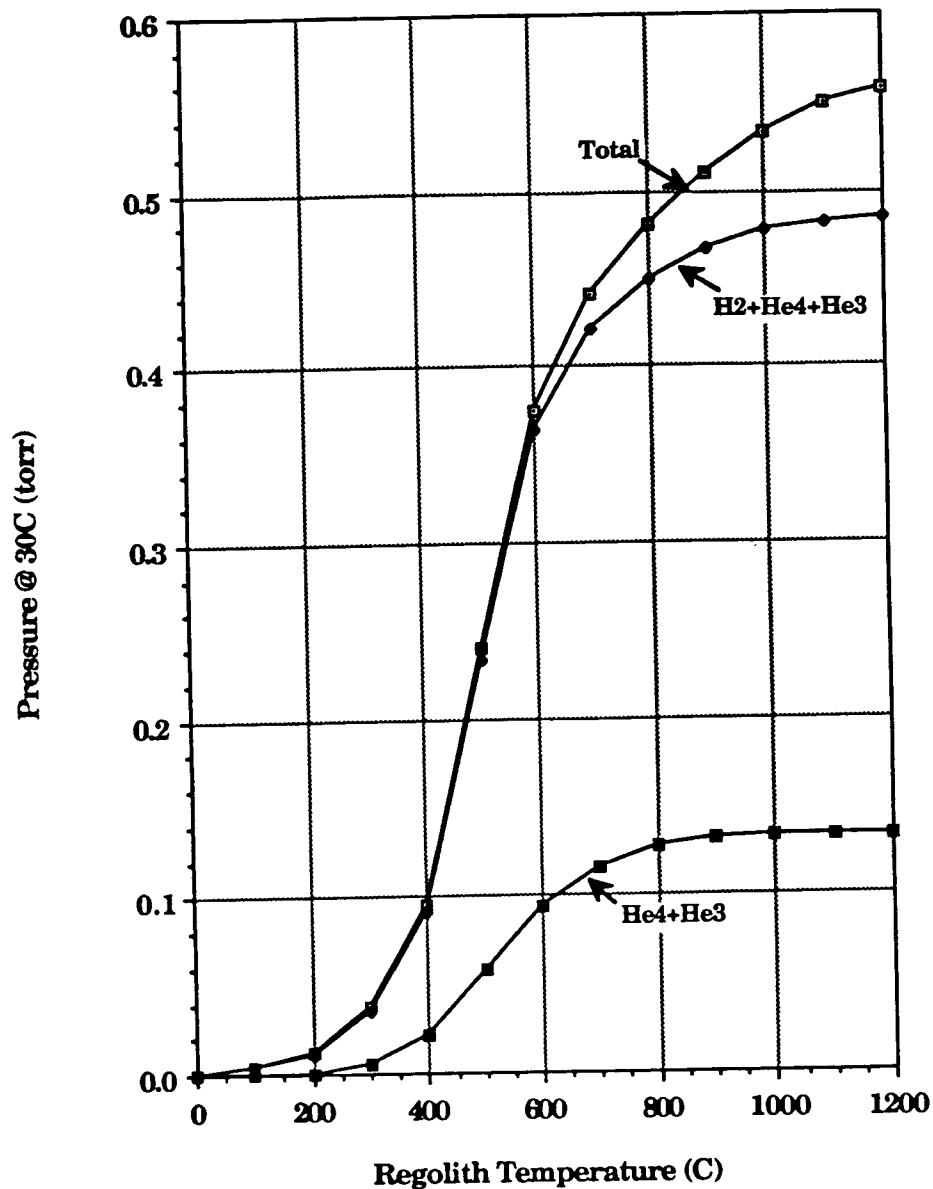


Figure II.4 Pressures of solar wind products from one gram of regolith as a function of heating temperature collected in a 1000 cc container for total , H₂ + He⁴ + He³ and for He⁴ + He³ measured at 30°C

Table II.1 Summary of Solar Wind Products from 1.0 gram of Regolith

Species	Mol. Wt	Mass (gm.E-6)	Fraction (%) by weight	Partial Pr. (torr) at 30°C
H2	2.016	58	23.9	4.9E-1
CH4	16.043	12	4.9	1.3E-2
He3	3.016	8.9E-3	3.7E-3	5.0E-5
He4	4.003	25.1	10.3	1.1E-1
CO	28.011	73	30.0	4.4E-2
CO2	44.011	22	9.1	8.5E-3
N2	28.014	30	12.3	1.82E-2
H2O	18.016	23	9.5	2.1E-3

* Heated to 1200°C, Collected in 1000 cm³

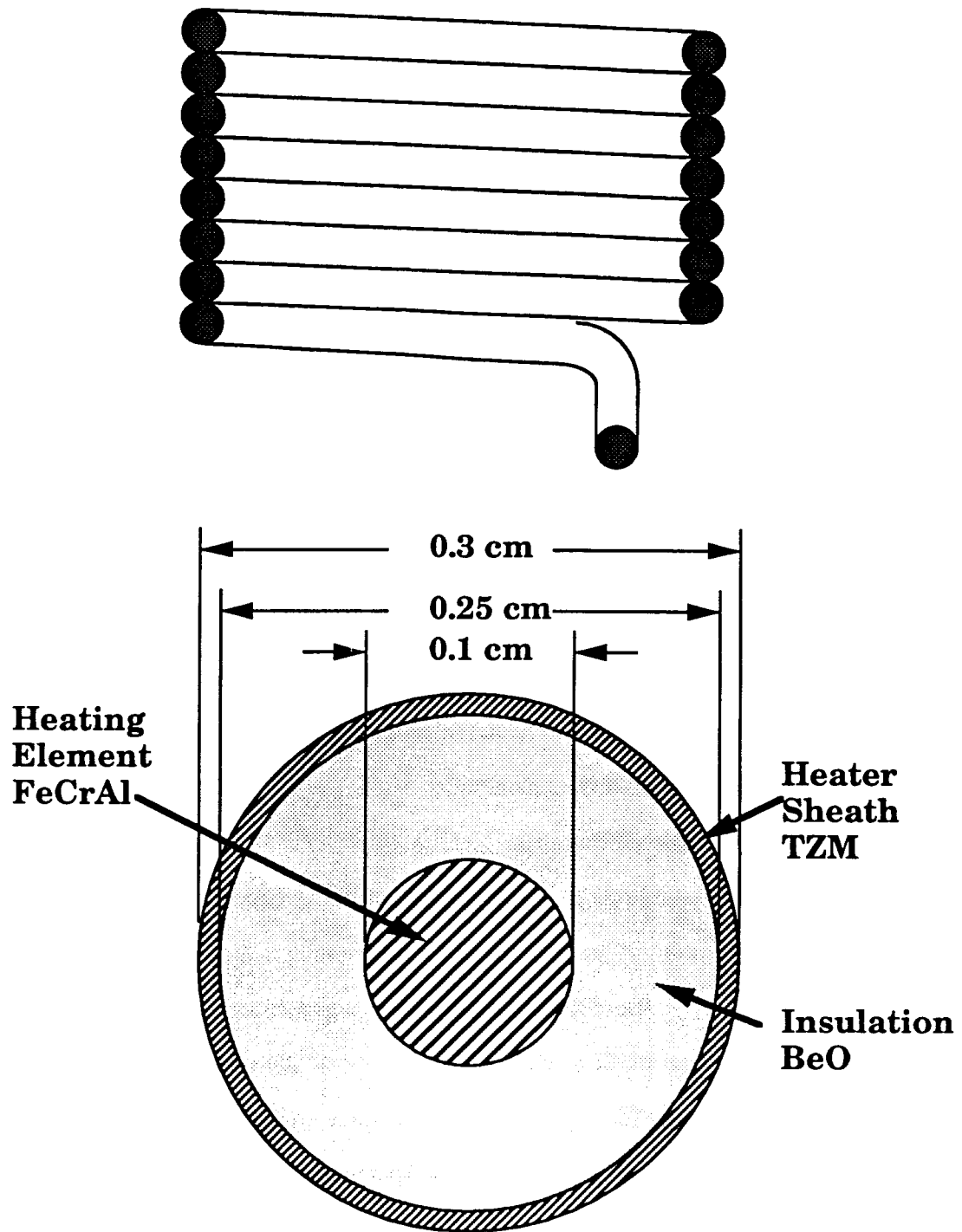


Figure II.5 Coiled sealed heater shown on top with a cross-section of heater shown on bottom

Figure II.6 shows the energy needed to heat the sample to 1200°C as a function of container diameter. By far the largest amount of energy is needed by the heater and its surrounding parts while that needed for the regolith and container is very low. Nevertheless there is almost a factor of two difference in the total energy for an OD of 0.5 cm compared to an OD of 1.0 cm.

Figure II.7 shows the overall time needed to heat one sample of regolith from 300°K to 1473°K using a 50 watt heater. The time for heating the sample is dominated by the thermal conductivity of the regolith and can be seen to vary by almost a factor of four. When the time for heating the heater and the time for heating the regolith are added together, the total shows a shallow minimum between OD of 0.7 cm to 1.0 cm. In the actual case the two would be heated simultaneously and not consecutively, however, the optimization with respect to the container dimensions would not change. On this basis, we have selected a container with an OD of 0.8 cm, a height of 1.57 cm and a wall thickness of 0.1 mm. The actual time for heating will be determined by a computer program, and will be less than 560 s.

3. Obtaining a Sample of Regolith

Figure II.8 shows a lunar rover platform of arbitrary configuration with sampling equipment mounted on it. A scoop is shown in a lowered position with the detail of the scoop shown separately. The function of the scoop is to pick up some regolith from the lunar surface. This can be done by forward motion of the rover with the scoop in a lowered position scraping the upper 0.5 cm of the lunar surface. The front of the scoop is covered with a grid which performs the initial screening, allowing only particles of <0.2 cm to pass. Once a sample is picked up, the scoop is rotated and the charge is dumped through a chute into two progressively smaller sieves. The sieves are vibrated and the fraction which passes through is collected into a funnel which fills the sample container located immediately below the funnel. The fraction which does not pass through the sieves falls off the open side of the sieves back onto the lunar surface.

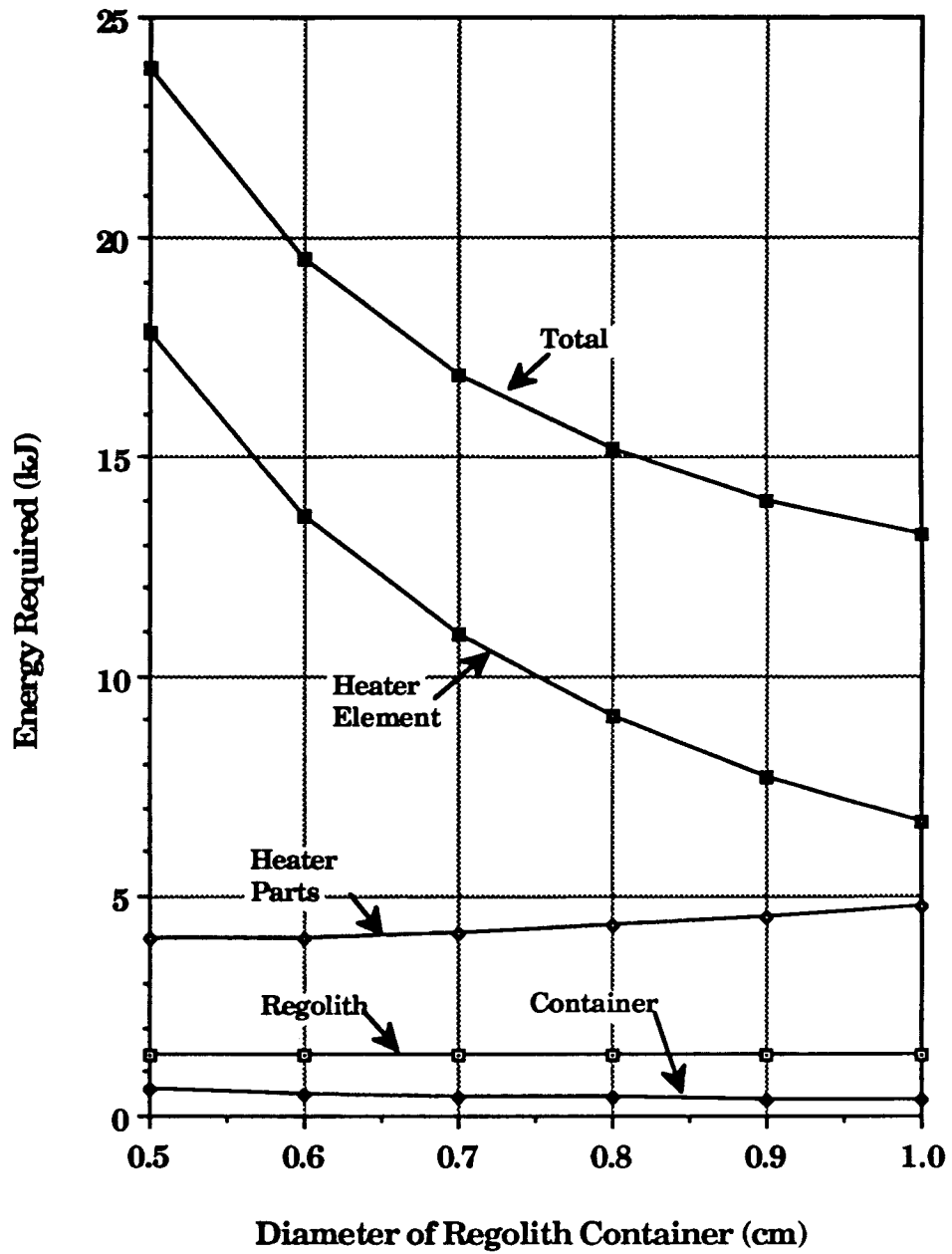


Figure II.6 Energy required to heat a one gram sample of regolith to 1200°C as a function of container diameter

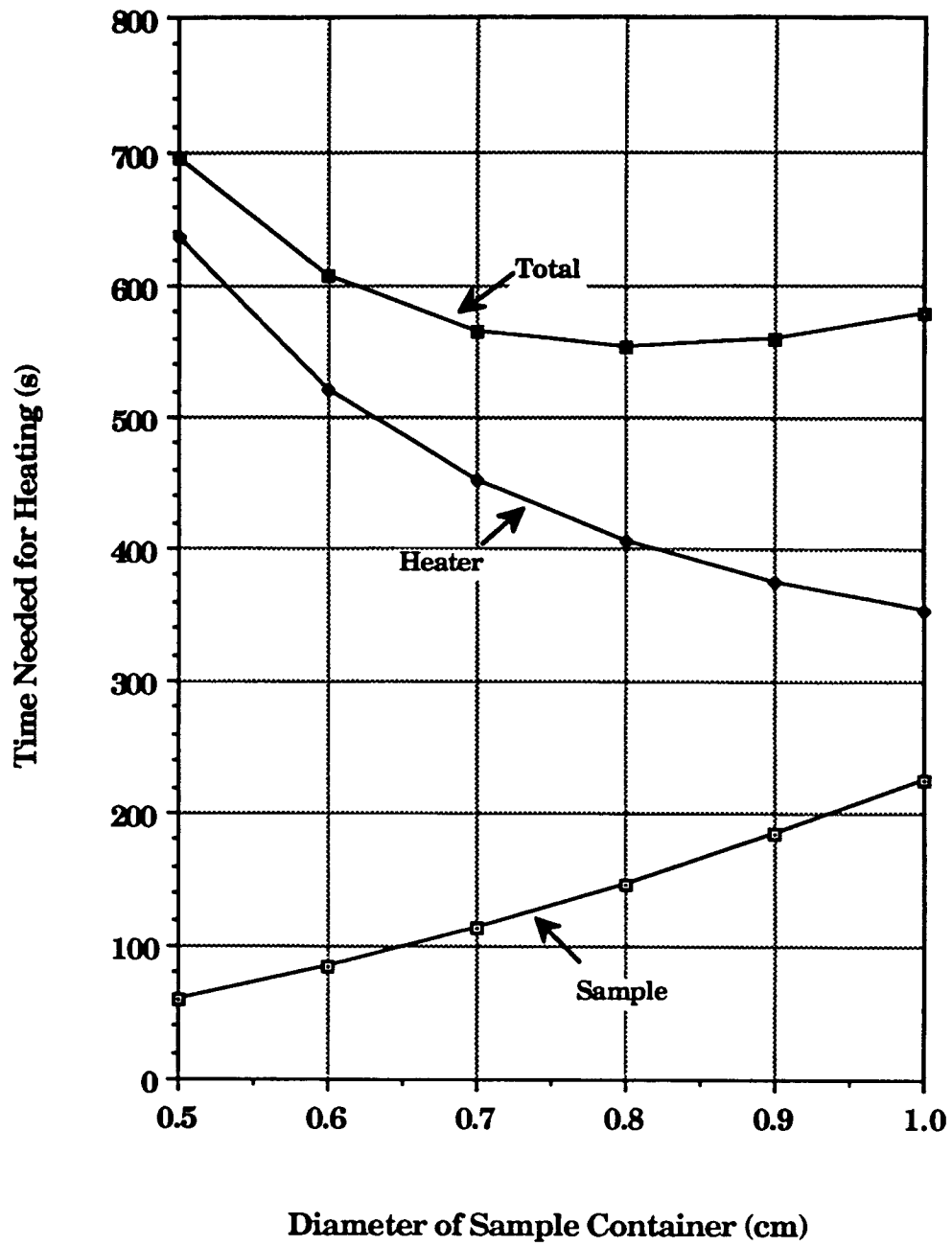
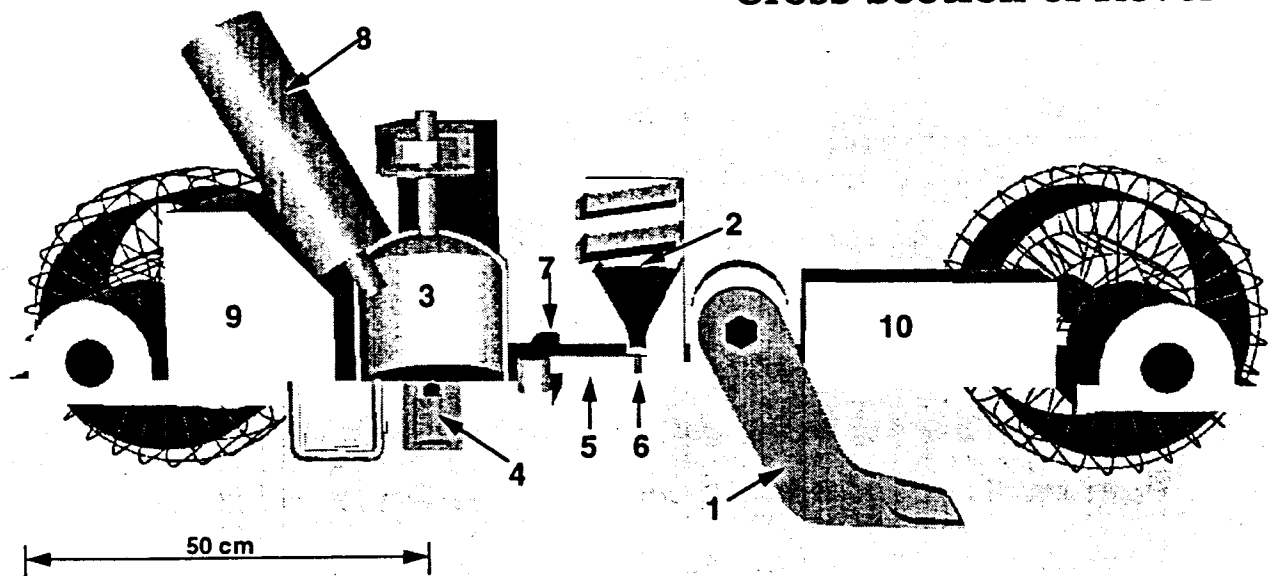


Figure II.7 Time needed to heat a one gram sample of regolith from 30°C to 1200°C as a function of container diameter using a 50 watt heater.

Cross Section of Rover



- | | |
|--------------------|----------------------|
| 1) Scoop | 6) Sample Container |
| 2) Sieves & Funnel | 7) Scale |
| 3) Heater Dome | 8) Laser |
| 4) Heater | 9) Mass Spectrometer |
| 5) Rotary Arms | 10) Capacitor Bank |

Figure II.8 Lunar rover of arbitrary configuration showing the sampling and heating equipment

The figure also shows the top view of a double arm rotating mechanism equipped with magnetic chucks at the ends. The two arms are at 90° to each other and rotate counter clockwise. The mechanism is controlled by a stepping motor which can index onto various stations located along the path of the arms.

4. Weighing the Regolith Sample

Each sample is collected into a ferritic stainless steel container 0.8 cm in diameter and 1.57 cm high with a wall thickness of 0.1 mm. Ferritic stainless steel was selected because it is magnetic and thus can be picked up with a magnetic chuck.

The first arm of the rotating mechanism holds a one gram calibrated weight. This calibrated weight is used to calibrate a scale just prior to weighing of the sample itself. In this way all uncertainties that can influence the weight measuring are removed by this calibration. These uncertainties may have to do with the level of the platform on which the scale is mounted, it may be for some other reason such as the uncertainty in the correction for lunar gravity. The scale is calibrated by depositing on it the one gram weight, which is held by the magnetic chuck on one arm of the rotating mechanism. Once the scale is zeroed, the weight is removed by energizing the magnetic chuck, and the arm rotate to index the sample onto the scale. The sample is deposited on the scale and is weighed. Since the mass of the container is the same for all the samples, the absolute weight of the regolith can be obtained. When the weight is registered, the sample is picked up and the arms are rotated to the next station.

5. Heating the Sample

The oven consists of a cylindrical oven dome with a heater built into its base. The cover dome can be raised ~10 cm while the heater stays in the base.

After the sample is weighed, the oven dome is raised and the arms rotate to index the sample on the heater. The container with the regolith sample fits inside the heater with only one mm gap between the heater coils and the container. The arms are rotated out of the way and the dome cover lowered onto a seal built into the base of the oven.

6. Vaporizing Sample Material

A laser is fired onto the surface of the regolith, evaporating some of the regolith. A plasma is formed from which ions are ejected and enter into the mass-spectrometer where they are analyzed as discussed in Section II.A. The energy density needed is $\sim 10^{11}$ w/cm³ [20]. The 2J laser which is built into the oven cover dome is focused onto a spot 0.16 cm in diameter. Assuming an average particle diameter of 100 μ , this spot will expose at least 100 particles to the laser beam. Statistically, this should give an adequate indication of the composition of the regolith in the sample.

Once the elemental composition of the sample is known, the sample can be heated. The next section gives a description of the heater.

7. Description of Heater

Figure II.9 is a full scale cross section of the heater enclosure. It shows the cylindrical regolith sample container located in the heater which consists of effectively six coils, wound in a cylindrical configuration. There are upper and lower insulating washers squeezed between metallic washers. There is a TZM radiation shield surrounding the heater at a distance of 2 mm and surrounding that is a 3 mm thick insulating cylinder, separated from the radiation shield by 2 mm. The heater is supported on four long rods made from Hastelloy R-235, which is characterized by a very low thermal conductivity. The upper metallic washer is attached to the bottom support plate by six metallic spring loaded straps. The whole heater assembly fits within an insulated cavity which is sealed from the oven enclosure. Electrical leads are admitted from the bottom and are made from TZM, which has a very high electrical conductivity and a very high melting temperature. Outside the enclosure the electrical leads can be made of copper.

The design of the heater minimizes energy losses to its surroundings. At maximum temperature, the total conduction losses are 1.1 watts in the support rods, 2.3 watts in the electric leads and the I^2R losses from the leads are 0.7 watts. Thus the total

conduction losses are <5 watts. To account for these losses in the thermal analyses of the heating time needed to raise the temperature of the regolith, 5 watts were subtracted from the available heating power. Thus when a 50 watt heater was used, only 45 watts were assumed to be available in the heater, similarly when a 25 watt heater was used, 20 watts were available. Radiation losses are modelled directly in the 2D ANSYS program which was used to determine heating time.

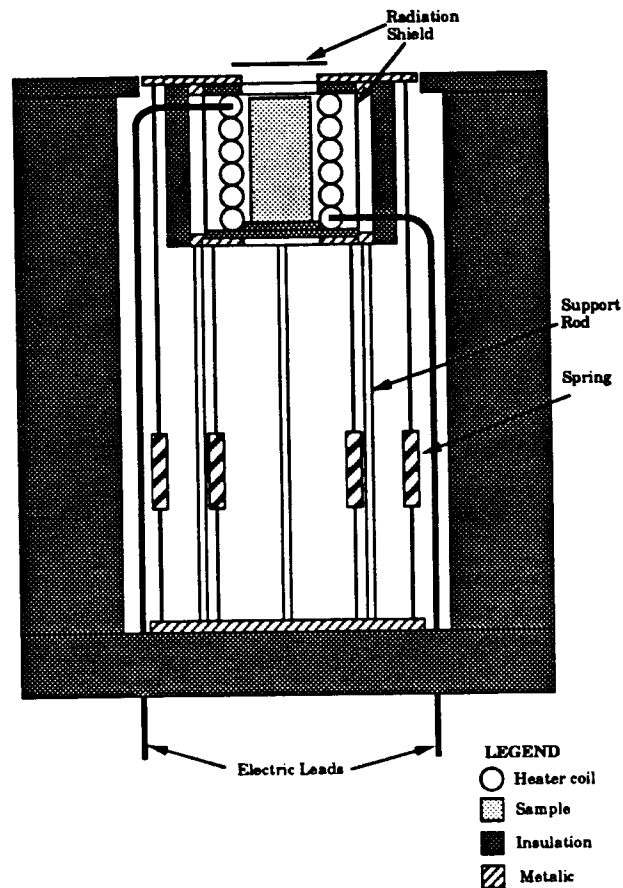


Figure II.9 Full scale cross-section of heater enclosure

Table II.2 gives the heater materials and their properties which were used in the analysis of heating time.

Table II.2 Heater Material Properties

Component	Material	Density (g/cm ³)	Specific Heat (J/gK)	Thermal Conductivity (w/mK)	Electrical Resistivity (μohm cm)	Emmissivity
Heater Element	Fe-Cr-Al	7.15	0.45*	n/a	166.2	n/a
Heater Element Insulation	BeO	3.01	1.09*	20*	5x10 ¹²	n/a
Heater Sheath	TZM	10.2	0.75*	98*	n/a	0.14*
Heater Insulation	Fireclay brick	0.23	0.96	1.09	n/a	0.65
Radiation Shields	TZM	10.2	0.75*	98	n/a	0.14*
Regolith Container	Ferritic Steel	7.8	0.76*	29*	n/a	0.4
Electric Leads	TZM	10.2	0.75	98	31	n/a
Support Rods	Hastelloy R235	8.8	0.45	18	n/a	n/a
Sample	Lunar Regolith	1.265	1.17	0.1	n/a	n/a

n/a Not Applicable

* Properties at 1000°C

8. Analysis of Sample Heating

Analysis of the heating of the regolith samples has been performed using the ANSYS 2D finite element thermal and static stress analysis code [21]. The heater and the sample were modeled as a 10° slice of the complete cross-section shown in Figure II.10. It shows the model starting at the regolith center proceeding left to right: 4mm of regolith (diameter of sample is 8mm), 0.1 mm ferritic steel sample container wall, 1.0 mm vacuum gap, 3 mm heater, 2 mm vacuum gap, 0.2 mm TZM radiation shield, 2 mm vacuum gap, 3 mm fireclay brick insulation, and finally a vacuum gap of arbitrary dimension followed by a heat sink also made of fireclay brick. This heat sink is assumed to stay at 30°C. The components of the heater which could not be explicitly modeled in the code, such as the upper and lower washers were included as part of the specific heat of the heater. Thus, whereas the actual specific heat of the heater is 0.814 J/gk, the effective specific heat used is 1.25 J/gk.

The mode of analysis is the following. The sample is enclosed in the oven and all the components are at 30°C. The heater is turned on for a period of time and when its temperature exceeds some value (~1300°C) it is turned off and the components are allowed to equilibrate in temperature. This analysis is done iteratively until the proper time and temperature are determined.

Figure II.11 is a plot of the temperature histories of the various heater components for the 50 watt input heat case. At $t = 0$ all components are at 30°C. The curves are for sample center ($r=0$), sample midpoint ($r= 2\text{mm}$), sample outer surface ($r=4\text{mm}$), inner heater surface ($r=5\text{mm}$), radiation shield ($r=10\text{mm}$) and finally, the inner insulation ($r=12\text{mm}$). Active heating is stopped at $t = 280\text{s}$ and at $t = 324\text{s}$, the sample center reaches 1200°C. We can say that six minutes are needed to perform the sample heating when a 50 watt heater input source is used.

For completeness, it was decided to do the analysis for a heater input of 25 watts, and the results are shown in Figure II.12. In this case only 20 watts were used for

heating, and it can be seen that the spread between the curves is much smaller, because the effect of thermal inertia is negligible. Active heating is stopped at $t = 800\text{s}$ and the sample center reaches 1200°C at $t = 825\text{s}$. Thus about 14 minutes will be needed for the 25 watt case.

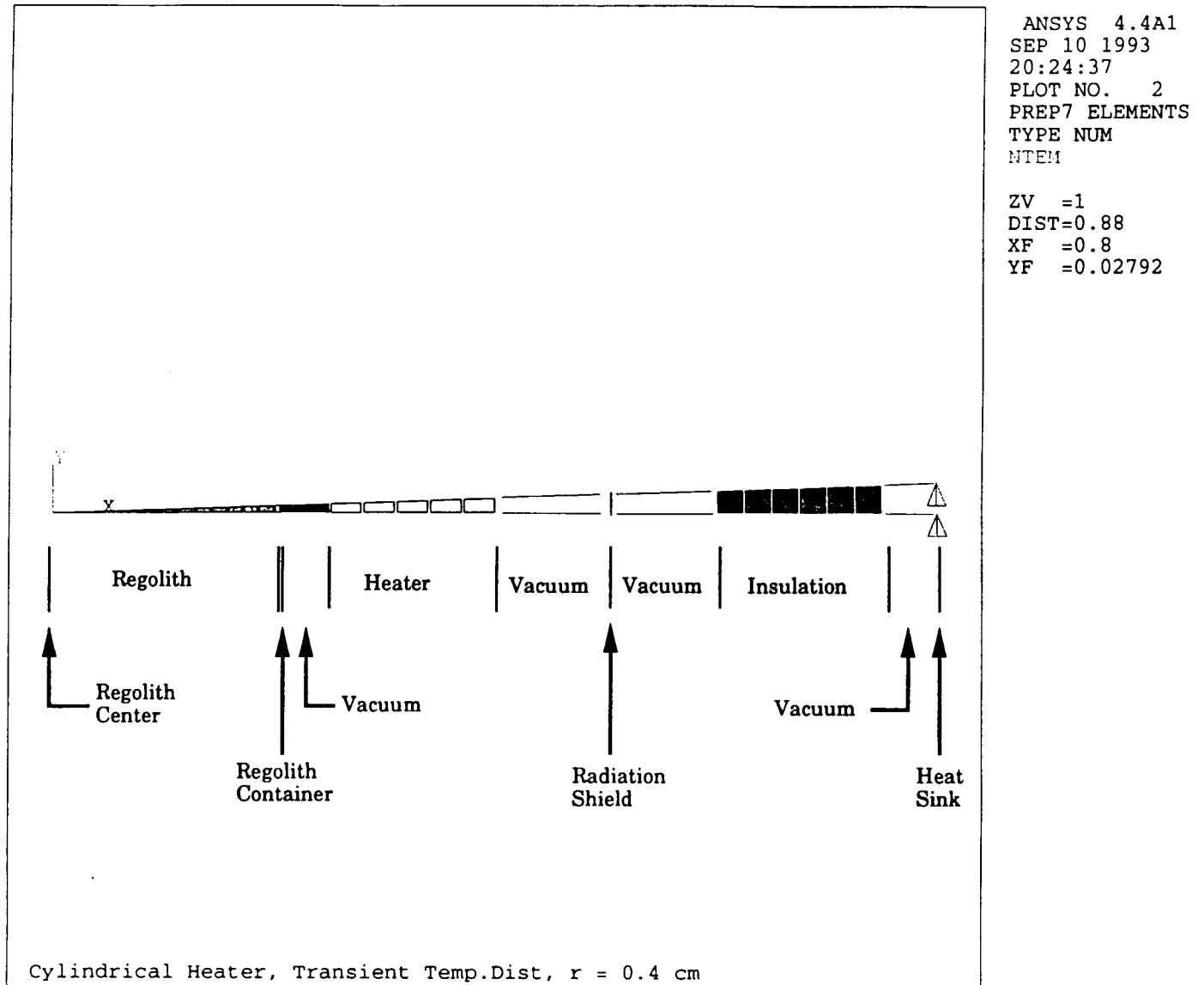


Figure II.10 Model for the regolith sample in the heater for analysis by ANSYS

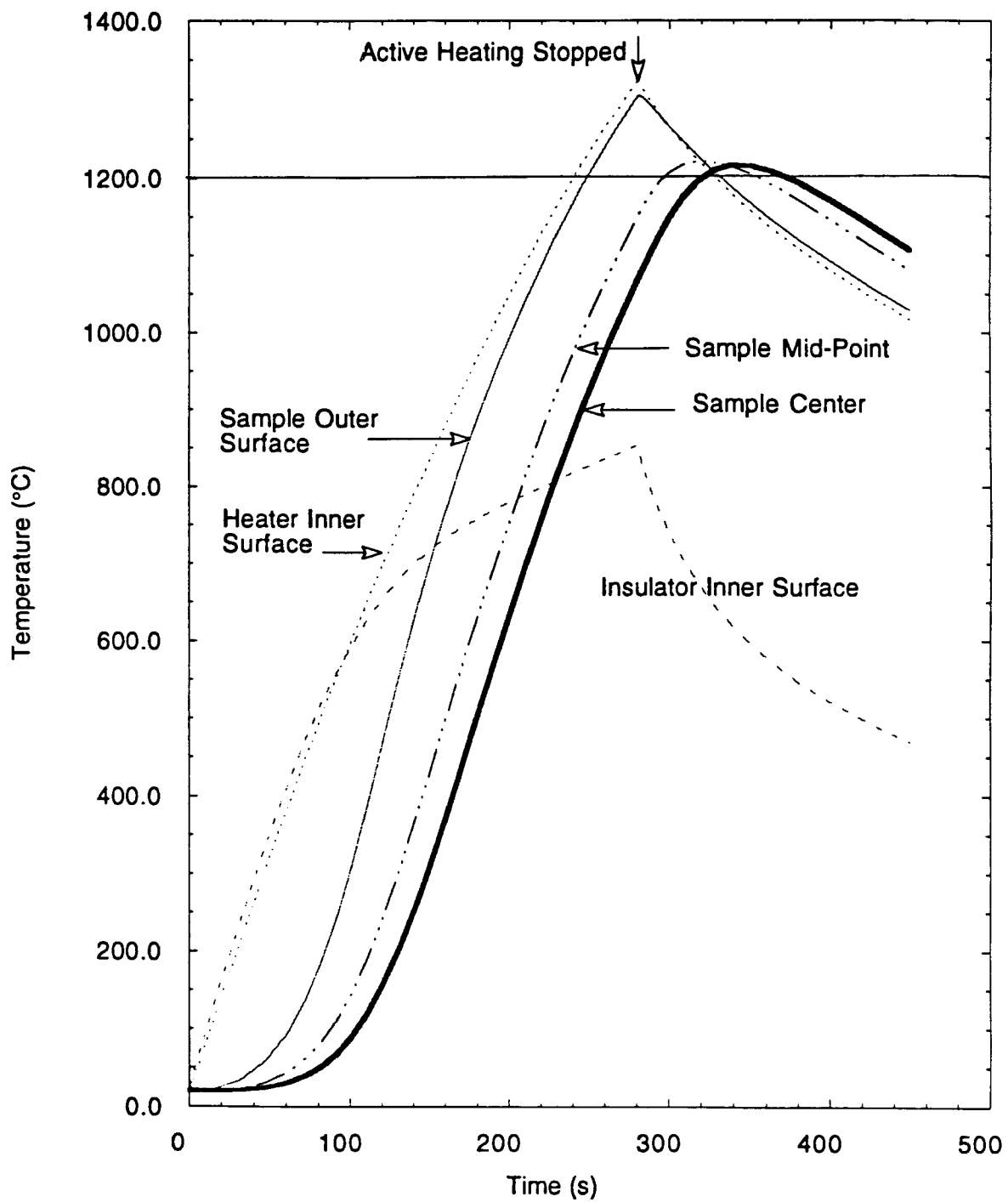


Figure II.11 Temperature history of various parts in the heater for a sample of 0.8cm diameter and 50W power input. The heavy curve represents the regolith center

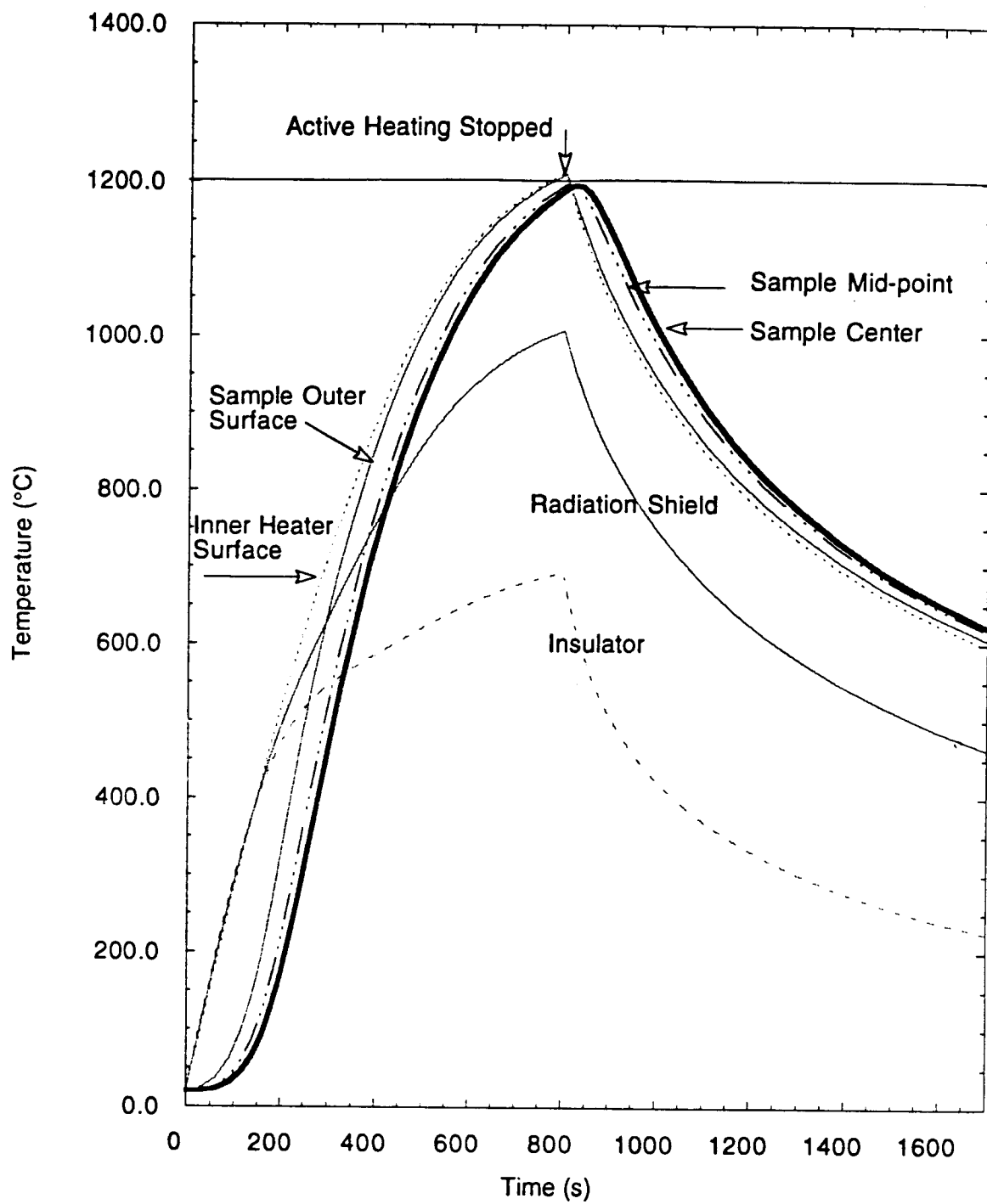


Figure II.12 Temperature history of various parts in the heater for a sample of 0.8cm diameter and 25W power input. The heavy curve represents the regolith center

It should be mentioned here that subsequent sample heating times will depend on the duration between sampling. If a new sample is inserted into the oven while the components are still hot, the heating times will be shorter. Also, these calculations are conservative, because we have assumed that the insulated enclosure remains a heat sink at 30°C. In the actual case, it will not, and the times for heating will be somewhat reduced.

9. Sample Characterization Sequencing.

The procedure for sampling and analyzing lunar regolith is summarized in the following section, where the numeration refers to that in Figure II.8.

Procedure for Sampling and Analyzing Lunar Regolith.

- With the scoop (1) elevated, the carriage travels to the desired sampling area.
- The scoop is lowered and a sample is taken by forward motion of the carriage. Initial screening is accomplished by the grid on the scoop.
- The scoop is rotated upwards and the sample is deposited into two vibrating screens and into a funnel (2) which directs the fines into a sample container (6)
- The sample container is held by a magnetic chuck (6) at the end of an arm of a two arm rotating mechanism (5)
- The second arm also has a magnetic chuck which holds a one gram calibrating weight (7). At the time the sample is collected, the arm is positioned over a piezo-electric or strain-gauge scale (7)
- When all the vibration stops, the weight is deposited on the scale and the scale calibrated. The weight is then picked up.
- The oven cover(3) is retracted, by means of a mechanical screw mechanism protected with a rubber bellows.

- The arms rotate and the sample stops at the scale. The magnetic chuck releases the sample, it is weighed and then picked up again.
- The arms rotate again and the sample is deposited into heater cavity (4)
- The arms rotate again and clear the oven enclosure (8)
The oven cover (3) is lowered and a seal is made with an "O" ring in the base of the cover.
- Experiments on the sample can now begin. This laser is fired and the elemental characterization is made. This can be repeated several times. All other instruments can access the oven enclosure throughout the base. Once the heater is turned on, gas samples can be periodically drawn into the mass-spectrometer.
- After the experiments are completed, the gasses are exhausted, the oven cover retracted and the sample discarded.
- A new sample container is picked up (9) and the whole process is repeated.

C. Mass and Power Requirement

An estimate has been made of the mass and power requirements of the instrumentation package which deals directly with acquisition and characterization of the lunar samples.

The scoop and the rotary arms are made from a Ti alloy (Ti-GAl-4V). Indeed all the external parts which do not come in contact with the solar wind products when they are released will be made of Ti alloy for its strength and light weight. No parts of the heater or the oven dome will be made of Ti because it is a H₂ getter at low temperatures and will hold up H₂. This will give erroneous readings of the H₂ content of lunar regolith. The hot parts of the heater which will be exposed to H₂ are made of TZM (Molybdenum alloy) with the exception of the sample container which will be made of ferritic steel, because it is magnetic. A magnetic chuck is used to manipulate the sample container during sample acquisition and weighing.

The laser is a Nd:YAG unit, diode pumped with a 10% efficiency, and is tunable to deliver from 0.45J to 2.0J per pulse at a wavelength of ~1000 nm. It needs 25J capacitor bank, where only 20J are discharged during one pulse. The capacitors are recharged in 10 s using 2.0 watts of power. Since it takes ~ 10 s to perform the mass spectrometer analysis, the capacitor bank will be recharged in case another laser firing is needed. As mentioned in II.A, the weight of the mass spectrometer was taken the same as that used on Rocky II, namely 12 kg.

To avoid the contamination of any sample with residue of previous samples, we have decided to use clean containers each time a new sample is taken. The containers are made from a ferritic steel, have a diameter of 0.8cm and are 1.0 cm high. The material is 0.1 mm thick, making the mass of each container 0.45 g. Assuming an inventory of 1000 containers on board, the total mass will be 450 g. Table II.3 gives the masses of the equipment and the estimated power requirements for operating them.

Table II.3 Mass and Power Requirements

Component	Mass (g)	Function	Power (w)
Scoop	244	Lower	2.0
		Raise	3.0
Sieves	100	shake	1.0
Funnel	50	-	-
Rotary Arms	124	Rotate	1.0
		Magnetic chuck	1.0
Drive for Rotary Arm	200	-	-
Scale	50	Weigh	0.5
Heater	40	Heat Sample	24--50
Heater Insulation	480	-	-
Oven Dome	690	-	-
Oven Dome Drive	500	Raise	7
		Lower	5
		Seal	10

Laser	500	Evaporate regolith	2×10^9
Capacitor	2500	Recharge	2
Mass Spectrometer	12000	Analysis	25
Sample Containers	450	-	-
Total Mass	17,928		

We have assumed that 25 watts of power is needed for housekeeping functions, and any power requirements needed to operate the instruments are over and above that. Table II.4 gives sequential time and power requirement for obtaining a sample and characterizing it. Two second stop intervals are used between most operations.

Table II.4 Time and Power Sequencing for Obtaining and Characterizing Lunar Regolith Samples.

No.	Operation	Time (s)	Cumulative Time(s)	Indiv. Power (w)	Total Power (w)
1	Rover Moving	15	15	13	38
2	Rover Stopped	2	17	1	26
3	Scoop Lowered	10	27	2	27
4	Stop	2	29	1	26
5	Forward Motion	3	32	13	38
6	Stop	2	34	1	26
7	Scoop Raised	20	54	3	28
8	Stop	2	56	1	26
9	Shake Sieves	10	66	2	27
10	Stop	2	68	1	26
11	Release Calibration Weight	5	73	0	25
12	Stop	2	75	0	25
13	Calibrate Scale	10	85	0.5	25.5

14	Pick up Calibration	2	87	1	26
15	Stop	2	89	1	26
16	Rotate Arms	5	94	2	27
17	Stop	2	96	1	26
18	Release Sample on Scale	2	98	0	25
19	Stop	2	100	0	25
20	Weigh Sample	10	110	0.5	25.5
21	Pick up Sample	2	112	1.0	26
22	Raise Oven Dome	10	122	7	32
23	Stop	2	124	1.0	26
24	Rotate Arms	5	129	2.0	27
25	Stop	2	131	1.0	26
26	Release Sample in Oven	2	133	0.0	25
27	Rotate Arms	5	138	1.0	26
28	Stop	2	140	0	25
29	Lower Oven Dome	10	150	5	30
30	Seal Oven Dome	3	153	10	40
31	Stop	2	155	0	25
32	Fire Laser	10 ⁻⁹	155	2e ⁹	25
33	Mass Spectrometer On	10	165	25	52
34	Stop	2	167	0	25
35	Fire Laser	10 ⁻⁹	167	2e ⁹	25
36	Mass Spectrometer On	10	177	25	52
37	Stop	2	179	0	25
38	Heater On	800	979	25	50

39	Stop	2	981	0	25
40	Temp. Equilibrium	25	1006	0	25
41	Mass Spectrometer On	10	1016	25	50
42	Stop	2	1018	0	25
43	Raise Oven Dome	10	1028	7	32
44	Stop	2	1030	0	25
45	Rotate Arm	5	1035	1	26
46	Stop	2	1037	0	25
47	Pick Up Sample	2	1039	1	26
48	Stop	2	1041	1	26
49	Rotate Arms	5	1046	2	27
50	Stop	2	1048	1	25
51	Release Sample	2	1050	0	25
52	Rotate Arm	5	1055	1	26
53	Stop	2	1057	0	25
54	Pick Up New Container	2	1059	1	26
55	Stop	2	1061	1	26
56	Rotate Arm	5	1066	2	27
57	Stop	2	1068	1	26
58	Transmit Information	30	1098	25	50

The whole sequence from start to finish takes ~1100s or 18.3 minutes. It is interesting to note that 73% of that time is needed for heating, using a 25 watt heating input.

Figure II.13 is a plot of the sequential power requirements for obtaining a regolith sample and placing it in an oven. This takes 150 seconds. Figure II.14 shows the

sequence from start to the point at which solar wind products are characterized, or step Number 42 in Table II.2. The remaining steps describe recovery and disposal of a new sample.

To communicate the information directly to an earth-based station, some 40-50 watts of power are needed. This means that all available power, including housekeeping will be used to transmit the acquired data. During this time, only the bare essentials (such as the magnetic chucks) will be drawing power, and the rover will be stationary.

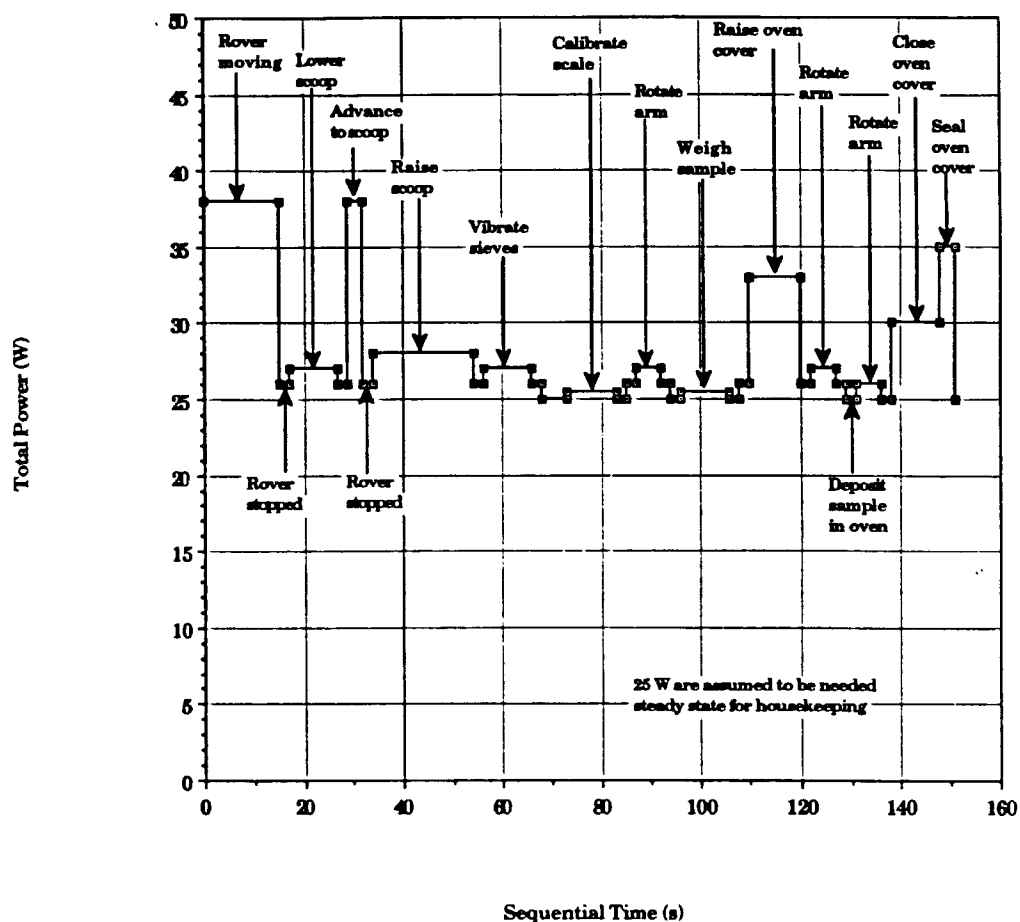


Figure II.13 Sequential Power Requirements for Obtaining a Sample of Lunar Regolith and Placing it in the Oven.

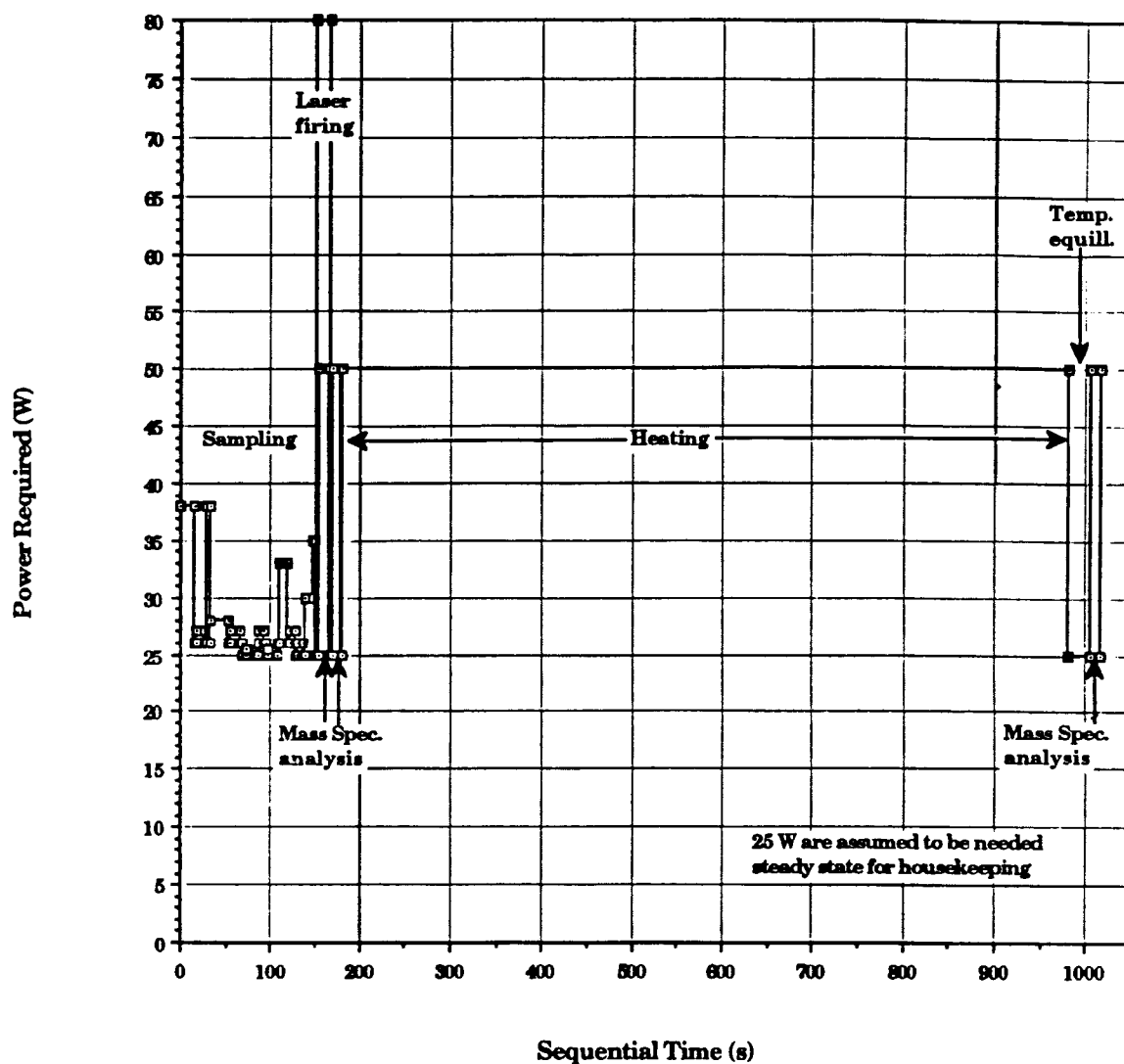


Figure II.14 Sequential Power Requirements for Obtaining and Characterizing a Sample of Lunar Regolith

II.B SELECTING A SOIL SAMPLE COLLECTING INSTRUMENT FOR AN AUTOMATED LUNAR ROVER.

A. Introduction

The objective of this section of the study was to select a surface soil sample collecting instrument for an automated lunar rover. A sampling system is required to collect 10 cubic centimeters of lunar soil and deliver it to the analyzing instrument. Eight sampling concepts and eight criteria to judge them are presented. Mass, power requirement, reliability and simplicity are the most important criteria for the mobile

sampling system. The concepts were arranged according to each criterion and the most promising ideas were identified. Finally the flip scoop is proposed as a sampling instrument for the rover. Data sheets for the sampling concepts are presented in appendix A.

B. Sample Acquisition Concepts

So far some real experience in sample acquisition on planetary surfaces has been gained through manned Apollo-missions and unmanned Luna, Surveyor and Viking-missions. During Apollo-missions a portable core drill, drive tubes driven with the aid of a hand held hammer and different types of penetration cones were used [22]. Russian Luna-landers examined the lunar surface with a simple rotatable penetration cone [22]. Surveyor III and Surveyor VII used lazy tongs to reach the surface with a sampling scoop [25, 26, 27]. Viking mars landers made use of reel stored extendible booms to locate sampling scoops on surface [28, 34].

Below are listed, with brief comments, the most interesting ideas of the sampling concepts which were found in literature or presented by the author. Illustrations and short data lists of eight ideas are enclosed in appendix A. Concepts such as a 40 kg and 236 watts core drill were rejected immediately as inadequate for mobile use. In addition to geometries presented in the data sheet pictures, some sampling systems needed mechanisms to unfold and position the sampler. Estimated masses of the mechanisms are included in the mass shown on the data sheets.

1. Brush Sweeper

In reference [29] a brush sweeper was designed to meet the efficiency of an enormous 120 cubic-ft of regolith per hour device which is too large for surface sampling purposes. However, scaling the whole system down by a factor of about one hundred, the size and energy requirements will be reasonable and efficiency still adequate. The brush sweeper appears to be a relatively simple and efficient device.

2. Extendible Reel Stored Boom

A boom is a relatively strong and powerful tool for taking surface samples within a radius of three meters from the lander or rover [28]. The boom system is somewhat complex and during a mars mission some anomalies took place but the problems were solved and the experiment was successful [34].

3. Flip Scoop

A flip scoop minimizes the amount of moving parts and therefore is very simple. However, very strong horizontal movements of the rover may break scoop if it hits a large rock or stone. The rover may also get stuck due to the cutting resistance of the scoop but this shouldn't be a problem because of TV-feedback from the rover back to Earth. The idea of the flip scoop was presented by Igor Sviatoslavsky.

4. Lazy Tongs

Lazy Tongs are simpler and lighter than but not as strong as the reel stored boom. Lazy tongs were successfully used on the Surveyor III and Surveyor VII missions although an anomaly in telemetry prohibited feedback of motor currents which eliminated the possibility to calculate forces encountered [25, 26, 27]. This design appears to be a relatively efficient way to take soil samples when there is a need to reach away from the lander or rover.

5. Robotic Arm Sampler

Very little information can be found on this type of robotic arm. The data sheet shows that the mass of the arm may be relatively low but a power estimation is missing due to lack of information. The robotic arm is presented in reference [35].

6. Surface Drill

This is a strongly simplified version of the core drill. Only a few rotations are required to collect a 10 cc sample of loose lunar soil. This design appears to be very simple although the moments may require a stronger positioning mechanism. The idea of a surface drill was presented by author.

7. Surface Sample Collection System

This system presented in reference [30] is in principle similar to the flip scoop. It is however, unnecessarily large and the energy consumption is very high.

8. Wheel Collector

The idea of a wheel collector presented by the author is based on the Apollo Lunar Roving Vehicle (ALRV). Accidentally the rear fender of the ALRV was broken so the astronauts were concerned about sand and rocks that would come in contact with the rover when driving. To collect the regolith off of the rover wheels would require driving the rover at a high speed which may cause other difficulties. If the dust doesn't have enough velocity to flow into the scoop inside the fender, a small rotating brush may be used to loosen the dust from wheel. Mechanically this system is very simple although it requires some special adjustments to the wheel surface.

C. Concept Analysis

To find the most promising concepts, the proposals are judged according to several different criteria. Eight criteria are presented and the most important of these gets number eight as a value of weight and least important gets one. If several criteria seem to be of equal importance they all get same value.

Table II.B.1 Weights and Criteria

Criterion:	Weight
Mass	7
Power	7
Dimensions	5
Complexity	8
Energy per 10 cc Sample	1
Working Volume	2
Positioning Accuracy	3
Flexibility	4

The best concept according to each criterion gets value of 8 and the worst gets 1 (there are 8 concepts). The meanings of values are given below.

Table II.B.2 Meanings of Values

Criterion:	Value	Meaning
Mass	8	the lightest
Power	8	the lowest
Dimensions	8	the smallest
Complexity	8	the most simple
Energy per 10 cc Sample	8	the lowest
Working Volume	8	the largest
Positioning Accuracy	8	the most accurate
Flexibility	8	the most flexible

A comparison value for each concept is the weighted sum of values. The lowest possible value is $1 \times 1 + 2 \times 1 + 3 \times 1 + 4 \times 1 + 5 \times 1 + 6 \times 1 + 7 \times 1 + 8 \times 1 = 36$, the highest possible value is $1 \times 8 + 2 \times 8 + 3 \times 8 + 4 \times 8 + 5 \times 8 + 6 \times 8 + 7 \times 8 + 8 \times 8 = 288$. The orders (and therefore values) of sampling concepts according to each criterion are presented in Table II.B.3.

Table II.B.3 Orders of Sampling Concepts

Criterion							
Mass		Power		Dimensions		Complexity	
Wheel Co	8	Wheel Co	8	Wheel Co	8	Wheel Co	8
Flip Sc	7	SFace Dr	7	Flip Sc	7	Flip Sc	7
Robot	6	Flip Sc	6	Tongs	6	SFace Co	6
SFace Dr	5	Brush Sw	5	Robot	5	Brush Sw	5
SFace Co	4	SFace Co	4	SFace Co	4	Tongs	4
Tongs	3	Tongs	3	Brush Sw	3	SFace Dr	3
Brush Sw	2	Robot	2	SFace Dr	2	Robot	2
Boom	1	Boom	1	Boom	1	Boom	1

Energy		Working Vol.		Accuracy		Flexibility	
Wheel Co	8	Robot	8	Robot	8	Robot	8
Tongs	7	Boom	7	Boom	7	Tongs	7
SFace Dr	6	Tongs	6	Tongs	6	Boom	6
Brush Sw	5	SFace Co	5	SFace Dr	5	SFace Co	5
Flip Sc	4	Brush Sw	4	Flip Sc	4	Flip Sc	4
Robot	3	Flip Sc	3	SFace Co	3	Brush Sw	3
Boom	2	SFace Dr	2	Brush Sw	2	SFace Dr	2
SFace Co	1	Wheel Co	1	Wheel Co	1	Wheel Co	1

Table II.B.4 presents the values of each sampling concept according to each criterion, the weighted values (*in italic font*) and the sum of the weighted values. The most promising sampling concepts are highlighted.

Table II.B.4 Values, Weighted Values and Sum of Weighted values of Sampling Concepts for the Rover Sampler.

Rover Sampler																	
Criteria																	
	Mass		Power		Dim.		Compl.		Energy		W. Vol.		Accur.		Flexib.		
Weight	7		7		5		8		1		2		3		4		37
Concept																	Sum
Brush Sw	2	14	5	35	3	15	5	40	5	5	4	8	2	6	3	12	135
Boom	1	7	1	7	1	5	1	8	2	2	7	14	7	21	6	24	88
Flip Sc	7	49	6	42	7	35	7	56	4	4	3	6	4	12	4	16	220
Tongs	3	21	3	21	6	30	4	32	7	7	6	12	6	18	7	28	169
Robot	8	56	2	14	5	25	2	16	3	3	8	16	8	24	8	32	186
SFace Dr	6	42	7	49	2	10	3	24	6	6	2	4	5	15	2	8	158
SFace Co	5	35	4	28	4	20	6	48	1	1	5	10	3	9	5	20	171
Wheel Co	8	56	8	56	8	40	8	64	8	8	1	2	1	3	1	4	233

1. Conclusions

According to Table II.B.4 the Flip Scoop and Wheel Collector are both very efficient sampling instruments for the rover.

The wheel collector is a very good choice because of its low mass, low power requirement, low complexity and therefore low cost. However, on the lunar surface the alternating soil characteristics and low roving velocity make sample acquisition unreliable. The soil may be too hard or there may be too many rocks or too roughly grained regolith on surface which makes sample acquisition impossible. Also it is impossible to tell the exact source of the sample collected.

The flip scoop has very good points according to the criteria applied but in the case of rocks or hard soil the forces acting on it may be of significant importance because the mass and power of the rover and may be hazardous for the scoop and overall experiment. Therefore there should be some flexibility and perhaps a force detection design in the scoop's structure.

2. Proposal

The proposed sampling instrument is the flip scoop.

II.C. A PRELIMINARY DESIGN OF A SAMPLE HANDLING APPARATUS AND A SAMPLE ACQUISITION DEVICE FOR AN AUTOMATED LUNAR ROVER

A. Introduction

During previous studies various soil sampling methods were examined and the flip scoop was selected for the automated lunar rover. Here sample handling, measuring and weighing concepts are discussed and a few designs are presented. Finally a design for the flip scoop and the overall system integration layout are proposed.

B. Sample Manipulating Arrangement; Proposal II

A Sample Manipulating Arrangement takes care of sample handling after it is received from the sample acquisition device. The concept presented here was developed from Proposal I presented in appendix B and it uses two separate units for sample measuring/weighing and container lifting/chamber sealing. The linkage to close the chamber and dump the sample is similar to Proposal I. The main parts of a measuring unit are the inner flipper and the outer slider. These cylindrical parts are connected to each other by a gearing mechanism so, that when the flipper rotates one degree clockwise, the slider rotates 0.381 degrees counter clockwise.

The Figure II.C.1 below illustrates system principle and more accurate drawings are enclosed in appendix C.

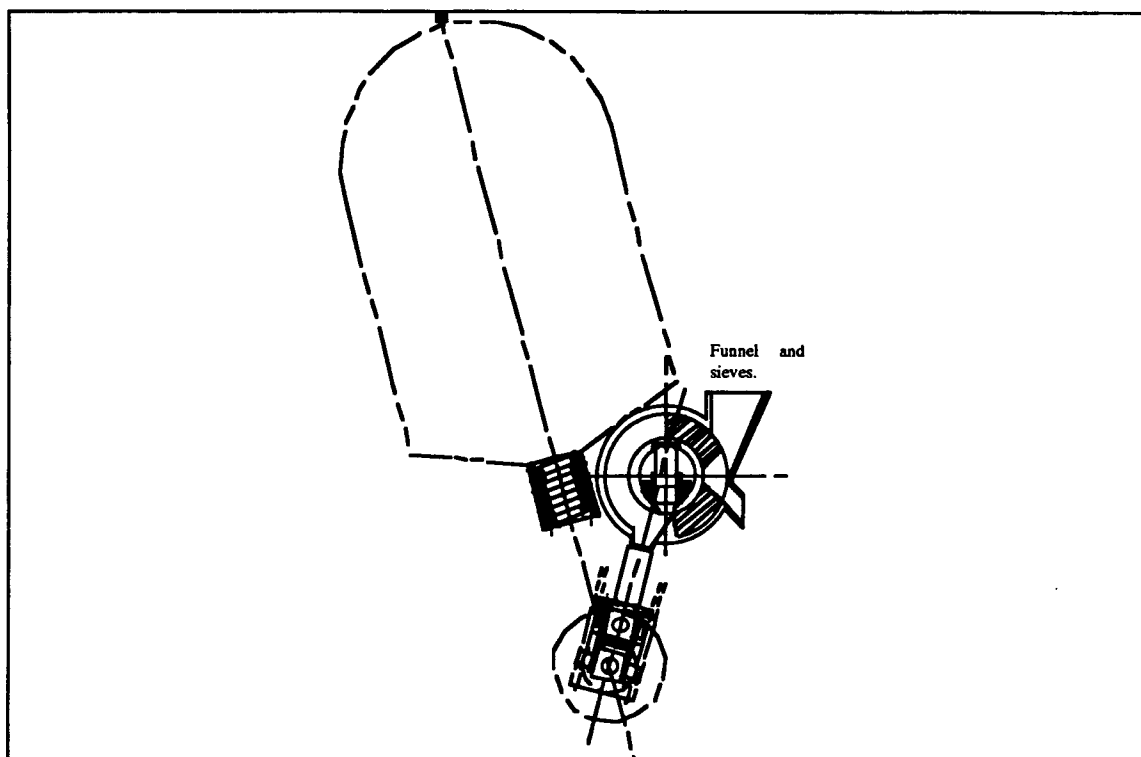


Figure II.C.1 Sample Manipulating Arrangement; Proposal II.

1. Function

Sketches describing the structure and function are enclosed in appendix C.

Lifting Unit:

- 1) In the lower position the linkage is stretched out to the limits and a clockwise rotation of the lead screw causes the linkage support to turn stretching the spring. In 15 degrees clockwise tilted position the heating container receives a measured and weighed sample from a measuring unit, as illustrated in sketch 06-02, figure I.
- 2) When a stepper motor is rotated 30 degrees counter clockwise the spring pulls the linkage support structure into a position of 15 degrees counter clockwise from vertical position, where the movement is stopped by mechanical limits.
- 3) When the linkage support structure has reached its rotational limit, the rotational movement of the lead screw extends the linkage and lifts the container into the heater.

The base for the container seals the vacuum chamber. This is illustrated in sketch 06-02, figure II.

4) After heating, while the spring keeps the linkage support steady, the stepper motor is rotated clockwise and the linkage lowers the container.

5) When the lowest position is achieved, the motor starts to rotate the linkage support and stretches the spring. The motor is rotated 195 degrees and the soil in the container falls out. Look at sketch 06-02, figure III.

6) The motor is rotated counter clockwise and the spring pulls the linkage support back to the initial position.

Measuring Unit:

1) When the scaling container inside the flipper is upside down, -as in sketch 07-01, figure I- the sample flows from the scaling container into a heating container, and anything that is in or is put into the funnel flows through a measuring hole in the slider into a dumping channel.

2) As the flipper is rotated 50.6 degrees clockwise the slider closes the dumping channel and receives a sample from the funnel. See sketch 07-01, figure II.

3) When the flipper is rotated clockwise into a vertical position, the slider closes the funnel channel and encloses one cubic centimeter of soil into a conical hole. This is illustrated in figure III.

4) The calibration weight is resting on rings around the scaling container and one gram calibration point may be recorded.

5) Activation of an electromagnet lifts the calibration mass off the scale and a zero point may be recorded.

6) When the flipper is rotated 15.51 degrees clockwise, a hole in the flipper and the conical hole in the slider meet. The measured sample flows into the scaling container, as figure IV illustrates.

7) After the flipper is rotated 15.51 degrees counter clockwise the sample may be weighed. Figure V in sketch 07-01 presents the situation.

8) When the flipper is rotated 180 degrees counterclockwise the sample flows from the scaling container into the heating container and the funnel is emptied into the dumping channel, as in figures VI and I.

2. Analysis

Table II.C.1 System Characteristics for Proposal II.

Linear Pairs	2
Resolute Pairs	8
Screw Pairs	2
Gear Pairs	2
Sliding Surfaces	2
Stepper Motors	2
Electromagnets	1
Power	~2 W
Container Mass to be heated	0.43 g
Container Mass to be weighed	0.27 g
Height	~269 mm
Length	~159 mm
Width	~152 mm
Lift Unit Mass	200 g
Measuring Unit Mass (Aluminum)	220 g
2 Motors, Magnet and Bearings	600 g
Electronics Cards	300 g
Overall Mass	~1320 g

3. Problems

1) Inside the measuring unit are two pairs of sliding surfaces between which regolith grains may enter. Grains may cause rapid abrasion or mechanism jamming.

Solution 1: Use seals.

Consequence: Enlarged complexity and power requirement.

Solution 2: Make slider of softer material which allows grains to penetrate into it. (This technique is used in car engines, which, however, have oil lubrication.)

2) Gears inside the measuring unit may be damaged by regolith grains passed through sliding surfaces.

Solutions: Same as above.

3) Wires for the scale and electromagnet have to rotate 195 degrees.

Solution 1: Use long wires which are wound around the measuring unit.

Solution 2: Use slip rings.

Consequence: Enlarged complexity.

4) Passages for regolith flow are quite narrow: minimum diameter is four millimeters.

Solution 1: Make whole unit larger.

Solution 2: Use vibrator.

5) In case of linkage support structure jamming the linkage tends to extend which may be hazardous.

Solution 1: Use strong spring.

Consequence: Enlarged power requirement.

Solution 2: Use separate motors for linkage extension and linkage support rotation.

6) When pulling the container out of the heater, friction or jamming cause moment to the linkage support which leads to jamming of the system.

Solution 1: Use strong spring.

Solution 2: Use separate motors for linkage extension and linkage support rotation.

7) Electromagnet may disturb a scale made of steel.

Solution 1: Make scale of another material for example aluminum or beryllium copper.

4. Conclusions

This design is twice as heavy as Proposal I and the measuring unit is very complex in structure, although its function is simple. Presence of gear pairs adds one more unreliability issue to the system. In Viking Mars Landers two measuring units also had two pairs of sliding surfaces and the principle of functioning was very similar to this. However, instead of cylinders horizontal rotary disks were used. [22] Therefore

problems 1) and 2) with sliding surfaces should be solvable. Problem 3) is solved by right selection of wire and adequate wire support. Dry, sieved and fine lunar regolith shouldn't have any difficulties to flowing through holes of 4 mm diameter. The solution to problems 5) and 6) is either more controllability with some mass penalty or a risky use of a plain force. It is evident that the major problems with this design are the mass and complexity.

C. Installing the Flip Scoop on the Rover

Selected rover design will probably be a three-body, six wheeled 75 kg Marsokhod developed in Russia, or a 100 kg, six wheeled rocker-bogie type of rover from the Jet Propulsion Laboratory, USA. Navigation by dead reckoning is possible therefore a scooping procedure should disturb the rover movement as little as possible. Unintended changes in direction may cause severe miscalculations about the rover's location. For this reason the scoop should be installed on the rover's centerline between the wheels. The rover will be partly teleoperated and therefore requires at least one pair of TV-cameras. The TV-cameras are aligned forward and are used to guide the rover and examine surrounding environment. It would be very useful to see what the scooping instrument is doing and if the sampling procedure is successful. This may be done by using the same TV-cameras if the scoop is installed in front of the rover.

1. Sampling Procedure

When the rover arrives at an interesting sampling site, the surface is studied with the aid of a TV-picture and a safe sampling location is selected. At the sampling area the scoop is lowered to the surface and the rover is driven a few decimeters.

It now makes a difference whether the sample acquisition is carried out by a forward or backward rover motion. Forward scooping is illustrated in picture 2, where F_r is a traction force of the rover which is equal to soil cutting resistance F_c , and M is a moment of a scoop motor. In forward scooping, the motor moment M is kept constant, increased cutting resistance F_c causes the scoop to turn against the surface and penetrate

deeper into ground, which again increases the cutting resistance. There is a kind of mechanical positive feedback from cutting resistance to sampling depth. For backward scooping, illustrated in Figure II.C.3, an increased cutting resistance causes the scoop to arise on the surface, which decreases the cutting resistance and the system is stable and the scoop may easily and safely be kept at a desired depth. For these reasons the backward scooping is preferred.

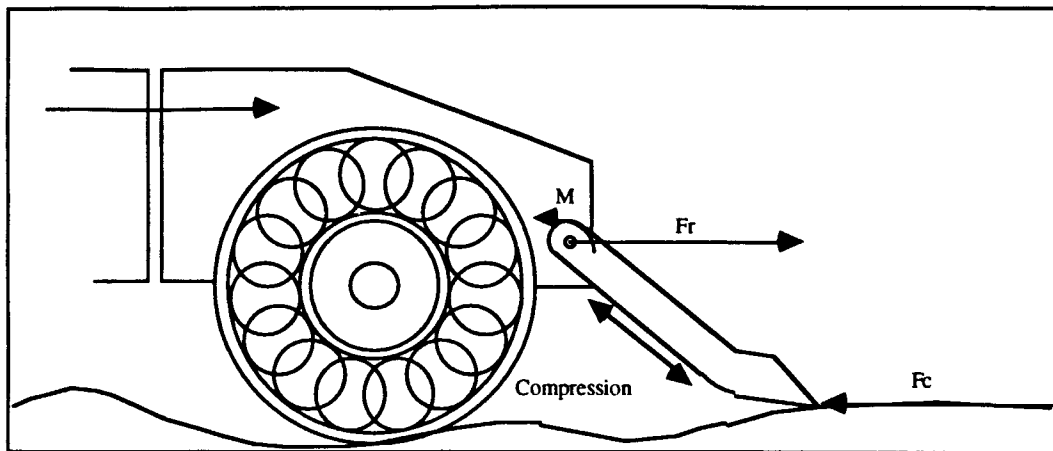


Figure II.C.2 Forward Scooping.

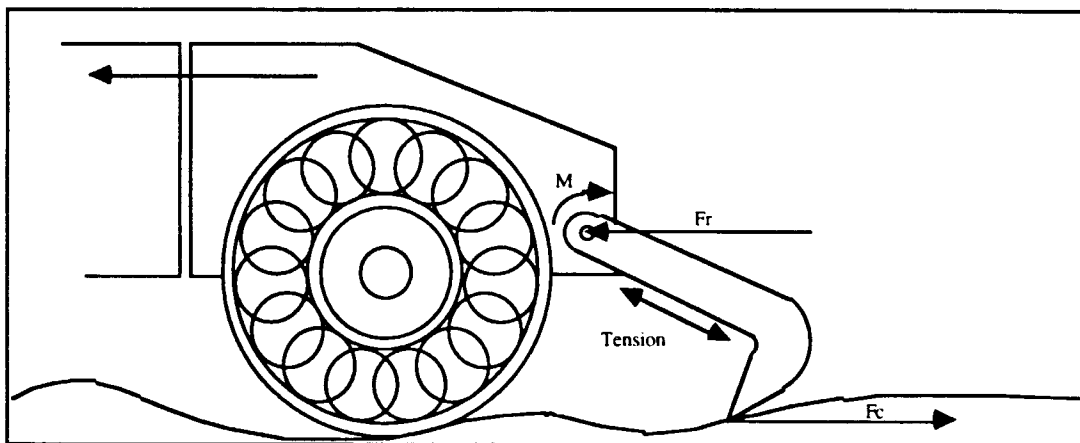


Figure II.C.3 Backward Scooping.

To protect the scoop, the rover's traction force may be limited to powering only the front wheels instead of all six wheels when scooping. In addition to that there may

be electromagnetically controlled slip clutches which set a limit for the maximum moment on the wheels.

D. A Preliminary Design of the Flip Scoop

Figure II.C.4 below illustrates approximate sampling system dimensions and arrangement. More accurate drawings are enclosed in appendix D.

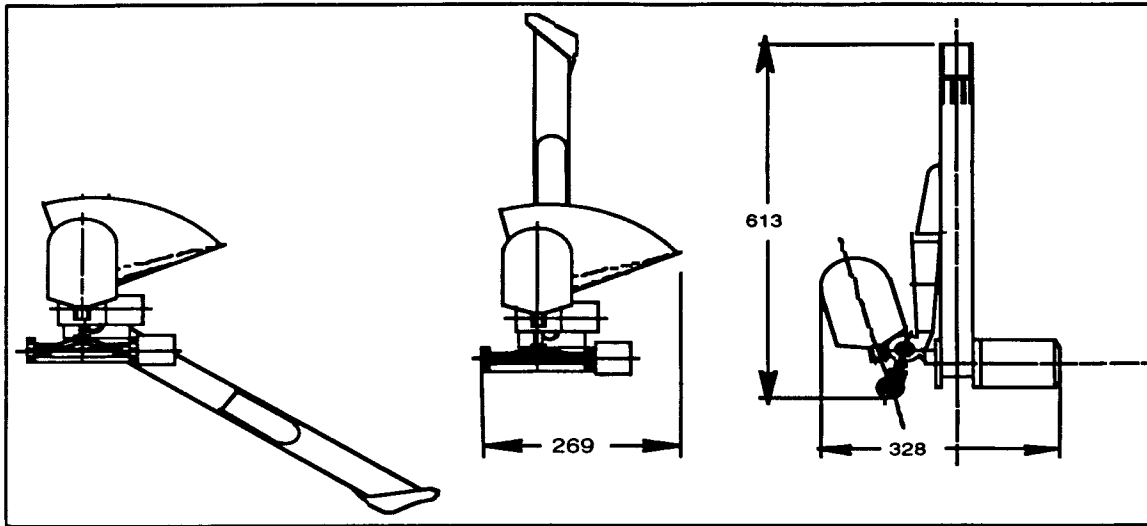


Figure II.C.4 Sampling System Arrangement.

1. Function

When the scoop is lowered to the surface and pulled, it acts like a cheese slicer. The base of the scoop prevents penetration that is too deep as the cutting blade lifts a thin layer of soil into the scoop. Small fins (part number (6) in sketch 13-01) protect the blade from rocks greater than 10 mm in diameter. A lid (number (7)) allows the soil flow in, but not out when the scoop is lifted off the surface. The moment needed to keep the scoop in a constant depth is approximately 1.4 Nm. Estimation was done using 3.4 N cutting resistance, which was calculated for the Drag Line sample acquisition concept, and assuming a 60 cm long arm to be at a 45 degree angle causing axis to be located 42 cm above surface.

When the scoop is lifted the sample goes inside the scoop arm and falls through an opening (number (3) in sketch 12-01) inside of the arm into a sectorial funnel (number (1)). A pair of sieves are installed inside the funnel and the sieved sample is received by the measuring unit just below the funnel.

2. Scoop Arm Control

The force with which the scoop is pressed against the surface may be adjusted by a closed loop controlled servo motor or it may be kept approximately constant by a pre stressed spring. The scooping system requires some flexibility for safe sample collecting on rough lunar surface. The required flexibility may be achieved in three different ways:

1) Adding compliance in the arm.

Scoop is lowered on the surface and is kept there by a stressed spring. When the spring is stressed by the motor it may be locked by a brake or a self-holding gearing and the spring allows the scoop to yield along surface without damaging the motor or structure.

2) Use of active force control.

Here the forces acting on the arm are measured with strain gauges and information is used to control motor moment. When lowering or lifting the arm the force control loop is replaced by a position control loop.

3) Use of a soft closed loop position control.

A soft response to disturbances on the scoop requires low gain and doesn't allow use of an integrator. The scooping moment is generated by commanding the scoop to penetrate deeper into the surface than it in reality can and therefore the controller adds some moment to the arm continuously. An integrator is forbidden because it makes the force increase in time, which is not what we want. However, the controller works like a spring causing the scooping force to increase or decrease as the distance from the surface decreases or increases. For lifting the scoop, a more accurate controller with greater gain and integrator may be needed.

In each case the use of a DC servo motor is possible either for position or force control. A stepper motor may be used to position the arm and to extend or compress a spring and in that way adjust the force in an open loop manner.

A detailed study on a scoop/surface interaction and a dynamic behavior of the arm is presented in appendix D. To estimate the mass and power requirement of different systems, some typical motor and gearhead examples from vendors' brochures are discussed, and the result is, that no significant profit may be achieved by using a closed loop force or position control.

3. Analysis

Table II.C.2 System Characteristics for the Flip Scoop.

Resolute Pairs	1
Stepper Motors	1
Power (Stepper motor)	2.5 W
Height	~600mm
Length	~240 mm
Width	~200 mm
Scoop + Funnel Mass	~300 g
Motor and Bearings	~400 g
Gearhead	~215 g
Electronics Cards	~200 g
Overall Mass	~1115 g

4. Conclusions

Use of a stepper for positioning the scoop and a spring to provide needed scooping force appears to be the simplest and the least power consuming solution. Another consideration is that control of the stepper is easy. There should be strain gauges attached to arm. Measuring the elongation of the arm provides information of moments acting on it, and if the moment appears to be too small, (or too large), the stepper is commanded to increase, (or decrease), the spring tension. The lifting action occurs simply by rotating the stepper until the desired position is achieved.

Although the mass of the scoop is almost twice the mass used when selecting the sampling concepts in previous study, the result of the selection remains unchanged since the next best solution weighs 4 kilograms.

E. Summary

Table II.C.3 presents estimated mass and dimensions for the entire sampling system utilizing Sample Manipulating Arrangement; Proposal II and the Flip Scoop presented above. The mass for the interface is adapted from the Surveyor surface sampler instrument substructure and mounting hardware. [26]

Table II.C.3 Sampling System Characteristics.

Height	613mm
Length	269 mm
Width	328 mm
Power	2.5 W
Scoop Mass	1115 g
Lift Unit and Measuring Unit Mass	1320 g
Interface (Aluminum)	~1000 g
Overall Mass	~3435 g
Marginal 20%	687 g
Total	4122 g

1. Reducing the Mass

The system includes three stepper motors: the scoop motor, the lift unit motor and the measuring unit motor, each weighing about 250-300 g with gearhead. These motors were designed for on-earth use and are very well shielded against dust and water. Some mass reduction might be possible by reducing the shields, but it should be emphasized, that we are dealing with fine grained lunar sand and shielding against dust is very important. On the other hand, heat transmission by conduction must be

increased because convection is absent on the moon. Therefore, it is impractical to rely on reduced motor mass.

Combining the functions of two motors into one by a gearing or clutch may save about 200 grams with a penalty of increased number of moving parts and complexity. One opportunity is to connect all functions to the scoop arm motor by a chain or a toothed belt. This means that all systems rotate at the same time requiring more moment and causing shorter lifetime. For the proper sequencing of functions, two relay operated lids control the time of regolith flow into and out of the measuring unit. In this way the overall mass may be reduced by 400-500 grams with the penalty of two relay operated lids, two chains or belts and a bit larger motor. If the speed of these functions is kept slow, the inertias of the scoop and other systems shouldn't cause any trouble and no clutches for power transmission are not needed. Optimization of the scoop structure saved an additional 50-100 grams.

III. MISSION AND SYSTEMS DESIGN

A. Mission Study Overview:

The flowchart of Figure III.1 shows how various components of the mission system design process are interrelated. Top level mission requirements “flowdown” or impose requirements on each of the major subsystems: science instrumentation, rover, lander, and launch vehicle. In addition, each of the subsystems impose constraints on each other due to their interrelationships.

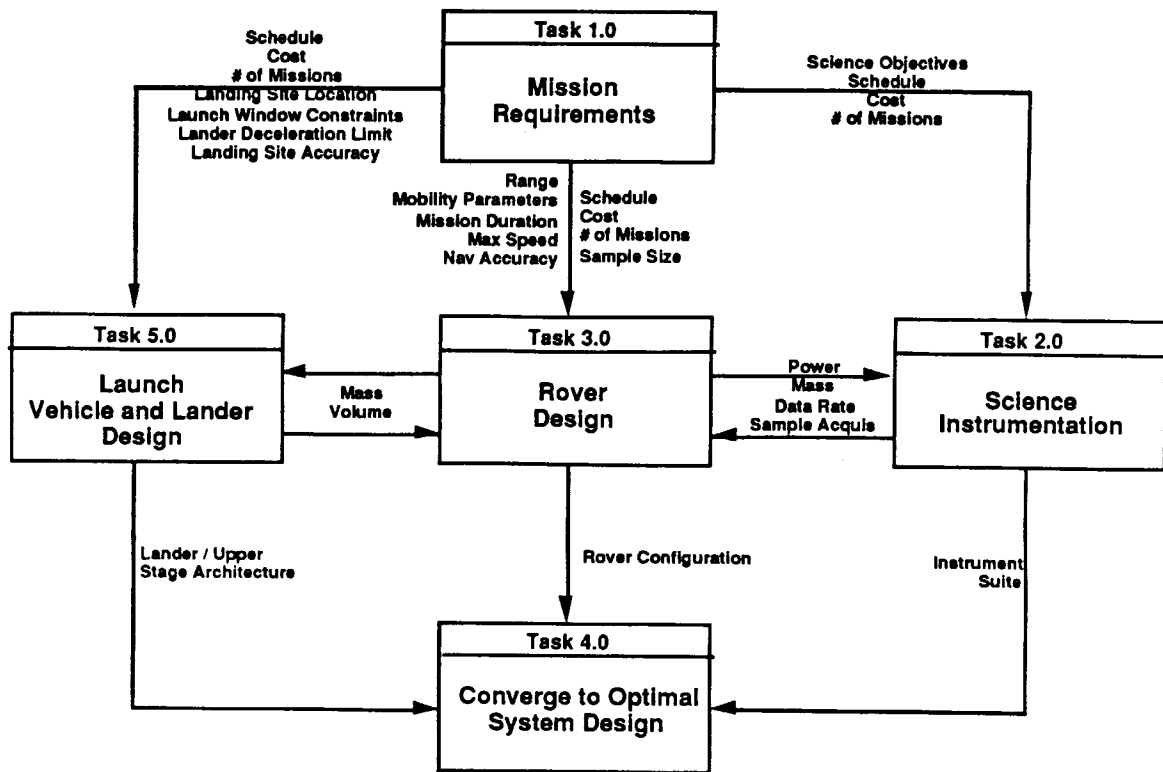


Figure III.1 Mission Study Overview

The mission study progressed in two different directions. First, a strawman list of science objectives was compiled including volatile gas analysis, regolith properties, chemical composition, mineralogy, and soil maturity. Instrumentation requirements were then developed in terms of mass and power. These requirements were then imposed on the rover (Figure III.1). Rover design proceeded with these requirements and those derived from desired mission requirements (range, speed, mobility, etc.). The resulting rover design was then input to the lander design process. Finally, the science package, rover, and lander designs were input to the launch vehicle and upper stage design process. The resulting mission package was too large to fit on any of the launch vehicles currently in production.

The next step in the study was to propagate requirements in the opposite direction: from the launch vehicle to the lander to the rover to science instrumentation

(Figure III.1). This was done for each of the current United States launch vehicles in production from the medium class and larger (Delta, Atlas, Titan) considering different possibilities for native upper stages, strap-on solid rocket motors, and three different staging architectures for the lander. The result was a trade study/optimization performed at the rover level for rover mass, rover power, rover range, science instrumentation mass, science instrumentation power, and total mission life cycle cost. Two solutions emerged one being based on the Delta launch vehicle and the other based on the Atlas launch vehicle.

The following sections discuss the issues related to mission objectives, requirements, science instrumentation, rover, lander, and launch vehicle design. Primary design parameters which were discriminators in converging to the baseline design are given. Two design solutions, one primary, and another secondary, are given in the recommendations section.

B. Ground Rules

One important ground rule adopted was that this study involved only one lunar mission. This assumption is very important because it affects how advantageous new design and development is with respect to total mission life cycle cost. This is due to the fact that Research Development Test and Evaluation (RDT & E) costs (nonrecurring costs) are historically 2 - 3 times the unit (hardware) costs [ref. 40 pg. 678]. Consequently, if development costs cannot be amortized over several missions, minimizing RDT & E usually results in lower total mission life cycle cost. Various life cycle cost components are discussed in more detail in Section III.F.

The second ground rule was to baseline flight qualified hardware, if available, or use an existing design which has already been studied and / or tested in preference to proposing new design. This usually results in sub-optimal design with respect to mass and power utilization because the original design was optimized to a different set of

requirements. However, as discussed above, this approach generally minimizes total life cycle cost especially for a single flight mission.

The third ground rule was that all mission requirements were subject to trade until the resulting mission design was “acceptable” in terms of technical objectives, schedule, and cost. The basic objective function applied was: maximize science data necessary to make long lead lunar resource utilization decisions subject to the constraint of fitting the entire single mission on a medium class launch vehicle (Delta or Atlas). The end result was to provide an incremental investment path to obtain the science data of highest priority.

C. Mission Objectives and Requirements:

The ground rules given in the previous section are mission design constraints which are not subject to trade. This section defines two mission objectives which are qualitative statements describing the mission goals. They also are not subject to trade. This section then defines the preliminary mission requirements which quantify how well we wish to achieve the mission objectives subject to the ground rules. All mission requirements are subject to trade throughout the design process.

A primary mission objective, as discussed in Section I, is to measure insitu volatile gas concentrations embedded in the lunar regolith. Insitu measurements are necessary because the lunar environmental conditions of high vacuum and extreme dryness is difficult to maintain throughout the entire process of sample acquisition, transport, handling, storage, and terrestrial laboratory analysis. For example, the Apollo 12 documented sample box leaked during the return to Houston. When tested at the Lunar Receiving Laboratory (LRL), the internal pressure was a significant fraction of atmospheric pressure and the ratios of nitrogen, oxygen, and argon approximated those in Earth’s atmosphere [ref. 36 pg. 26]. Insitu volatile gas concentration measurements will improve the available lunar data base so long term lunar resource utilization decisions can be made.

Another objective is to establish spatial distribution of volatile gas concentrations for a representative area of the lunar surface. Volatile gases resource maps can then be made for similar areas and the technical / economic feasibility of candidate mining processes can be evaluated. Digital multispectral 2 km resolution images of selected lunar surface regions were obtained with Earth-based telescopes in a 150 km field of view (e.g. McCord et al., 1976, 1979, Johnson et al., 1977). Images collected at 0.38 mm (negative) and 0.62 mm (positive) are sensitive to the Ti abundance of lunar mare soils and are particularly useful for identifying and mapping the spatial distribution of different basaltic surface units having different Ti contents [ref. 36 pg. 601]. He-3, a constituent of regolith volatiles, is a candidate fuel for earth based nuclear fusion and has been empirically associated with TiO₂. Validation of this relationship with spatial insitu measurements would allow extrapolation of existing Ti maps to estimate global lunar He-3 resources. Global lunar knowledge of He-3 resources in turn would provide the information necessary to make long lead fusion reactor design and development decisions.

Making spatial distribution measurements of volatile gas concentrations will require an automated roving vehicle. Vehicle range is key requirement and a design driver for most subsystems due to its close relationship with mission duration, average speed, and power consumption. To correlate ground measurements to remote sensing measurements rover range needs to be greater than the 2 km resolution of these images. Vehicle range which is a significant fraction of the image 150 km field of view would be most useful for these “ground truth” measurements. As a point of comparison astronauts made traverses up to 8 km in radius from the landing site with the Lunar Roving Vehicle (LRV) during the later Apollo J-class missions. Apollo 17 total distance traveled was 35 km. Similarly, the Soviet Lunokhod 1 automated vehicle traveled a total distance of 10 km while exploring a 1.5 km x 0.5 km area. Lunokhod 2 traveled a total distance of 37 km.

Measuring volatile gas concentration as a function of regolith depth was found to significantly increase mass and power requirements of the sampling system as well as significantly reduce vehicle range. Taking core samples takes much longer than surface samples so more time and power resources are spent digging rather than roving. In addition, returned Apollo cores indicated the existence of a “reworked zone” at or near the surface where meteor impacts are small and frequent. The resulting mixing and turnover of this zone occurs often enough to expose most of the soil particles to the near-surface environment for time periods long enough to saturate it with solar-wind volatiles [ref. 36 pg. 337]. Therefore, measuring volatile gas concentration vs. regolith depth was not made a mission requirement. If the technical and economic feasibility of lunar volatiles resource utilization is indicated from this initial mission then depth measurements will be required later to provide design data for mining equipment.

Returning a volatile gas sample to Earth was initially considered but rejected because it significantly increased mission cost with marginal contribution to the primary mission objective. Returning 100 grams of volatile gases would require excavation, beneficiation, and heating of approximately 900 kg of regolith followed by collection, compression and storage of the gases. Estimates for vehicle sub-systems to provide this processing capability were approximately 1,000 kg with about an additional 350 kg necessary for a single earth return ascent stage. Since these initial mass estimates were well beyond the capability of the target launch vehicles even for a fixed lander architecture consideration of sample return was discontinued.

Any vehicle with round wheels will perform satisfactorily on the lunar surface, provided the ground contact pressure is no greater than about 7-10 kPa [ref. 36 pg. 522]. However, there is an almost infinite combination of wheel sizes, geometry, numbers, and configurations that can have the same contact area but different performance characteristics. Obstacle step height capability of a rover is related to the number of wheels. However, fewer, larger wheels tend to be mechanically simpler,

weigh less, and are generally easier to package on a lander and launch vehicle fairing. The LRV was not permitted to have six wheels due to Lunar Module packaging restrictions. Addition of frame articulation allows the vehicle wheels follow irregular ground contour and improves obstacle crossing capability. Bekker states [ref. 42] that frame articulation adds more obstacle mobility to a vehicle than any other structural feature. However, articulation adds complexity, mass, and joints that must be protected from lunar dust.

Geometry of the terrain surface and the physics of the soils affect design requirements of the rover mobility system. The baseline landing site is Mare Tranquillitatis (9° N 20° E \pm 10 km) due to predicted high Ti content ($\sim 10\%$) from multispectral image maps (see Section I.B.6). Since this site is located within a mare basin it is expected that the terrain surface will be similar or less rough than the three Apollo LRV sites because they were located either in the Lunar Highlands (Apollo 16) or on the Highlands-Mare Boundaries (Apollo 15 & 17). Likewise, it is expected that the soil physics of this site will be similar to the Apollo LRV sites. An analysis by Costes concludes that at least for the Apollo 14 through 17 and Luna 17 landing sites, the surficial lunar soil appears to have similar mechanical properties regardless of initial origin, geologic history, gross chemical composition, or local environmental condition. These findings, which agree with the results of astronaut footprint analysis, are also corroborated by calculations on the LRV energy consumption at the Apollo 15, 16, and 17 sites [ref. 43 pg. 8-17]. Therefore, it is expected that a vehicle design with mobility parameters similar to the Apollo LRV will meet or exceed requirements the volatile gas resource experiment.

Smaller hummocky craters will be the primary obstacles for the volatiles rover. During LRV evaluation Apollo 15 astronauts noted the terrain conditions in general were very hummocky having a smooth surface and only small areas of fragmental debris. Approximately 90% of the craters encountered had smooth subdued rims which were, in

general, level with the surrounding surface. Fragmental debris was clearly visible and easy to avoid on the surface. The major problem encountered was recognizing the subtle subdued crater directly in the path due to the lack of topographic definition as the vehicle passed over the hummocky terrain. In general, 1 meter craters were not detectable until within 2 to 3 meters of the front wheels. Avoidance of these craters seemed necessary to prevent controllability loss and bottoming of the suspension system and caused the most problems in negotiating the traverse [ref. 39].

The LRV had four flexible wheels (82 cm diameter and 23 cm wide) fabricated from 0.033 inch diameter piano wire mesh with chevron shaped titanium treads covering 50% of the contact area. Shocks are absorbed by the wire mesh wheels and a pair of parallel triangular suspension arms at each wheel. Other features included independent four wheel drive and double Ackerman steering (front and rear independent steering). Vehicle mass was 218 kg empty and 708 kg fully loaded.

A summary of the mission objective and requirements is shown in Table III.1. Individual sections discuss their impact at the subsystem level.

Table III.1 Summary of Mission Objectives and Requirements

Primary Mission Objective:	Measure insitu spatial distributions of volatile gas concentrations embedded in the lunar regolith to evaluate technical and economic feasibility of candidate mining processes
Number of Missions	One
Sample size	1 gram
Sample Depth	0 - 5 cm
Rover Range	20 to 150 km; longer ranges would be beneficial
Rover Terrain and Soil	Lunar Mare
Wheel Contact Pressure	Less than 7 to 10 kPa
Cost	Delta or Atlas Class Mission
Schedule	1998 launch

D. Rover Design

1. Overview:

Of all the mission components the rover design is the least technically mature. The United States has yet to operate a mobile robotic vehicle on a planetary surface. The Soviet Union operated two vehicles in the early 1970's but speed and range were limited. Lunokhod 1 took over 10 months to travel 10 km (ave. speed for daylight operations = 3 meter / hour). Lunokhod 2 moved faster traveling 37 km in 4 months but according to an Eagle Engineering study may have rolled over as it crossed the lip of a crater [ref. 40 pg. 54].

As stated in the ground rules, the purpose of this mission study was not to propose new design but choose from existing designs which most closely meet our mission requirements. However, since rover technology is relatively immature, existing design means either conceptual design, analytical studies, or hardware testbeds. This covers a wide range of vehicle concepts because specific requirements for various planetary exploration programs have yet to be agreed upon. Missions proposed in recent literature include science, exploration, landing site certification, human transportation, materials transportation, construction, and mining either for the Moon, Mars, or both. Therefore, the resulting vehicle concepts have ranged from 1 kg micro-rovers to multi-metric ton planetary mobile habitats.

Initial sizing of the volatiles mission rover needed to consider launch vehicle capabilities, lander mass, science instrumentation mass, and power requirements because the science instrumentation is payload to the rover, the rover is payload to the lander; and the lander is a payload to the launch vehicle. Current United States launch vehicle capabilities for dry soft landed payload estimates (rover mass) ranged from: 78 - 109 kg (Delta II 7925), 196 - 269 kg (Atlas II), 222 - 298 kg (Atlas IIA), 389 - 472 kg (Atlas IIAS),

621 - 756 kg (Titan III / PAM-DII), and 996 - 1156 kg (Titan IV / Centaur) depending on lander staging architecture. Please refer to the next section for launch vehicle and lander estimate details and assumptions.

Figure III.2 was developed to trade rover mass, rover power, and science instrumentation mass. Moving upward along a vertical line in Figure III.2 trades reduced rover power for increased science instrumentation mass while holding total rover mass constant. Moving along a horizontal line to the right trades increased rover mass for increased rover power while holding science instrumentation mass constant. Moving upward along the 55° constant power line trades increased rover mass for increased science instrumentation mass while holding rover power constant.

The “average” rover of Figure III.2 has the subsystem mass distribution of Table III.2. This distribution was obtained from curve fits of several Jet Propulsion Laboratory (JPL) rover designs of masses 100, 290, 600, and 842 kg [ref. 41]. If a point is located on Figure III.2 by rover mass and science instrument mass coordinates; and if a point falls above the “average” rover line, then the rover point design has a higher payload mass fraction relative to the “average” rover. In addition if the actual rover power at this same point is less than the indicated power then the rover design also has either a lower specific power density than “average” or a higher “other” “average” subsystem mass fraction. All other subsystems include communication, thermal, manipulation, computation, control, chassis and structure. If lumped together these “other” subsystems have an “average” mass fraction of 0.72.

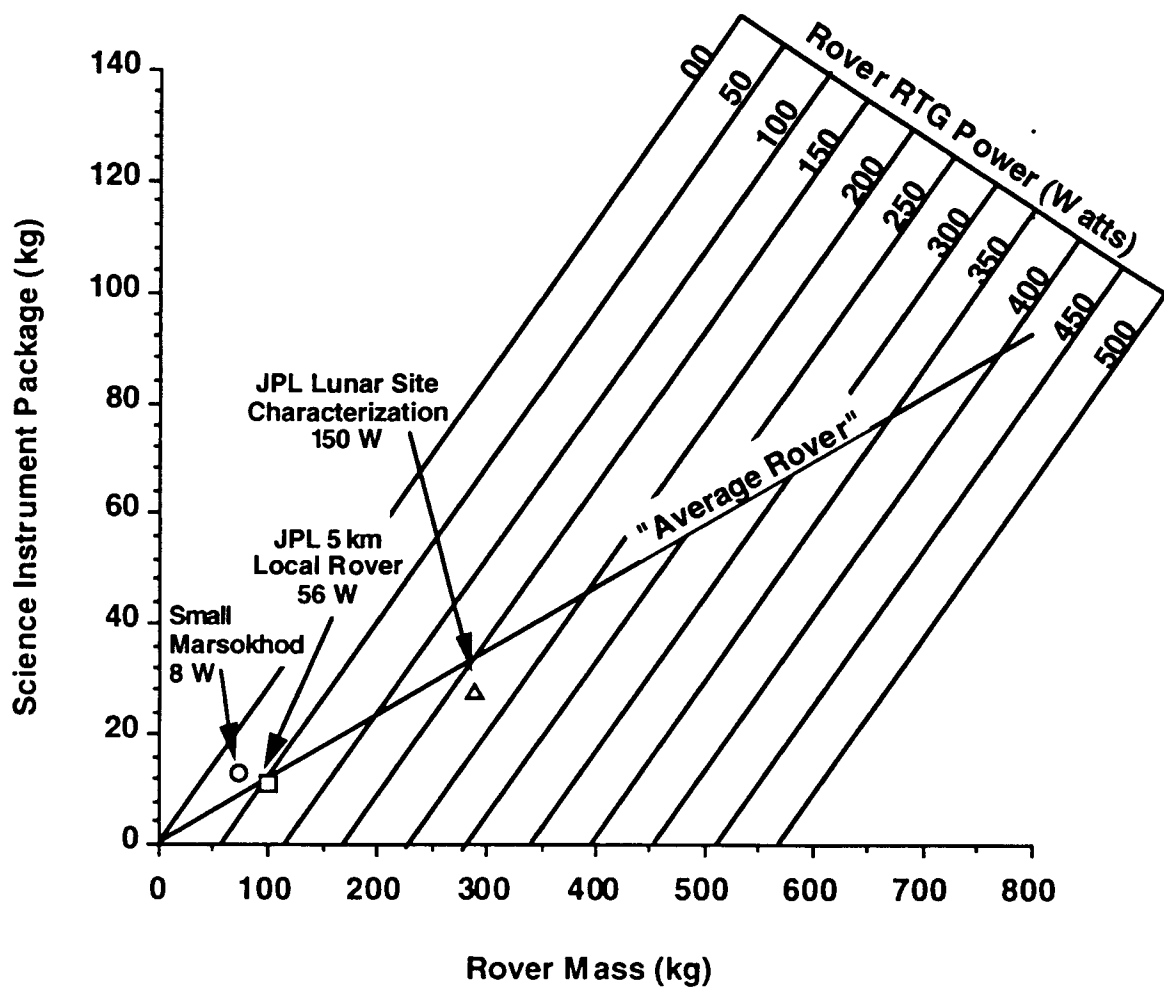


Figure III.2 Instrument Mass vs. Vehicle Power vs. Vehicle Mass

Table III.2 "Average" Rover Subsystem Mass Fractions

Power	0.16
Communications	0.05
Thermal	0.03
Manipulation	0.10
Computation	0.08
Control	0.14
Structure & Chassis	0.32
Science	0.12

The JPL reference designs utilized to derive Figure III.2 assumes a Radioisotope Thermoelectric Generator (RTG) provides rover power. Two crucial RTG advantages in the lunar rover application are lunar night thermal control capability and compactness. During the two earth week duration lunar night waste RTG heat can be used for thermal control rather than auxiliary electric heaters. According to Pivrotto, on the Moon a purely solar/battery system is infeasible. Either the rover must be allowed to freeze (as was Surveyor) and recover when the sun warms its batteries, or Radioisotope Heater Units (RHUs) must be provided [ref. 42 pg. 27]. Body mounted arrays require relatively large unobscured mounting areas. Articulated solar array booms on a moving vehicle present a substantially more difficult dynamic environment than current spacecraft applications. Although the Soviet Lunokhod utilized solar arrays to generate electric power during the daylight a separate RTG was utilized for nocturnal thermal control.

Power subsystem mass was calculated assuming state of the art RTGs qualified for the Galileo and Ulysses missions (General Purpose Heat Source or GPHS). Values utilized were: specific power of 5 W / kg, power conditioning / control components specific power of 12 W / kg, [ref. 43 pg. 261] and a power management battery of 30 W-hr / kg. Assumed Rover battery capacity was the RTG power in Watts times one hour. Therefore, peak power could be provided at twice the RTG rating for 24 minutes

assuming fully charged batteries and allowable battery Depth of Discharge (DOD) of 40%.

Using Figure III.2 the estimated current United States launch vehicle capability for an “average” rover science instrumentation payload is: 9 - 13 kg (Delta II 7925), 24 - 32 kg (Atlas II), 27 - 36 kg (Atlas IIA), 47 - 57 kg (Atlas IIAS), 75 - 91 kg (Titan III / PAM-DII), and 120 - 139 kg (Titan IV / Centaur) depending on lander staging architecture. These estimates are subject to the above stated assumptions and the linear scaling of the point designs limits their validity to Rough Order of Magnitude (ROM). Nevertheless, they provided a quantitative basis to trade science instrumentation and a focal point from which to pursue more detailed design.

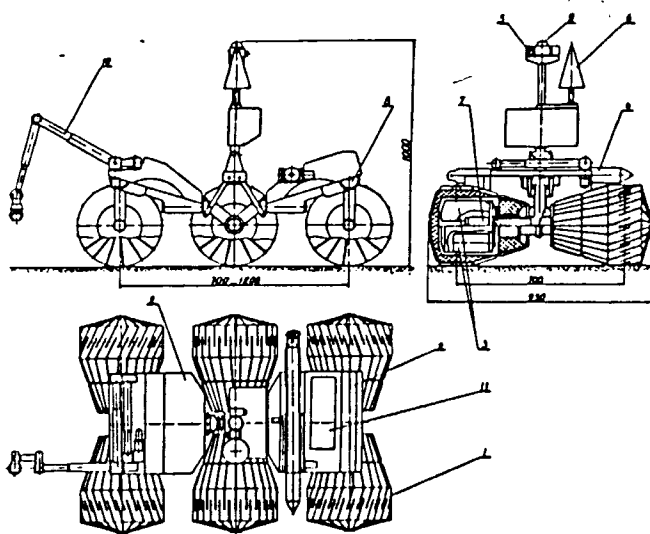
Two rover designs emerged as primary candidates for the volatiles mission: The 75 kg Small Marsokhod with 100 km range for a Delta class mission; and the JPL 290 kg Lunar Site Characterization rover with range up to 1,000 km for an Atlas class mission. Each rover is discussed individually in following sub-sections.

2. Small Marsokhod 75 kg Rover

The Small Marsokhod Rover (SMR) was developed by the Mobile Vehicle Engineering Institute (VNIITransmash) in St. Petersburg, Russia. It was the most technically mature rover chassis /undercarriage design found in the literature for a lunar Delta II class mission. Mockup tests on Mars-like volcanic terrain in the Kamchatka peninsula, Russia occurred in August 1991. In May 1992 the Russian team was hosted by the Planetary Society for tests at Dumont Dunes and Mars Hill in the Mojave Desert, California, USA. Most recently, Marokhod demonstrated a variety of capabilities at JPL, NASA Ames, McDonnell Douglas Aerospace (MDA), and Stanford University in January 1993. Figure III.3 details key SMR dimensions and subsystem mass fractions.

A principal advantage of the SMR is high mobility in heterogeneous terrain. The above mentioned testing has verified mobility performance in different terrain's including combinations of slopes, cracks, rocks, and granular sandy soil. Design

characteristics key to this mobility performance include six hollow cone-shaped titanium wheels, each with its own drive motor, and independent articulation of a three segment chassis capable of rotational motion about both the roll and pitch axis as well as translational motion of front and rear frame segments. Moving these various joints in different combinations enable SMR to develop different propulsive forces appropriate for changing terrain conditions. For example, to cross a crack, the mutual frame sections are clamped after the translational joint actuates to increase wheel base to the 1200 mm maximum. Similarly, during transit to the moon, the translational joint is fully retracted to 700 mm for minimal packaging volume. A “wheeled-walking” motion is used to ascend a 30° - 35° granular incline. To create this motion, which resembles that of an inchworm, the wheels are simultaneously rotated



Subsystem Masses (kg)	
Chassis	31.0
Radio System & Antenna	2.5
RTG & Battery	10.0
Science Instruments & Sampling	15.0
System Electronics	2.0
Sun Sensor, Vertical	1.0
Cables	2.5
Secondary P.S.	1.0
DPU + Mem	2.0
Structure, Term. Contr	8.0
	75.0

Figure III.3 SMR Dimensions and Subsystem Mass Fraction

forward while the frame translation joints are alternately expanded and contracted. To follow uneven terrain contour simultaneous frame pitch and roll articulation enable SMR to overcome boulders twice as high as the wheel diameter. A summary of SMR technical data from several reference sources is given in Table III.3.

Table III.3 Small Marokhod Data [ref. 44, 45, 46, 47,]

Number of Wheels	6
Wheel Diameter	350 mm
Track	700 mm
Wheel Base	Variable 700 - 1200 mm
Serviceability	100 km
Speed of Motion (max.)	0.5 km / hour
Mobility Duty Cycle	1 hour / day
Power System	8 Watt RTG w/ Batt
Mobility Power Consumption (flat area Mars conditions)	25 - 40 W-hr / km
Maximum Obstacles to Overcome	
slope with granular ground	20°
wheel mode	30° - 35°
wheel-walking mode	
Individual stones	0.75 m
Bench	0.75 m

A principal disadvantage of the SMR is increased design complexity associated with a multi-degree of freedom articulated chassis and the resulting higher chassis mass fraction (0.41). Particles smaller than 50 microns constitute 45% of the regolith and contain nearly 90% of the volatile gases. Therefore, high mobility performance is not required because volatiles concentration measurements can be constrained to the relatively flat areas of the lunar mare. Orbital photographs indicate that approximately 22% of the total area of Mare Tranquillitatis on the Julius Ceasar and Taruntius Quadrangles are occupied by major features (domes, ridges, craters, rilles, basement rocks, ray materials and miscellaneous non-mare features). An analysis by Bekker, [ref. 37, pg. 266] showed that a vehicle 3 m wide would encounter difficulties finding a

bypass when crater distribution covered approximately 40% of the total area. Therefore, it is not necessary to analyze Nose In Failure (NIF), Hang Up Failure (HUF), and vehicle performance to determine whether a vehicle could clear the obstacles.

SMR meets or exceeds the lunar volatiles gas concentration measurement experiment requirements. Science instrument mass capability is less than required but the shortfall is within estimation error. Since RTG power is 8 watts, and mobility power consumption is 30 - 40 W - hr / km, rover velocities approaching 0.20 - 0.26 km /hr require battery power assist. SMR would utilize 400 terrestrial days roving 100 km assuming day only operations and a 4.2% locomotion duty cycle at 0.5 km / hr [ref. 47]. Mission time would be reduced or range increased if Earth-light is sufficient for local navigation during the Lunar night.

3. Lunar Site Characterization 290 kg Rover:

The Lunar Site Characterization Rover (LSCR) is a conceptual design developed by JPL for characterizing potential human landing sites on the Moon for their safety, “buildability”, and possible resources [ref. 42]. Although site characterization is a different mission than measuring volatile gas concentrations, the rover requirements are similar in terms of total rover mass, science instrumentation mass, range and mobility. LSCR is essentially a “paper design” but the basic mobility concept has been tested in similar but smaller JPL prototypes Rockey 3 (15 kg total mass) and Rockey 4 (6.8 kg total mass).

Figure III.4 shows the LSCR configuration which is a JPL design known as Rocker Bogie featuring six wheels with a pitch axis frame joint. Obstacle clearance capability of 0.5 m is provided for a chassis mass fraction of 0.34. Figure III.4 shows the 4 RTGs mounted vertically on the aft structure. This orientation prevents dust from settling on the RTGs and provides a good angle for heat rejection. Table III.4. summarizes key characteristics of the rover subsystems: power, communication, system control, vehicle control, computation, and navigation.

Subsystem Masses (kg)		
Power	4 Galileo class RTGs for 150 W total	46.0
Communications	S-band Earth direct at 2 mbps	17.0
Thermal	Passive & Active from RTG heat	6.0
Manipulation	Pile Driver Device & Sounding Antennas	24.0
Computation	General Purpose Computer	20.0
Control	Electronics, Sensors, Cameras	49.0
Structure	Chassis, Body, Motors, and Wheels	100.0
Science	Resource and Seismic Analysis	28.0
		290.0

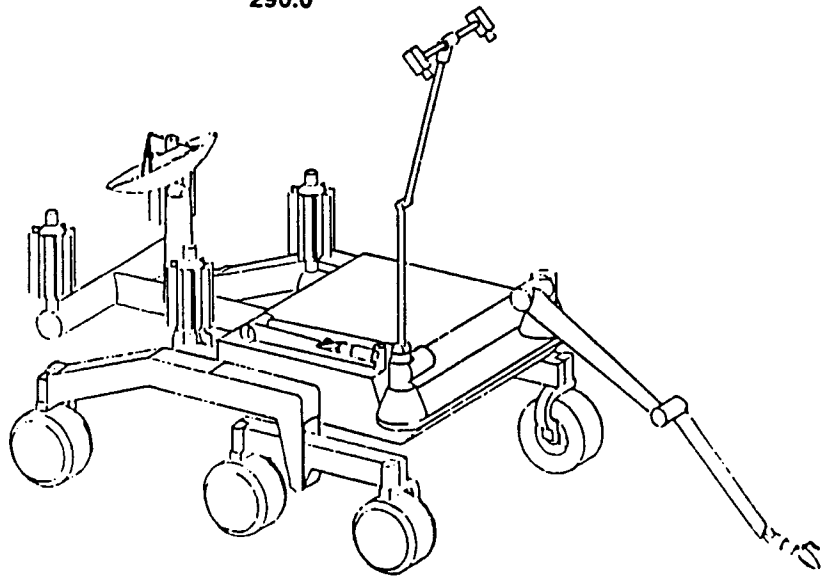


Figure III.4 LSCR Configuration

A major advantage of the LSCR rover concept is increased range due to sizing of the power system. The Galileo class RTGs provide enough power with respect to total mass for continuous roving at 0.36 km / hr (10 cm /sec). Moving continuously at this speed the rover could conceivably cover 120 km / Lunar day in a wide ranging volatile gas resource survey spanning the entire width of Mare Tranquillitatis within 8 lunar days assuming day only operation. Range would be further increased if Earth-light is sufficient for local navigation during the Lunar night.

Actual range would be dependent on how often and how long the rover need to stop for ground decision making processes. During the initial two or three lunar days the mobility duty cycle would be lower because driving experience would need to be gained at slower speeds, more detailed imaging surveys would be made, and samples would be taken closer together with higher positional accuracy. Assuming daylight operations only and 25% mobility duty cycle 90 km would be covered in the first three Lunar days. It is possible that the rover could be kept moving continuously during the second mission phase because, except for sample acquisition, the resource survey would emphasize existence and concentration of volatile gases over an extended area rather than their exact location (up to 1,200 km total for a one year mission). Measuring insitu volatile gas concentration near Apollo 11 sampling locations approximately 300 km away from the proposed landing site would be possible. This could provide "insitu ground truth" for the rest of the Apollo site samples with respect to volatile gas concentrations.

The LSCR science payload is more than required for the volatiles mission. This excess could be used either for margin or additional experiment instrumentation. The recommendations section discusses the possibility of scaling the rover down slightly to optimally fit the Atlas II launch vehicle.

Table III.4 LSCR Subsystem Characteristics [ref. 42]

Mission Duration:	Up to one year
Range:	Up to 1,200 km
Configuration:	Rocker Bogie 0.5 meter obstacle clearance Max. Speed 0.36 km / hour (10 cm / sec) Daylight operations with night operation if Earth-light is sufficient for local navigation
Power:	4 Galileo class RTGs for total 150 Watts w/ capacitor bank for power management
Communication:	S-band rover direct to Earth at 2 mbps to a 34 meter Deep Space Network antenna via a hemi-directional antenna on the rover (assumes Lunar Nearside)
System Control:	Teleoperated, incremental movement of rover with standard types of onboard spacecraft fault detection. Commands direct from Earth (no communication relay)
Vehicle Control:	Provides steering, proximity sensors for obstacles ("curb feelers") pointing, and directional sensing
Computation:	Requirements assumed to be similar to Comet Rendezvous Asteroid Flyby (CRAF) computer. Digital tape recording not used
Navigation:	Six rover navigation cameras mounted on a tilt-pan platform. Navigation conducted from ground control stations which receive near-continuous video downlink of the area in front of the rover. Operators command vehicle by indicating a path in appropriate directions around obstacles they observe in transmitted images utilizing a video screen cursor. Vehicle has preset engineering limits which are enforced in real time by acceleration and tilt angle measurements
Thermal Control:	Active, heat transferred from RTGs during Lunar night

E. Transportation: Lander and Launch Vehicles:

As shown in Figure III.1 the transportation system design is driven both by rover design and mission requirements. The rover primarily drives mass and center of gravity constraints for the lander in addition to lift capability and fairing volume constraints for the launch vehicle (or vice versa). Planetary landing mission technology is substantially more mature than automated mobile surface rover technology as there have been a number of both U.S. and Russian missions including: Luna, Surveyor, Apollo, and Viking. However, the last U.S. planetary surface landing took place in 1976 (Viking) and there are currently no planetary landers in production or on order.

The launch vehicle mission component is the most technically mature. Except for the Space Shuttle, all of the larger current production U.S. launch vehicles have been improved incrementally from versions first flown in the late 1950's or early 1960's. Most missions of the recent past are to either Low-Earth orbit (LEO) or Geosynchronous orbit (GEO). Therefore, current stage sizing and architecture's are optimized to put a spectrum of masses into these Earth orbits. Development of a new launch vehicle specifically optimized for a lunar mission would be prohibitively expensive for a single flight program. Therefore, the approach taken was to select a current production launch vehicle and optimize the lander as much as possible in terms of payload and cost. Table III.5 shows U.S. launch vehicle capability (medium class and larger) to a 185 km x 185 km x 28.5° Low Earth parking orbit and launch vehicle costs in Fiscal Year 1990 Millions of dollars (FY90\$M) [ref. 53]. Translunar injection mass capability is also shown for each vehicle.

Selection of the launch vehicle will principally size the mission both in terms of mass and cost. The mission cost requirement was stated in terms of an "Delta or Atlas class mission" because it constrains launch costs as well as lander, rover, and science instrumentation mass and thus indirectly limits their cost.

The objective of a recent NASA Johnson Space Center (JSC) study called Artemis Common Lunar Lander (CLL) is to develop a Lunar descent stage appropriate for a medium class launch vehicle (Delta II or Atlas) [54, 55]. Artemis would be functionally similar to an upper stage like PAM, IUS, TOS, in that they are bought “off-the-shelf” with little or no modifications and provide only a mounting interface for

Table III.5 United States Launch Vehicle Capability (kg) LEO = 185 km x 185 km x 28.5° from [ref 53]

	Low Earth Parking Orbit Mass Capability (kg)	Launch Vehicle TLI capability (kg) $\Delta V = 3135 \text{ m/sec}$	Launch Costs FY90\$M [ref 53]
Delta II 7925 (10 ft ϕ fairing) (native 3rd stage)	4925	1463	50
Atlas II	6395	2024	80
Atlas IIA	6760	2145	90
Atlas IIAS	8390	2945	120
Titan III / PAM-DII	14515	4054	150 + Upper Stage
Titan IV / Centaur	17700	5844	227

the payload. Producing “common” landers in quantity for a variety of Lunar science missions would reduce total program costs by amortizing development costs over several missions and achieve economy of scale by learning curve effects. The Artemis concept and many corresponding assumptions were adapted as the baseline for the volatiles mission based on our ground rule to utilize existing design. However, since in this study, RDT & E costs are charged to the volatiles mission for hardware not yet developed (includes the lander) various perturbations of the Artemis lander design were evaluated in attempt to minimize cost for our single mission application.

Many assumptions of the Artemis Phase 2 Artemis study dated March 10, 1992 were adapted (mass estimates from Baseline C Rev 1 mass statement dated February 26,

1992). Assumptions for the mission velocity budget shown Table III.6 include: Low earth parking orbit at 185 km x 185 km x 28.5°, all lunar landing sites accessible, provide transfer capability to Moon at anytime during the 18.6 year Lunar cycle, 4-5 day transfer time, and 100 km Lunar parking orbit.

Table III.6 Mission Velocity Budget (m / sec) (ref. 55)

Translunar Injection (TLI)	3135
Mid-Course Correction	30
Lunar Orbit Insertion (LOI)	887
Deorbit	18
Terminal Descent	1550
Constant Rate Descent	285
Total	5905

Perturbations of the Artemis design evaluated included three different staging architecture's for medium class launch vehicles and larger. First, a single stage bipropellant lander (BL) which would utilize the launch vehicle's native upper stage if available was considered. The baseline propulsion system features integrated Attitude Control System (ACS) and Main Engines (ME) for ΔV thrust, monomethylhydrazine (MMH) and nitrogen tetroxide (NTO) propellants, and ME Isp = 311 seconds. The primary advantage of this option is reduced RDT & E since only one stage is developed. The primary disadvantage is reduced payload performance. Lunar landed dry mass, lander propellants, and delivered payload mass estimates are given in Table III.7.

The second staging architecture evaluated featured a Bipropellant Lander upper stage with a Solid Lower Stage (BL + SLS) which would utilize the launch vehicle's native upper stage if available. The upper landing stage which includes the payload has the same characteristics as above but will only perform midcourse correction and landing ΔV burns totaling 197 m / sec. The solid lower stage will perform a single direct lunar insertion burn of 2573 m / sec . Assumed solid motor propellant mass fraction = 0.85 (0.92 motor, 0.07 for interstage) and Isp = 292 seconds. Primary advantages are increased payload performance due to staging and reduced propulsion system cost (\$ solid < \$ biprop, see cost section). Primary disadvantages are increased RDT & E for additional stage, decreased landing site accuracy due to direct insertion burn, and reduced payload volume envelope due to additional height requirement of solid motor packaging inside fairing. Solid motor mass, lunar landed dry mass, lander propellants, and delivered payload mass estimates are given in Table III.8.

Table III.7 Bipropellant Lander (BL) Mass Summary (kg)

	Gross Stack Mass (kg)	Lunar Landed Dry Mass inc P/L (kg)	Propellant Mass (kg)	Payload Mass (Rover) (kg)
Delta II 7925 (10 ft f fairing) (native 3rd stage)	1463	590	873	79
Atlas II	2024	816	1208	196
Atlas IIA	2145	865	1280	222
Atlas IIAS	2945	1188	1757	389
Titan III / PAM-DII	4054	1635	2419	621
Titan IV / Centaur	5844	2357	3487	996

Table III.8 Bipropellant Lander plus Solid Lower Stage (BL + SLS) Mass Summary (kg)

	Gross Stack Mass (kg)	Solid Motor Mass (kg)	Lunar Landed Dry Mass inc P/L (kg)	Lander Propellant Mass (kg)	Payload Mass (Rover) (kg)
Delta II 7925 (10 ft f fairing) (native 3rd stage)	1463	932	489	42	90
Atlas II	2024	1289	677	58	212
Atlas IIA	2145	1366	717	62	238
Atlas IIAS	2945	1876	985	84	412
Titan III / PAM-DII	4054	2582	1356	116	653
Titan IV / Centaur	5844	3722	1955	167	1041

The third staging architecture evaluated featured a Bipropellant Lander upper stage with a Bipropellant Lower Stage (BL + BLS) which would replace the launch vehicle's native upper stage (except for the Titan IV / Centaur case). Both the upper landing stage and lower stage utilize MMH and NTO as propellants with an Isp = 311 seconds. The total 5905 m / sec ΔV is split between the launch vehicle second stage (except Titan IV for which third stage is used), the bipropellant lower stage, and the lander. Primary advantages are increased payload performance due to staging and Isp of MMH & NTO. Primary disadvantages are increased RDT & E for additional stage, increased cost of a second liquid propulsion system engines and tanks, and reduced payload volume envelope due to additional height requirement of additional stage packaging inside the fairing. Table III.9. shows the contribution of an optimized launch vehicle TLI ΔV for the BL + BLS case in terms of velocity added and final mass. Table III.10. estimates bipropellant lower stage mass, lunar landed dry mass, lander propellants, and delivered payload mass.

Table III.9 United States Launch Vehicle Capability (kg); Split TLI with New Bipropellant Upper Stage

	Mass Injected from 185 x 185 Parking Orbit (kg)	Velocity added by Launch Vehicle for TLI (m / sec)
Delta II 7920 (10 ft ø fairing) (No Native 3rd stage)	3150	1132
Atlas II	2950	2256
Atlas IIA	3100	2278
Atlas IIAS	3300	2846
Titan III / PAM-DII	10100	906
Titan IV / Centaur	5844	3135

Table III.10 Bipropellant Lander plus Bipropellant Lower Stage (BL + BLS) Mass Summary (kg)

	Gross Stack Mass (kg)	Biprop Lower Stage Mass (kg)	Lunar Landed Dry Mass inc P/L (kg)	Lander Propellant Mass (kg)	Payload Mass (Rover) (kg)
Delta II 7920 (10 ft ø fairing) (No native 3rd stage)	3150	2250	560	340	109
Atlas II	2950	1850	798	302	269
Atlas IIA	3100	2000	837	263	298
Atlas IIAS	3300	1900	1105	295	472
Titan III	10100	7300	1658	1142	756
Titan IV / Centaur	5844	3250	2166	428	1156

Figure III.5 shows distribution of the launch vehicle payload mass (total mass bolted at launch vehicle interface or “stack mass”) for each of the staging architecture’s in the medium launch vehicle class. For a particular launch vehicle both the BL and BL + SLS case have the same total stack mass because the launch vehicle in both cases provides full TLI ΔV . In the BL + BLS case the total stack mass varies depending on

how much TLI ΔV is performed by the launch vehicle as determined by a three way optimization between the launch vehicle, lower stage and lander. The single stage BL case gives the highest landed dry mass but the lowest payload mass. Adding the solid

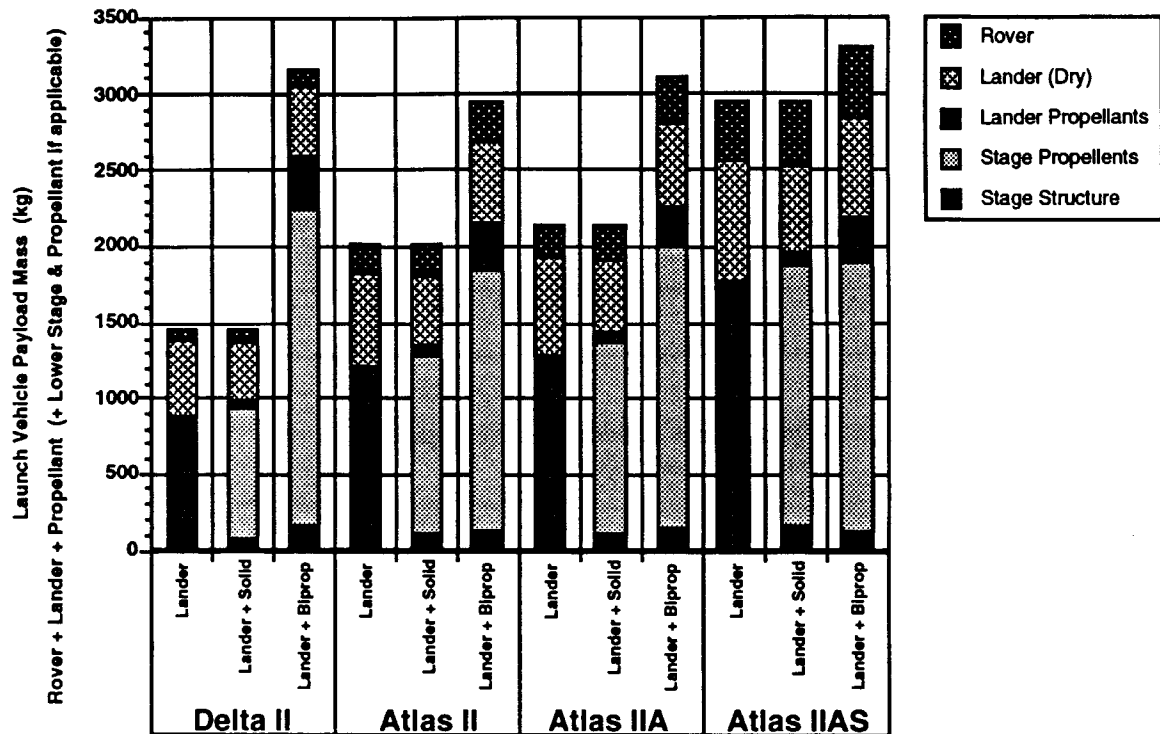


Figure III.5 Mass Distribution vs. Architecture vs. Launch Vehicle

motor increases payload due to staging. However the staging effect is small (approx. 5 - 10%) since the stage is separated near the Lunar surface. This results in the smallest liquid propulsion system requirement (reduces cost) and the smallest landed dry mass. Adding the lower bipropellant stage gives the highest payload capability due to the three way optimization.

Figure III.6 graphically illustrates the relationship between lander payload (rover mass), launch vehicle size, and lander staging architecture. Launch costs are

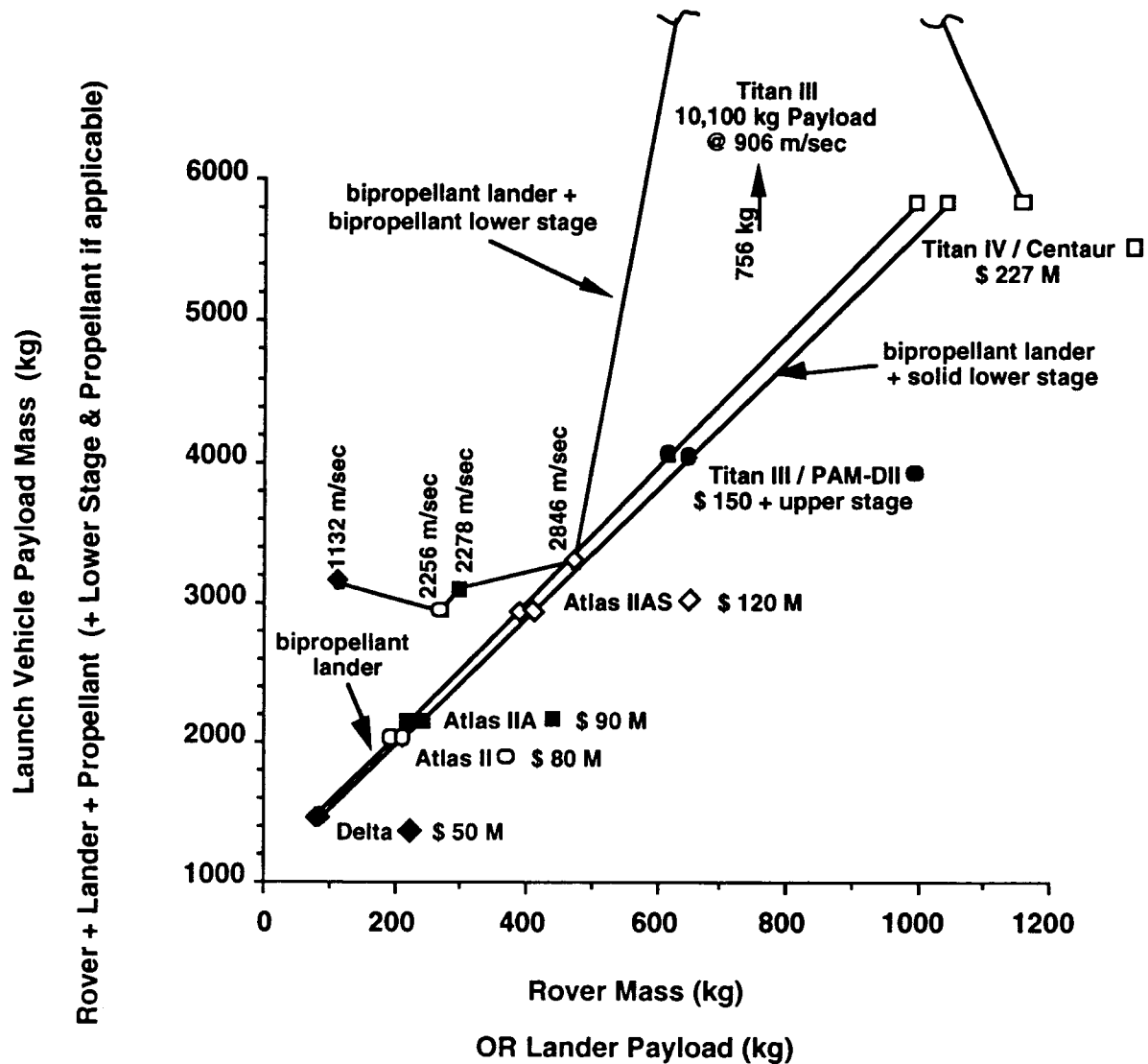


Figure III.6 Launch Vehicle Payload vs. Rover Mass vs. Stage Architecture

shown to help quantify the trade of increasing rover mass for increased launch vehicle capability. The lines between the launch vehicle points are somewhat misleading since there is no continuum between the launch vehicles (select nearest vehicle with positive or zero mass margin). The lines are shown to identify points belonging to the proper architecture.

The validity of the mass estimates are limited to ROM since they utilized linear scaling of Artemis lander mass estimates over a considerable mass range. Avionics and power sub-system masses were held constant at 98 kg and 125 kg respectively. Structural mass was scaled linearly with gross mass with allocations of 4% primary structure, 1% secondary structure, and 0.7% for the payload attach fitting. Other subsystems including propulsion minus tankage 11.9%, landing gear / pyrotechnics / Mech. 6.8%, and margin 9.8% were scaled with dry mass. Tankage was estimated from propellant volume and a curve fit of MMH / NTO propellant tanks and He pressurant bottles manufactured by TRW Pressure Systems Incorporated, Los Angeles, CA (based on flight qualified tanks). Figure III.7 shows Lander payload mass fraction plotted against dry landed mass. Mass fraction increases with total dry mass because avionics and power subsystems become a smaller percentage as total mass increases. There are two historical data points at the extreme end of either side of the spectrum to indicate an existence of this trend: Surveyor at 0.183 mass fraction with dry landed mass of 284 kg and the Apollo Lunar Module with an inert total mass of 4359 kg and a inert ascent stage to inert descent stage mass ratio of 1.01.

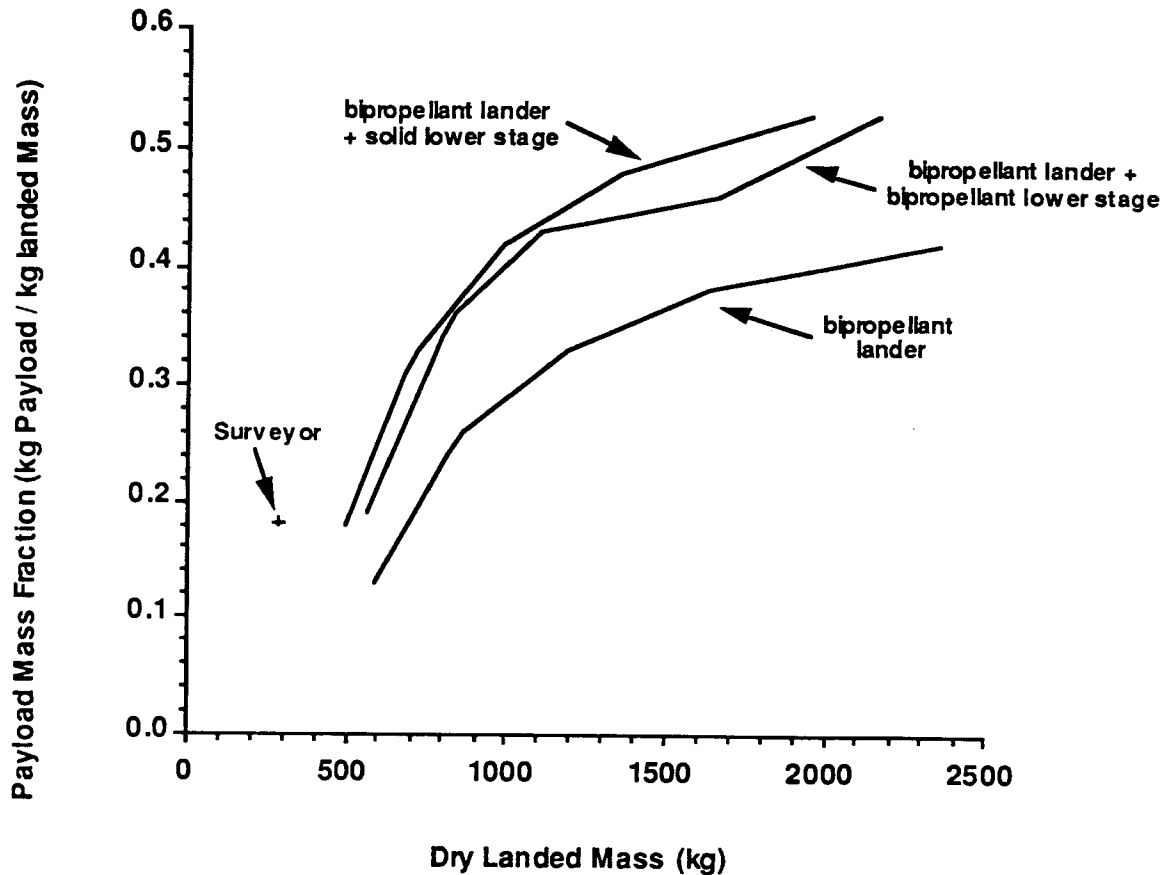


Figure III.7 Lander Payload Fraction vs. Dry Landed Mass vs. Stage Architecture

F. Cost Estimation:

There are three basic techniques used to develop cost estimates including: detailed bottom-up estimating, analogous estimating, and parametric estimating. In detailed bottom-up estimating sufficient design detail is required to estimate the cost of material, labor, and equipment to design, develop, and manufacture each system component. Bottom-up estimating is generally more accurate but also more time consuming because it requires design definition, vendor pricing or quotes, and coordination with different specialists (engineering, management, test labs, manufacturing, etc.). Usually this level of detail is not available until a concept has been developed far enough to formulate a contract bid.

In analogous estimating the cost of a similar item is used and appropriately adjusted for differences in size or complexity. However, this requires existence and knowledge of a similar design. This method is not well suited to conceptual trade studies.

In parametric estimating an equation called the Cost Estimating Relationship (CER) is used which relates cost as a function of a design characteristic (mass, power, dimension, etc.). CER's are derived from actual historical cost data with curve fits to appropriate design parameters. This method is appropriate for the detail level of this study.

The CER's utilized in the following estimates are from the USAF Unmanned Spacecraft Model, fifth edition, [Fong, F. et. al. 1981] USAF Space Division as reported in [ref. 40]. These CER's are based on a mix of government and commercial space programs, though weighted toward the government side. To compare competing concepts the relative dollar values can be compared. However, when evaluating absolute costs it is important to note that actual costs will depend greatly on program implementation (i.e. "skunk works", etc.). It is left as an exercise for the reader to apply appropriate factors for organizational / implementation assumptions, etc. All estimates are converted to fiscal year 1990 dollars.

Major cost categories of the total program life cycle cost are space segment, launch segment, ground segment, operations and maintenance, and 10% fee. The space segment consisted of RDT & E and Theoretical First Unit (TFU) cost for both the lander and rover. To estimate rover and lander cost sub-system mass and power estimates were used with appropriate CER's. Launch segment costs are given in Table III.5. Ground segment costs were held constant at \$M 83.3 for each competing concept based on a 162 K lines of Ada code ground software estimate. Operations & maintenance (O & M) costs consisted of labor and maintenance costs. For O & M labor a 25 government and 50 contract person load was assumed with rates of 90 K\$ /

year and 130 K\$ respectively. A one year mission length was generally assumed. Maintenance cost was estimated at 10% of ground software, equipment, and facilities cost per year (approx. \$M 14.3).

To gain some confidence in the volatiles mission cost model a comparison was made with various historical programs. Figure III.8 compares production cost and total program cost of the volatiles mission to various historical programs. The lander and rover production cost (theoretical first unit) was approximately \$ 20 -25 K / kg below the “historical average” of a variety of earth orbiting spacecraft (both military and commercial). This can be attributed to the volatiles mission lower mass fraction of high cost density components which occurs because higher cost density science instrumentation components are payload to the rover which itself is the payload to the lander. In earth orbiting spacecraft IR / Visible / optics or communications antenna’s/ electronics have larger cost densities as well as larger mass fractions. Figure III.8 also compares volatiles mission total program cost derived from the cost model with historical program costs. A minimum Delta class rover mission was approximately 3/4 of a Gamma Ray Observatory (GRO) mission. The largest rover Titan IV/ Centaur mission (1000 kg rover) was approximately 1/2 of a Space Telescope.

Figure III.9 gives estimated single mission total life cycle cost as a function of rover mass, lander staging architecture, and launch vehicle. It shows that choosing a staging architecture for the lowest total program cost is dependent on absolute rover mass. For example, if a 100 kg rover is required, than the Delta II with BL+BLS has the lowest total program cost at \$M 436. However, for a relatively modest increase in cost to \$M 456 rover mass can be increased to 212 kg by jumping to the next size launch vehicle and using BL+SLS architecture. This occurs due to different TFU and RDT & E costs associated with each architecture and the different performance characteristics of each architecture. It also occurs because of the particular performance and size characteristics of existing launch vehicles.

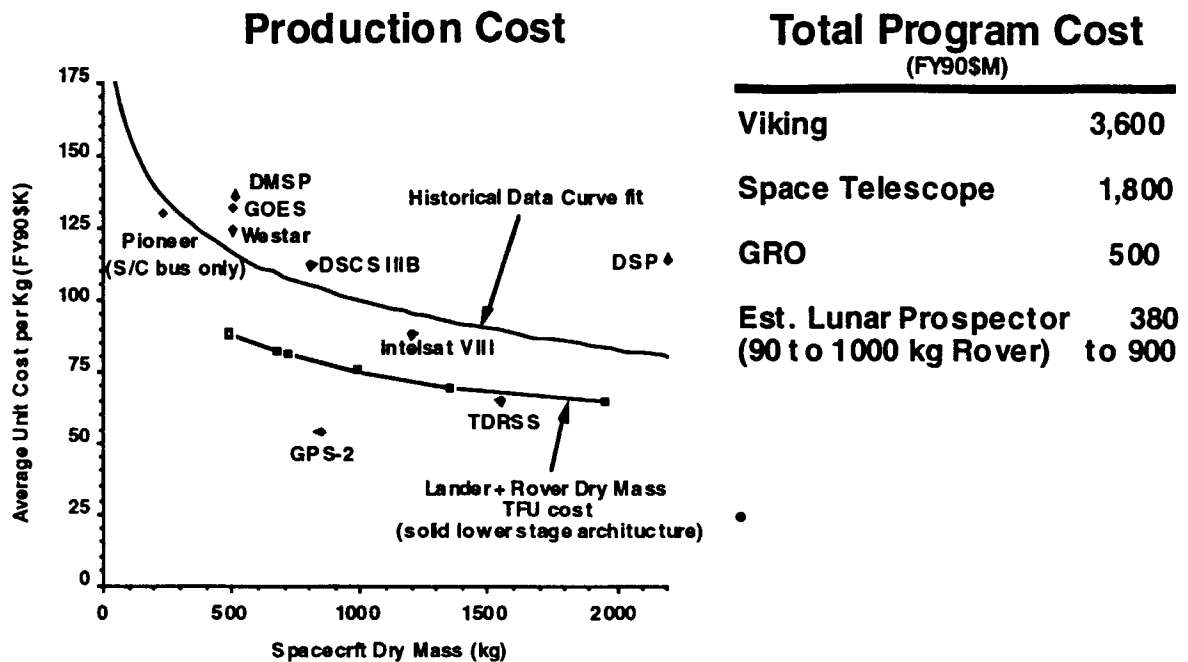


Figure III.8 Order of Magnitude Cost Comparison for Production Cost and Total Program Cost

The BL + SLS lander architecture had lowest estimated cost across the entire rover mass range (or lander payload). This results because a solid motor, for an equivalent ΔV , is generally less expensive than a liquid system (both RDT & E and TFU). However, as mentioned in section III.E, disadvantages of the solid are: reduced available height in payload fairing, lower landing accuracy (single burn), and less flexibility (only one solid stage burn can be performed).

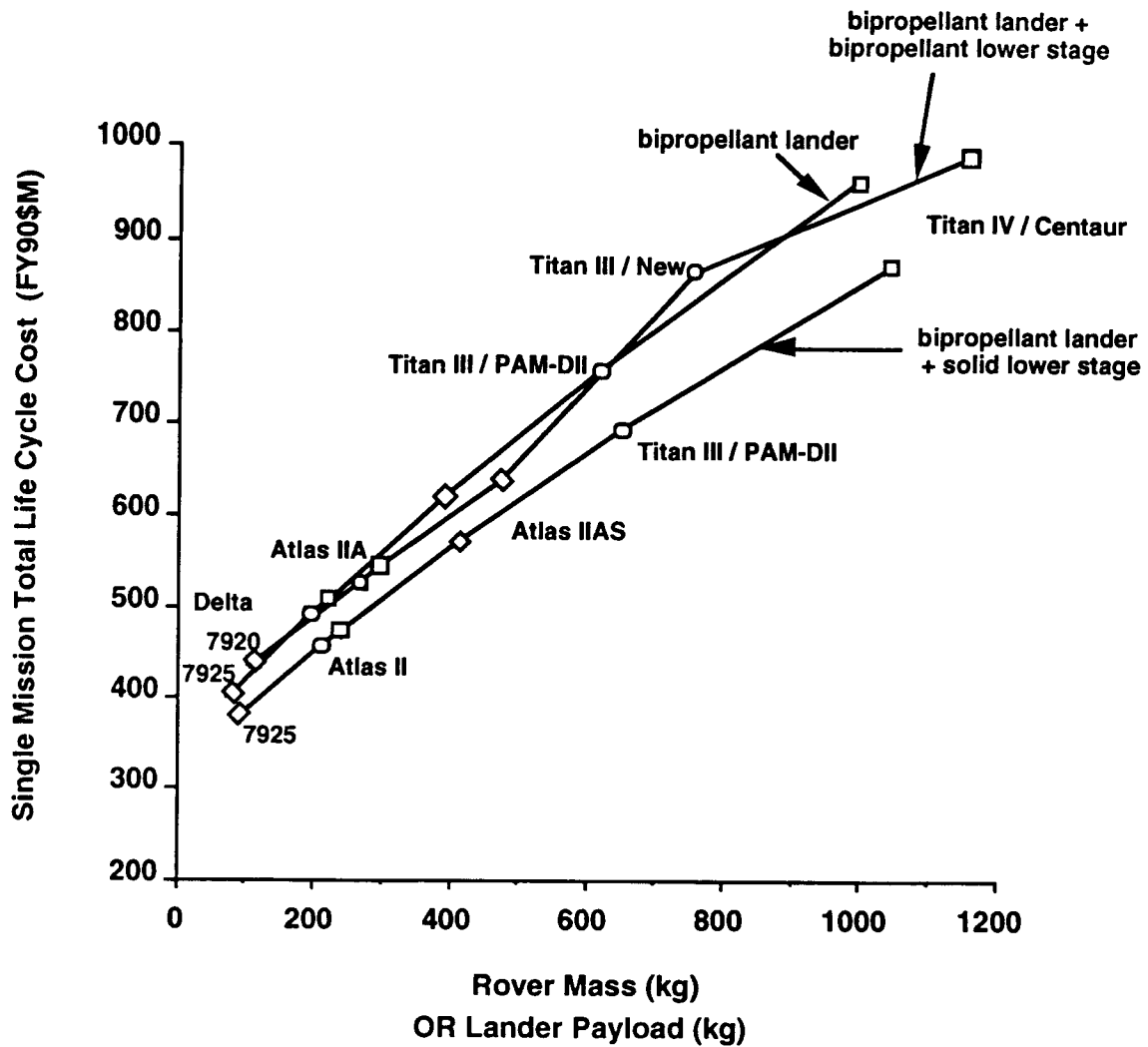


Figure III.9 Single Mission Life Cycle Cost vs. Rover Mass vs. Architecture vs. Launch Vehicle

If the disadvantages associated with the solid motor architecture are unacceptable, choosing between BL and BL+BLS for lowest total program cost will depend on absolute rover mass required. Referring to Figure III.9, lowest total program cost alternates between these two architecture's over the entire mass range. This results from dependencies of: existence of a native upper stage (use of an existing stage always costs less), ΔV of existing upper stage (it's optimality for use in lunar trajectory), and

absolute size of existing stage (developing a large liquid stage will cost considerably more for the larger launch vehicle offsetting the performance increase).

Figure III.10 shows single mission total life cycle cost per rover mass as a function of rover mass, lander staging architecture, and launch vehicle. It shows that BL+BLS gives the lowest cost per rover kg for the medium class launch vehicles (Delta + Atlas) but BL+SLS catches up and is slightly lower for the larger launch vehicle's (Titan III & IV). It also shows that the BL architecture has the highest cost per kg across the entire range of rover masses but the difference gets smaller for the larger launch vehicles. This indicates that the percentage of performance gain for utilizing lander staging, as well as using liquid propulsion, decreases relative to the increase of RDT & E and TFU costs as the rover mass increases.

Again, it is important to note that the objective is to minimize total program cost not cost per rover kg, etc. The lines connecting the points of Figures III.9 and III.10 indicating a continuum between launch vehicles that does not exist (lines are shown to identify points belonging to the respective architecture) and the absolute rover mass is critical to minimizing total program cost. For example, a Delta launch vehicle with a BL+SLS lander architecture gives the lowest total program cost for an "average" 75 kg rover (\$M 378) even though BL+BLS offers lower cost per kg (increased performance is not needed for this payload). If the solid stage had unacceptable landing accuracy or utilized too much packaging volume then the BL architecture would provide the next lowest cost (\$M 401).

Figure III.11 shows cost benefits associated with an extended commitment to Lunar exploration program. A 95% learning curve slope was utilized to account for productivity improvements as a larger number of lander and rover units were produced. RDT & E and ground segment costs are amortized over the number of missions. Operations and maintenance costs were held constant which is conservative since it assumes sequential missions rather than some overlap. Launch costs were also held

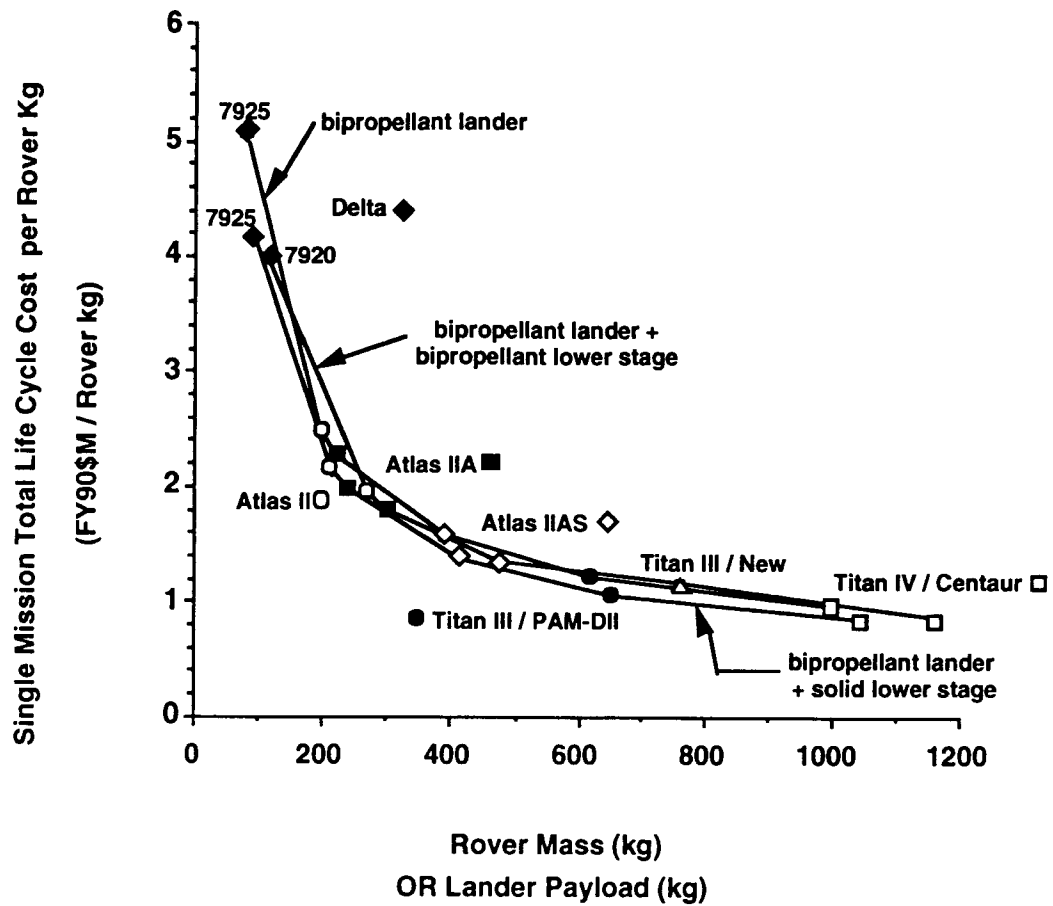


Figure III.10 Single Mission Life Cycle Cost per Unit Rover Mass vs. Rover Mass vs. Architecture vs. Launch Vehicle

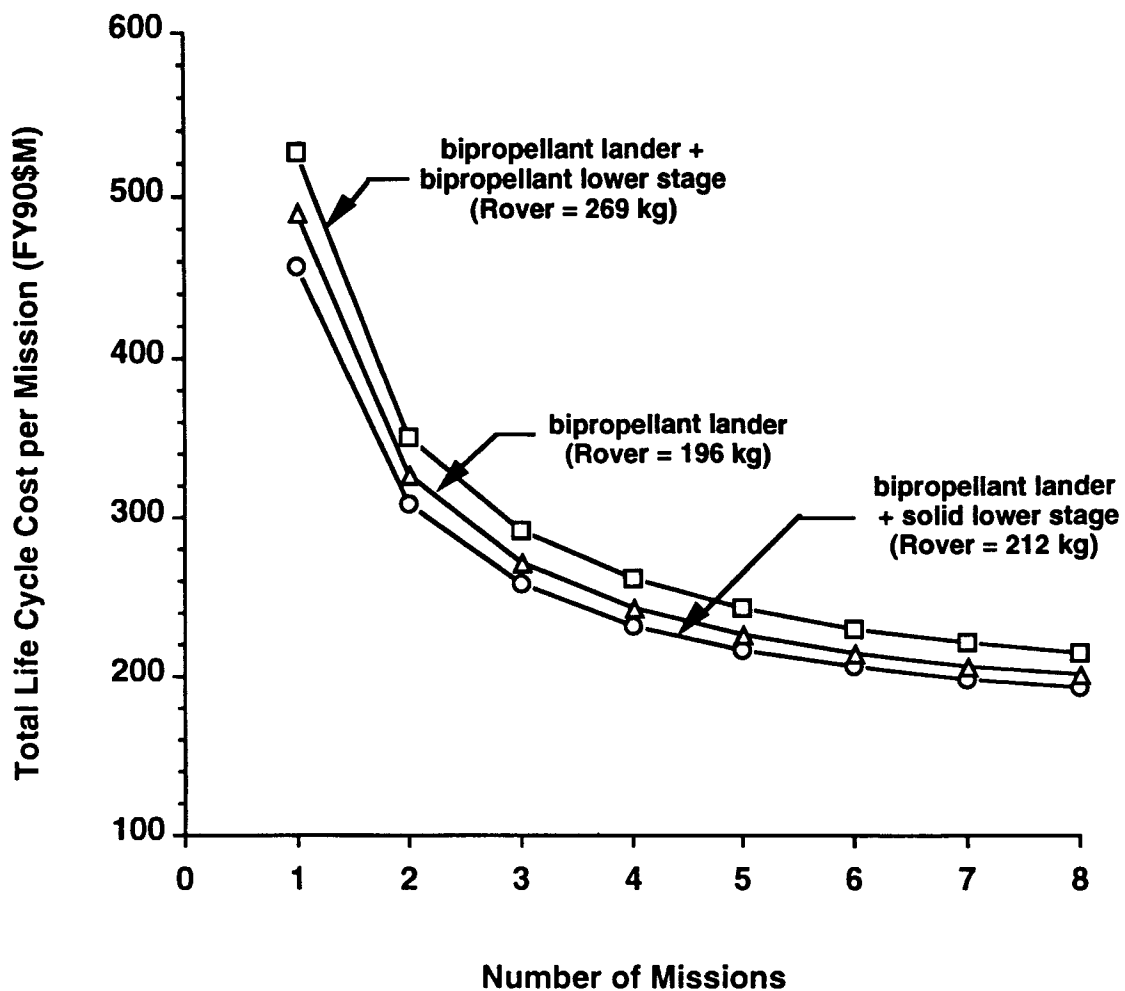


Figure III.11 Total Life Cycle Cost per Mission vs. Number of Missions vs. Architecture for Atlas II Launch Vehicle

constant which is also conservative since a multiple vehicle buy would generally result in cost reduction. For 8 missions total per mission cost was approximately \$M 201 for a 212 kg rover with a 25 kg science package based on an Atlas II launch vehicle. After only three missions the per mission cost was reduced over 44%.

A ROM comparison was also made comparing a large science mission to multiple smaller missions. A Titan IV/ Centaur with BL+SLS architecture could soft land a single 1,042 kg rover for a two year mission with a 125 kg science package and

526 Watt RTG power for continuous roving. Total estimated program cost was \$M 900. For the same total program cost four 212 kg rovers could be landed in four different locations with a 25 kg science package and 107 Watts of RTG power (continuous roving) based on an Atlas II launch vehicle and BL+SLS architecture. Science packages of the different smaller missions could be different but only one instrument suite RDT & E cost was included in the \$M 900. The large mission would be more appropriate for an extensive characterization of a smaller area (125 kg science), and the multiple smaller missions for less extensive characterization over a larger area (i.e. 1,200 km from single landing site vs. 1,200 km from four different landing sites). Although the volatiles experiment requires only one smaller mission these calculations show the cost benefits of an extended Lunar exploration program vs. a single mission.

G. Recommendations:

The Small Marsokhod Rover (SMR) was chosen as the baseline Lunar volatiles mission rover. The design meets key mission requirements including: science payload capability, range, and design maturity. SMR mobility capability significantly exceeds requirements for the Lunar mare landing site and volatiles traverse. This excess capability will reduce Clearance Failure Mode (CFM) probability and may also simplify vehicle guidance because avoiding smaller obstacles will not be of critical importance. However, the multi-degree of freedom chassis joints will have higher failure probability (Lunar dust, thermal cycling, etc.).

Another advantage of SMR is that the smaller Delta 7925 launch vehicle is sufficient to soft land SMR on the lunar surface with any of the three lander architecture's. The single stage bipropellant lander architecture was chosen due to the fairing envelope constraints (see Section III.E). Figure III.12 illustrates the Delta 7925 9.5 feet diameter payload fairing (GPS) with an "scaled" Artemis class lander and SMR. Lander subsystem mass estimates are shown in Table III.11.

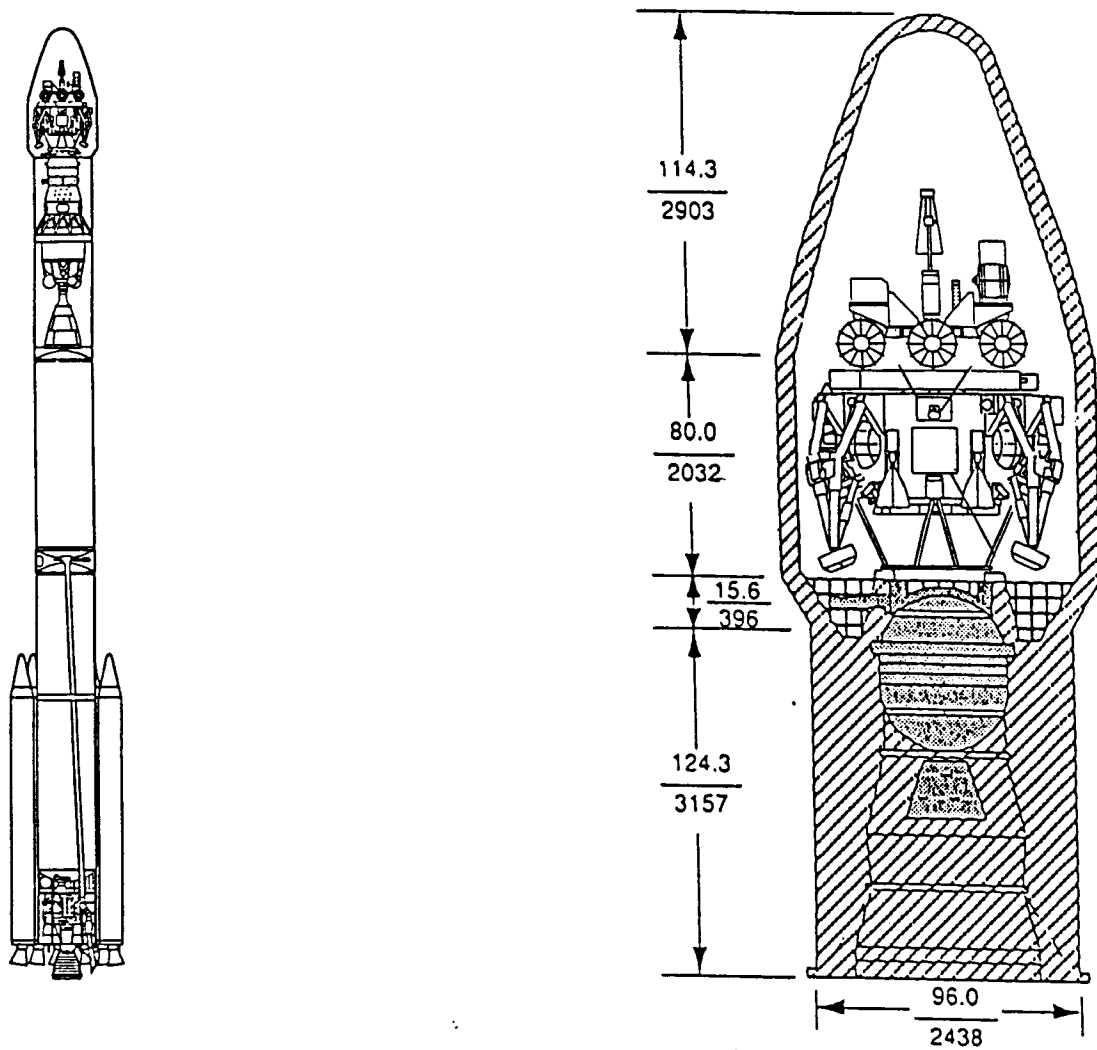


Figure III.12 Baseline Volatiles Mission: Small Marsokod Rover, Single Stage Bipropellant Lander, Delta 7925 Launch Vehicle w/ 9.5 feet diameter Fairing (GPS)

Table III.11 Baseline Lander Mass Estimates (kg)

Lander Power	125
Lander Attitude Determination	53
Lander Communication and Data Management	45
Lander Propulsion (dry)	105
Lander Structure	82
Landing Syst/ Mech./ Pyro	40
Lander Growth	57
SMR (see Fig. III.3 for details)	75
Lander Dry Mass	583
Lander Propellants	862
Gross Lander Mass	1445

Estimated SMR ROM total life cycle mission costs from the USAF Unmanned Spacecraft Model are shown in Table III.12. (see Section III.F). Included in the total from the USAF cost model is \$M 45.3 for rover RDT & E and \$M 10.4 for the rover flight unit. Russian involvement was not accounted for but the cost figures from the model are probably conservative possibly by as much as a factor of two or more. In [ref. 51], Garry Rogovsky, deputy director of the Babakin Center of NPO Lavochkin in Russia said that they had been working on the \$M 20 prototype for five years. However, it is important to note that the current Marsokhod prototype exists basically as a chassis/ undercarriage. The rest of the rover specifics have yet to be developed (control, computation, communication, manipulation, science instruments, thermal, etc.).

Table III.12 SMR Mission Total Life Cycle Cost (FY90\$M), (From USAF Unmanned Spacecraft Model, Fifth Edition, ref. 40)

Space Segment Cost			\$209
	RDT & E (Non-Recurring)	\$163	
	Theoretical First Unit Cost (Production)	\$46	
Launch Segment			\$50
Ground Segment			\$84
Operations & Maintenance over Mission Duration			\$14
Total Life Cycle Cost			\$357
Total Life Cycle Cost plus 10% Fee			\$393

SMR mobility performance, although more capable than necessary for the volatiles mission, could be more fully utilized in subsequent follow-on missions (chemical composition, mineralogy, soil maturity, etc.). After an initial volatiles qualification mission SMR and the associated lander could explore more difficult terrain: in and around craters, Lunar poles, Lunar highlands, Lunar dark side (need Comm. Link) or Mars.

If several follow-on missions were planned, making use of hardware qualified for the volatiles mission, it may be advantageous to have a more capable rover for increased mission flexibility. This concept, called Common Lunar Rover (CLR), would complement the Common Lunar Lander (CLL) development. CLL could deliver a fixed 212 kg payload, or deliver the 212 kg CLR with 25 kg of science instrumentation, 1,200 km maximum range, and 1 year mission life.

The JPL "rocker bogie" configuration was chosen for the CLR concept. It offers good mobility performance for a modest chassis/ structural mass fraction and moderate/ low design complexity (chassis articulation). It also offers significant range improvement of up to 1,200 km. The Lunar Site Characterization Rover (LSCR) discussed in section III.D.3. was scaled slightly down to fit on an Atlas II launch vehicle. Table III.13. gives scaled subsystem mass estimates for the CLR.

Table III.13 Common Lunar Rover (CLR) Design Optimized for Atlas Launch Vehicle based on JPL Rocker Bogie Configuration (mass in kg)

Rover Science	25
Rover Power (107 Watts)	34
Rover Communications	11
Rover Thermal	6
Rover Manipulation	21
Rover Computation	17
Rover Control	30
Rover Chassis	68
Rover Total	212

An initial layout indicated that the Atlas large payload fairing (13.75 feet diameter) could accommodate a two stage lander. Therefore, a bipropellant lander with a solid lower stage was chosen based on lowest cost. Mass estimates for the upper lander stage and lower solid stage are given in Table III.14.

Table III.14 Two Stage Common Lunar Lander (CLL) Design Optimized for Atlas Launch Vehicle(Kg)

Lander Power	125
Lander Attitude Determination	53
Lander Communication and Data Management	45
Lander Propulsion (dry)	13
Lander Structure	115
Landing Syst/ Mech./ Pyro	46
Lander growth	67
Rover (see table III.13)	212
Lander Dry Mass	677
Lander Propellants	58
Gross Lander Mass	735
Solid Motor Propellant	1188
Solid Motor Structure	101
Gross Stack Mass	2024

Estimated CLL / CLR first mission total costs from the USAF Unmanned Spacecraft Model are shown in Table III.15. The volatiles mission does not require the single mission cost increase from \$M 393 to \$M 457. The increased rover capability

would offer flexibility in planning several science missions utilizing the same hardware. Figure III.11 shows that the per mission total cost drops to \$M 258 for three missions and \$M 193 after eight missions. Therefore, it may be advantageous to utilize a slightly downsized JPL LSCR if several lunar missions were going to utilize the same hardware.

Table III.15 CLL / CLR First Mission Total Cost (FY90\$M), (USAF Unmanned Spacecraft Model, Fifth Edition)

Space Segment Cost		\$237
	RDT & E (Non-Recurring)	\$181
	Theoretical First Unit Cost (Production)	\$56
Launch Segment		\$80
Ground Segment		\$84
Operations & Maintenance over Mission Duration		\$14
Total Life Cycle Cost		\$415
Total Life Cycle Cost plus 10% Fee		\$457

IV. SUMMARY AND CONCLUSIONS

This report summarizes a one-year study of an unmanned lunar mission for Volatile Gas Recovery. The volatile gases evolved from the lunar regolith will have high value for use during future manned lunar colonies and the ^3He evolved has the potential to be used for fusion power on earth and in space.

In order to assess more fully the location and quantities of these volatiles located on the lunar surface, this study concentrated on the delivery of a mobile lunar rover to the moon which would transport a scientific package with the capability of determining the volatiles evolved from heating the lunar soil. The rover would have the capability to navigate approximately 100 km and include a retriever device to sample the top surface of the soil. Radioactive Thermoelectric Generators were proposed as the power source. A heat transfer analysis of the heater and sample indicated that 13.3 minutes were required to heat a 1 gram sample to 1200°C with a 25 watt heater. The entire sample analysis procedure was estimated to require 18.3 minutes.

The scientific package consisted of a sample loading device; a scale to determine the weight of the sample; a vacuum chamber in which the sample would be heated to 1200°C; and a mass spectrometer to measure the chemical constituents of the gases. In addition, the chemical assay of the sample would be determined when an energetic laser beam, directed to the surface of the sample, vaporized a small portion of the sample. The chemical content of the vapor would be analyzed by using the mass spectrometer.

The apparent relationship between He in the soil and the TiO₂ content of the soil was utilized during the selection of the landing site. An area with high soil concentrations of TiO₂ as determined by remote sensing, was selected on Mare Tranquillitatis at the location of 9°N and 20°E. As the rover traverses this area the samples of regolith should vary from 6 to >10 wt % TiO₂ with He concentrations in the range of 35-45 wppm (0.014-0.018 wppm ³He).

Several types of existing or currently designed rovers were surveyed for potential use on this mission. For the mass of the scientific package, ~18 kg, and the mobility required, the Russian Small Marsokhod 75 kg rover was selected as a prototype. Integration of the rover with a lander indicated that a launch vehicle of the Delta or Atlas class would be required to place the lunar transporter in an earth orbit of 185 km x 185 k x 28.5°. Several types of second stage architecture were considered. A bipropellant lower stage gave the highest payload capability. A cost analysis indicated that the R D T & E plus first unit production cost for the rover, lander, and science package could be accomplished for \$209M.

The principal conclusion of this study is that lunar missions with limited objectives, ie. only one or two analytical measurements, can yield a wealth of information at reasonable cost, ~\$200M, when existing equipment is utilized as much as possible. The planning, operation and data collection would be as faster and cheaper. Development and testing of the science package should proceed as rapidly as possible.

Further study of the integration of the rover, lander and science package designed for operation on the lunar maria is recommended in order to optimize the landed payload.

V. REFERENCES

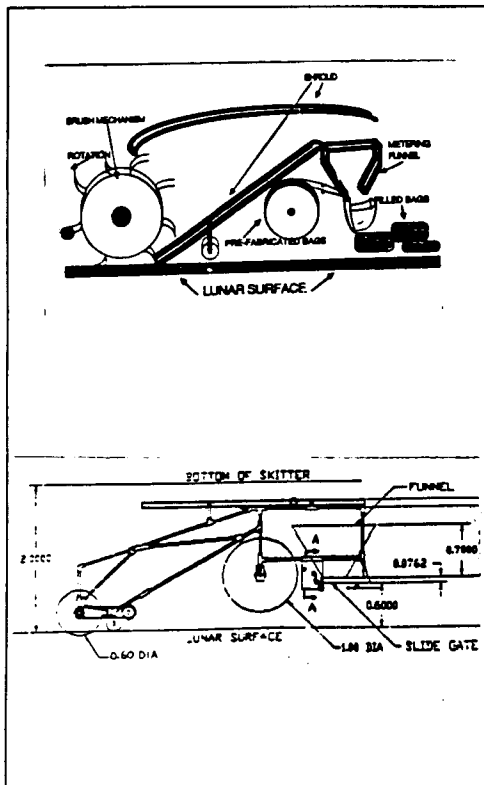
1. L. J. Wittenberg, et al. "Review of Helium-3 Resources and Acquisition for Use as Fusion Fuel ", Fusion Tech.,21, 2230 (1992).
2. H. Hintenberger, H. W. Weber, H. Voshage, H. Wanke, F. Begemann, and F. Wlotzka, "Concentration and isotopic abundances of the rare gases, hydrogen and nitrogen in lunar matter", Lunar Sci. Conf., Vol. 2. 1269 (1970).
3. P. Eberhardt, J. Geiss, H. Graf, N. Grogler, M. D. Media, M. Morgeli, H. Schwaller and A. Stettler, "Trapped solar wind in Apollo 12 lunar fines (12001) and Apollo 11 breccia (10046)", Third Lunar Sci. Conf.,2, 1821(1972).
4. E. N. Cameron. "Mining for Helium- Site selection and evaluation", Proc. Second Lunar Bases and Space Activities in the 21st Century,189-197, NASA Conf. Publ. 3166 (1992).
5. L. A. Taylor, "Generation of native Fe in the lunar soil", Proc. SPACE '88, Amer, Soc. Civil Eng. 67 (1988).
- 6 A. E. Metzger and R. E. Parker, "The distribution of Ti on the lunar surface", Earth Plant. Sci. Letters, 45, 155 (1980).
7. T. V. Johnson, R. S. Sanders, D. L. Matson and J. L. Masher, "A TiO₂ abundance map of the northern maria", Eighth Lunar Sci. Conf. 1, 1029 (1977).
8. J. R. Johnson, S. M. Larson and R. B. Singer, "Remote sensing of potential lunar resources, 1. Near-side compositional properties", J. Geophys. Res., 96, 18861 (1991).
9. M. J. S. Belton, et al, " Lunar impact basins and crustal heterogeneity: New western limb and far-side data from Galileo", Science, 255. 570(1992).
10. J. W. Head III, et al, "Lunar impact basins: New data for the near-side northern high latitudes and eastern limb from the Second Galileo Fly-by", (1993) in press.
11. E. N. Cameron, "Helium resources of Mare Tranquillitatis", Internal Rpt.: WCSAR-TR-AR3-9207-1 (July 1992).
12. K. Mauersberger, et al," Mass spectroscopy measurements of Martian Krypton and Xenon isotopic abundances", LPI Tech. Rpt. 92-07 (1992).
13. Lunar Sourcebook - A User's Guide to the Moon, Edited by G.H. Heiken, D.T. Vaniman and B.M. Frend. Cambridge University Press, 1991 p. 363
14. C. Köster, M.S. Kahr, J.A. Castoro and C.L. Wilkins "Fourier Transform Mass Spectrometry", Dept. of Chemistry, University of California, Riverside, Mass Spectrometry Review, 1992, II, 495-512

15. R. C. Elphic, H. O. Funsten, B. L. Barraclough, D. J. McComas, J. E. Nordholt, "Lunar and Asteroid Composition Using a Remote Secondary Ion Mass Spectrometer", Space Plasma Physics Group, Los Alamos National Laboratory, LPI Technical Report 92-06 (1992)
16. David E. Emerson and Elmer T. Suttle "Mass Spectrometric Method for Determining Parts per Billion He3 in the He" US Dept. of Interior, Bureau of Mines Report of Investigation No. 8119 (1976)
17. S. Chang, K. Lennon and E.K. Gibson Jr. "Abundances of C, N, H, He and S in Apollo 17 Soils from Station 3 and 4: Implications for Solar Wind Exposure Ages and Regolith Evolution", Proceedings of the 5th Lunar Conf. (1974)
18. S. Chang, J.W. Smith, I. Kaplan, J. Lawless, K.A. Kvenvolden and C. Ponnampuruma "Carbon Compounds in Lunar Fines from Mare Tranquillitatis - IV. Evidence for Oxides and Carbides", Proceedings of the Apollo 11 Lunar Science Conf. 1970
19. Y.T. Li and L.J. Wittenberg "Lunar Surface Mining for Automated Acquisition of He-3: Methods, Processes and Equipment." Proceedings of the 2nd Conf. on Lunar Bases and Space Activities of the 21st Century, Houston TX. 1988
20. R. J. De Young and W. Situ "A Remote Laser-Mass Spectrometer for Determination of Elemental Compositions" NASA Langley Research Center, Hampton, Va, LPI Technical Report 93-02 (1993)
21. G. J. DeSalvo and R. W. Gorman, "ANSYS Engineering Analysis System Users Manual" Revision 4.4, May 1989
22. W.D. Carrier III, G.R. Olhoeft, W. Mendell, "Physical Properties of the Lunar Surface" in G. Heiken, D. Vaniman, B.M. French, "Lunar Sourcebook, A User's Guide to the Moon", Cambridge University Press, 1991, pp. 475-594
23. D.C. Crouch, "Lunar Rock Coring Device Design Study, Final Report", Martin Co., Oct. 1965, NASA CR-65188, N66-15364
24. "Support Manual for Apollo Lunar Surface Drill (ALSD)", Martin Co., Mar. 15 1967, 105 p., NASA CR-65971, N68-18599
25. "Surveyor III, A Preliminary Report", 1967, NASA SP-146, N67-32588
26. E.R. Rouze, M.C. Clary, D.H. Le Croisette, C.D. Porter, J.W. Fortenberry, "Surveyor Surface Sample Instrument", JPL Technical Report 32-1223, 1968, NASA CR-93205, N68-17411
27. I.I. Cherkasov, V.V. Shvarev, "Lunar Soil Science", Moscow, 1971, Translated by Israel Program for Scientific Translations, Jerusalem, 1975
28. A) B. J. Hogan, "Thin Foil Booms Extend Nested Rocket Cones", Brunswick Defence, Design News, Cahners Publishing Company, May 25, 1982 B) Brunswick Corporation, Defence Division, "Brunswick Spacecraft Booms",

29. R. Cannon, S. Henninger, M. Levandoski, J. Perkins, J. Pitchon, R. Swats, R. Wessels, "Lunar Regolith Bagging System", 1990, 66 p., NASA CR-186683, N90-25223
30. "Study of Sample Drilling Techniques for Mars Sample Return Missions, Final Report", Martin Marietta Corp., 1980, NASA CR-160723, N80-27256
31. R.J. Amundsen, B.C. Clark, "Study of Sampling Systems for Comets and Mars", Martin Marietta Corp., 1987, 196 p., NASA CR-185514, N89-29292
32. V.I. Balovnev, "New Methods for Calculating Resistance to Cutting of Soil", Moscow Automobile-Highway Institute, 1963, Translated by Amerind Publishing Co, New Delhi, 1983
33. M.P. Nathan, F. Barnes, Hon-Yim Ko, S. Sture, "Mass and Energy Tradeoffs of Axial Penetration Devices on Lunar Soil Simulant" in Engineering, Construction and Operations in Space III, Space'92 Proceedings of 3rd Int. Conf., Denver, 1992
34. C.G. Cooley, "Viking 75 Project, Viking Lander System Primary Mission Performance Report", April 1977, Martin Marietta Corp., 105 p., NASA CR-145148, N77-29045
35. Eric Byler, "Design and Control of Ultralight Manipulators", SPIE Vol. 1387, Cooperative Intelligent Robotics in Space, 1990, pp. 313-327
36. N. A. Holmberg, R. P. Faust, H. Milton Holt, Viking '75 Spacecraft Design and Test Summary, Volume 1 - Lander Design, NASA RP-1027, NAS 1.61:1027/0.1, Nov. 1980
37. E.R. Rouze, M.C. Clary, D.H. Le Croisette, C.D. Porter, J.W. Fortenberry, "Surveyor Surface Sample Instrument", JPL Technical Report 32-1223, 1968, NASA CR-93205, N68-17411
38. Stock Drive Products, 2101 Jericho Turnpike, New Hyde Park, NY 11040
39. Maxon Precision Motors, inc. 838 Mitten Rd., Burlingame, CA 94010
40. James R. Wertz and Wiley J. Larson, "Space Mission Analysis and Design", Kluwer Academic Publishers, 1991
41. Grant H. Heiken, David T. Vaniman, and Bevan M. French, "Lunar Sourcebook", Cambridge University Press, 1991
42. M. G. Bekker, "Introduction to Terrain-Vehicle Systems", The University of Michigan Press, 1969
43. James K. Mitchell, W. David Carrier, Nicholas C. Costes, et. al., "Apollo 17 Preliminary Science Report", Chapter 8 Soil Mechanics, NASA
44. David R. Scott and Richard R. Gordon, "Apollo 15 Mission Report", The Society of Experimental Test Pilots, Symposium, 15th, Beverly Hills, CA September 16-18, 1971, pages 115-129

45. Eagle Engineering Inc., "Lunar Surface Transportation Systems Conceptual Design Lunar Base Systems Study Task 5.2", July 1988, NASA Contract NAS9-17878
46. J.R. Matijevic, W.C. Dias, et. al., "Surface Transport Vehicles and Supporting Technology Requirements", AIAA Space Programs and Technologies Conference, March 1992, AIAA 92-1485
47. D. S. Pivrotto, W.C. Dias, "United States Planetary Rover Status -- 1989", NASA-CR-186848, May 1990 (JPL Publication 90-6)
48. Roger Bedard, Brian K. Muirhead, et. al., "Planetary Rover Technology Development Requirements", Proceedings of the NASA Conference on Space Telerobotics, Jet Propulsion Laboratory, Jan. 31, 1989, pages 257-264
49. Alexander Kemurdjian, "Experiencing in Creating Self-Propelled Undercarriages for Planet Rovers", Journal of Aerospace Engineering, Vol 4, No. 4, October 1991
50. A. Kemurdjian, V. Gromov, V. Mishkinyuk, V. Kucherenko, P. Sologub, "Small Marsokhod Configuration ", International Conference of Robotics and Automation, IEEE, Nice, France, May 1992.
51. A. Kemurdjian, V. Gromov, "The Small Mars Rover", Space Engineering / Construction / Operations
52. "Russians to Test Rover in U.S.", Aviation Week and Space Technology, February 10, 1992, page 66
53. Steven J. Isakowitz, "International Reference Guide to Space Launch Systems", AIAA, 1991 Edition
54. Stephen A. Bailey, et. al., Common Lunar Lander, AIAA Space Programs and Technologies Conference, March 1992, AIAA 92-1481
55. Artemis Common Lunar Lander Phase 2 Study Results for External Review, NASA Johnson Space Center, March 10, 1992
56. William Boyer, "U.S. Rover may Hitch Mars Ride with Russians", Space News, December 1992
57. Tsutomu Iwata, Yoshio Toriyama and Mitsuru Yamada, "Lunar Rovers Exploration and Sample Return", Proceedings from an AAS/NASA International Symposium on Orbital Mechanics and Mission Design, NASA Goddard Space Flight Center, Greenbelt, Maryland, April 24-27, 1989, pages 525-537

Appendix A:
Sampling Concept Data Sheets.

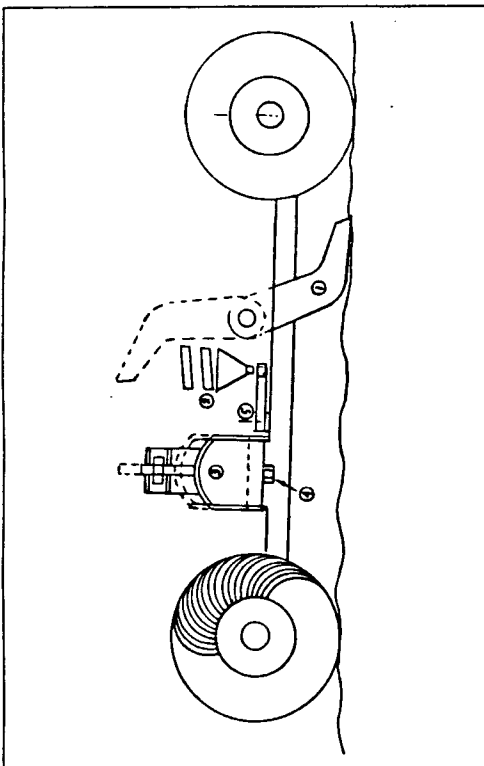


Brush Sweeper

Mass: 11.3 kg
Dimensions: width 1.6 m, brush dia 60 cm
Power: 3760 W
Depth: surface
Efficiency: 120 cubic-ft/hour = 3 398 021.6 cc/hour
 lift height 160 cm
Energy/10cc: ~0.68 W-min (takes rough 11 ms)

References: R. Cannon, S. Henninger, M. Levandoski, J. Perkins,
 J. Pitchon, R. Swats, R. Wessels:
 "Lunar Regolith Bagging System" (1990)
 NASA CR-186683; N90-25223

Notes: *Sweeper width of 2 cm, reduces mass flow and power to 1.5 cubic-ft/hour = 708 cc/min,
 P=47 W, sampling time 0.9 s.
 *Reduce lift height, sweeper diameter and speed for additional mass and power reduction.
 *Mechanisms to move brush are not included in power estimation.

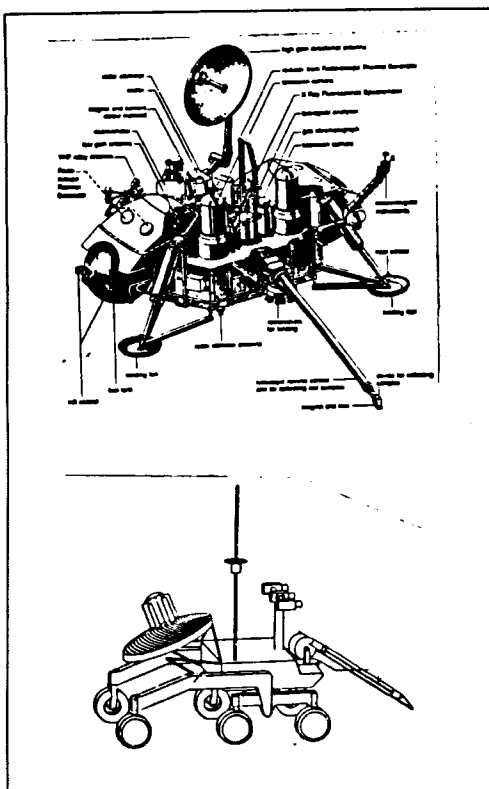


Flip Scoop

Mass: 0.165 kg
Dimensions:
Power: 2 W max (12 W for rover movement)
Depth: surface
Efficiency: 1 sample/33 s
Energy/10cc: 1.43 W-min

References: I.N. Sviatoslavsky,
 Senior Scientist, Fusion Technology Institute, Nuclear
 Engineering and Engineering Physics Department, and
 Wisconsin Center for Space Automation and Robotics,
 University of Wisconsin-Madison, Madison, WI, 53706

Notes: Uses back and forward movement of rover.



Extendible Reel Stored Boom

Mass: 11.3 kg
Dimensions: 61.48x23.37x34.29 cm
Power: 30 W max

Depth: surface
Efficiency: extends to full length of 3 m
 shear: 20 N
 digging: 133 N
 scraping: 88 N
Energy/10cc: 720-1440 W-min (very conservative)

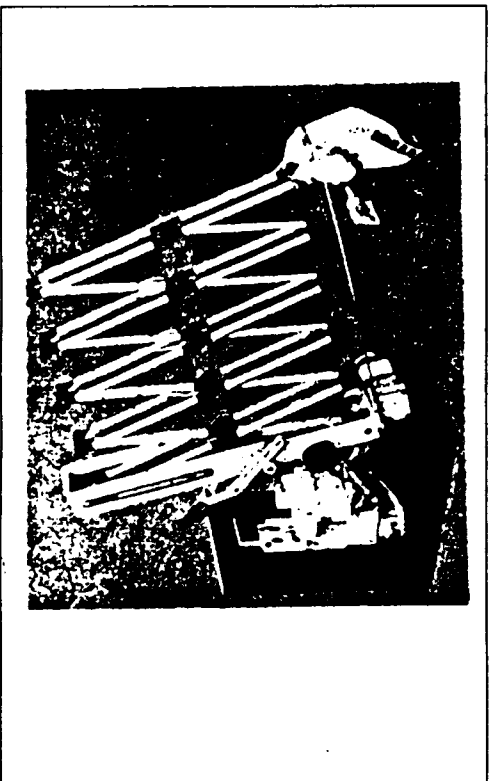
References: B. J. Hogan, "Thin Foil Booms Extend Nested Rocket Cones", Brunswick Defence, Design News, Cahners Publishing Company, May 25, 1982

Brunswick Corporation, Defence Division,
 "Brunswick Spacecraft Booms", 14 pp.

C.G Cooley, "Viking 75 Project, Viking Lander System
 Primary Mission Performance Report", 1977,
 NASA CR-145148, N77-29045

Notes: *Conservative estimation for energy/sample is estimated by assuming full power during whole sampling period taking typically 24-48 min.

TY 7/16/93



Lozy Tongz

Mass: 6.7 kg (mechanics + auxiliary equipment)
Dimensions: 13 x 42 x 8 cm, extended length 152 cm
Power: ~25 W

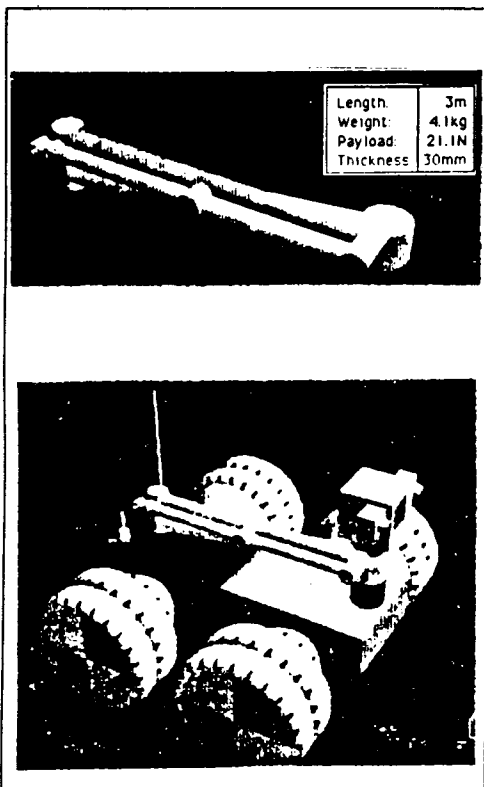
Depth: 5-7.5 cm 1st pass, 15-17.5 cm 3rd pass (width 5 cm)
Efficiency: 38-50 cm: 40 s 1st pass, 150 s 3rd pass
 89 N pull, 6.7 N push
Energy/10cc: ~0.2-0.8 W-min

References: "Surveyor III, A Preliminary Report"
 NASA SP-146, N67-32588, 1967

E.R. Rouze, M.C. Clary, D.H. Le Croisette, C.D. Porter,
 J.W. Fortenberry,
 "Surveyor Surface Sample Instrument",
 JPL Technical Report 32-1223, NASA CR-93205,
 N68-17411, 1968

I.I. Cherkasov, V.V. Shvarev,
 "Lunar Soil Science", Moscow, 1971
 Translated by Israel Program for Scientific Transla
 Jerusalem, 1975

Notes: *During Surveyor missions TV-camera provided feedback of manipulator position.



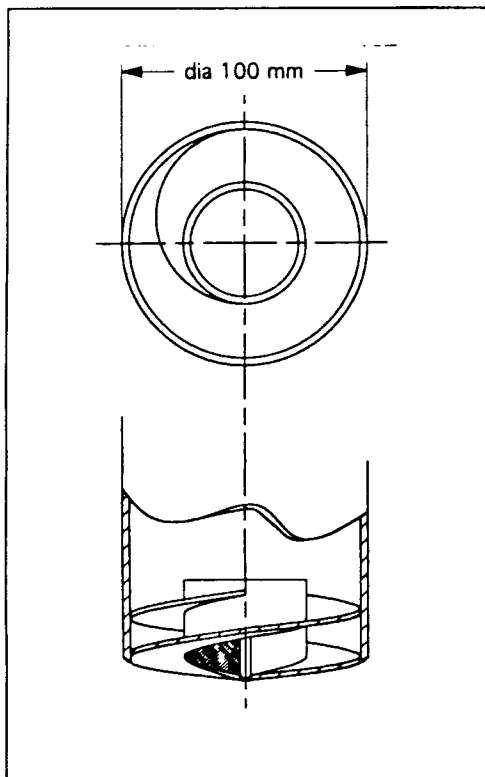
Robotic Arm Sampler

Mass: 4.1 kg (+scoop)
Dimensions: length 3 m
Power:
Depth: surface
Efficiency: payload 21.1 N; tool tip speed 10-50 cm/s
 max joint torque 22.9 Nm
Energy/10cc:

References: Eric Byler: "Design and Control of Ultralight Manipulators" SPIE Vol. 1387 Cooperative Intelligent Robotics in Space (1990) pp. 313-327

Notes: * Same arm may be capable of taking care of sample transfer and other functions.

TY 7/23/93



Surface Drill

Mass: ~5 kg (includes positioning mechanisms)
Dimensions:
Power: 1-5 W, moment 0.14-0.26 Nm
Depth: 1-5 cm
Efficiency: 10-50 cc/r
Energy/10cc: 0.02-0.04 W-min/r

References: -

Notes: *Positioning mechanism sets drill vertically on surface and drill is rotated 1-5 rounds. Drill is then lifted and turned in horizontal position and rotated backwards. Loose soil sample drops into funnel below drill.
 *Power estimation is based on cutting resistance to Drag Line and doesn't include friction or adhesion forces.
 *Mass is dominated by positioning mechanisms and is estimated to meet mass of Lazy Tongs or Robotic Arm Sampler or Surface Sample Collection System.

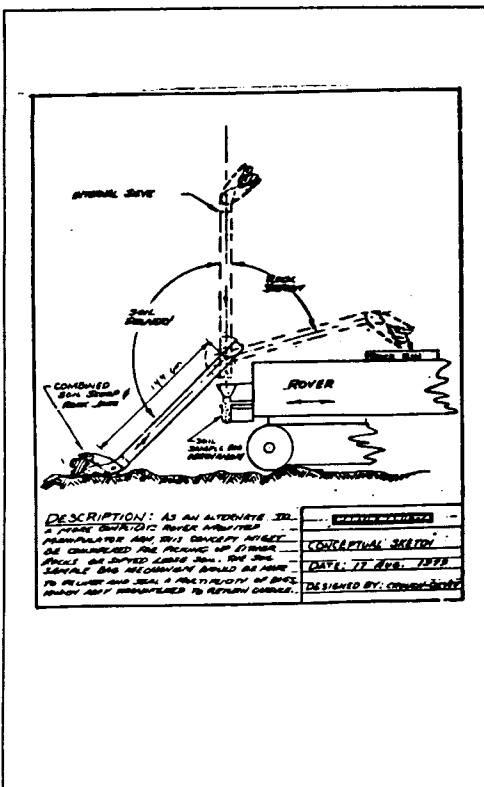
Surface Sample Collection Syst.

Mass: 5.2 kg
Dimensions: length 144 cm
Power: 24.5 W/8.8 min peak (arm+Sequencer)

Depth: surface
Efficiency: 1 sample/24 min; capable to grasp dia 10-20 cm rocks
Energy/10cc: 481 W-min/sample (Sample storage dropped off)

References: "Study of Sample Drilling Techniques for Mars Sample Return Missions -Final Report" (1980)
 NASA CR-160723; N80-27256

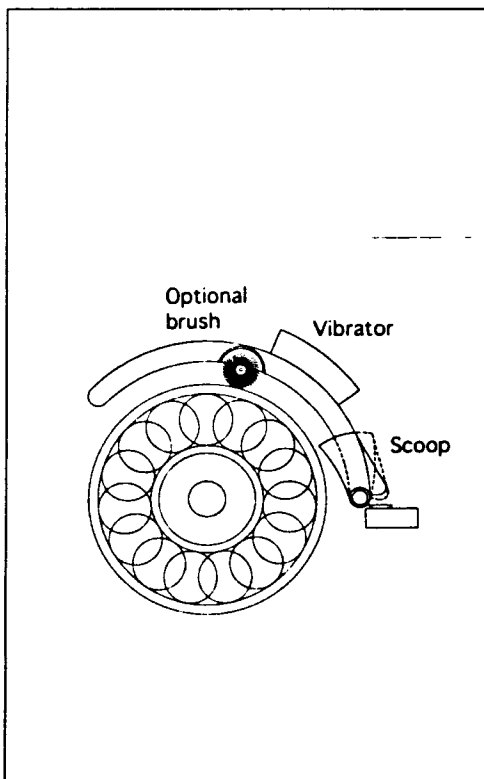
Notes: *Mass includes sample collection hand: 2.7 kg and Electronic Sequencing unit: 2.5 kg.
 *Uses back and forward movement of vehicle.

**Wheel Collector**

Mass: 0.5-1.5 kg (estimation)
Dimensions: -15 x 10 x 5 cm
Power:

Depth: surface
Efficiency:
Energy/10cc:

References: -



Notes: *Use vibrator or gas to clean fender of old dust.
 *Open scoop on sampling site.
 * When driving dust is blown to scoop. If not, additional brush may be used to give dust more velocity.

Appendix B:

Sample Manipulating Arrangement; Proposal I

Sample Manipulating Arrangement; Proposal I

A sample manipulating arrangement takes care of sample handling after it is received from the sample acquisition device. The main objective of this part of the study was to find the critical points of the design. Here the overall mass is minimized by integrating all functions into one structure utilizing only one stepper motor. Several problems were found and solutions to them are proposed. With the help of this knowledge a new and better design will be presented.

The Figure B.1 below illustrates system layout and more accurate drawings are enclosed in the end of appendix B.

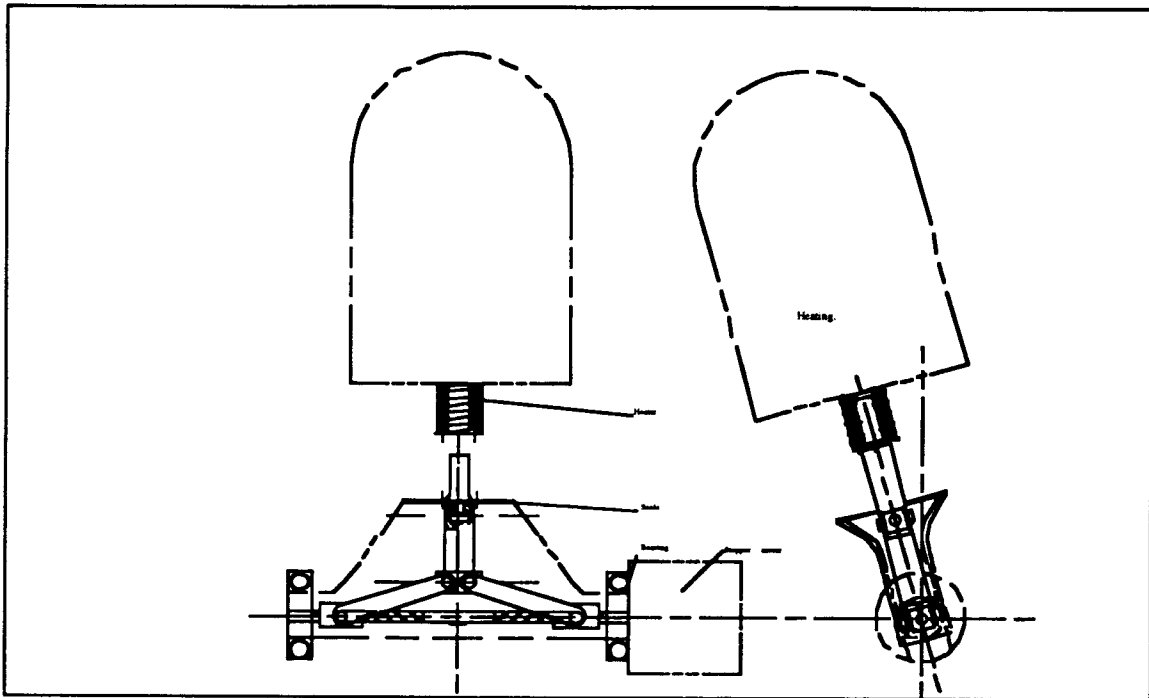


Figure B.1 Sample Manipulating Arrangement; Proposal I.

Function

- 1) In the lower vertical position the linkage is stretched out to the limits and the container is resting on the scale, as illustrated in sketch 01-02, figure I and sketch 02-01, figure I. To calibrate the scale, the calibration mass is lowered into the container by an electric motor.
- 2) After calibration a stepper motor rotates the lead screw 15 degrees clockwise. Because the linkage has met its limits, the moment of the motor is transferred to the support structure of linkages which now rotates stretching the spring. See figure II in sketch 01-02.
- 3) The soil sample is deposited into the funnel and flows through the sieves into the container. When the stepper motor is rotated 30 degrees counterclockwise the spring pulls the linkage support structure into position 15 degrees counter clockwise from vertical position, where movement is stopped by mechanical limits. As the container passes the sweeper, the level of soil in the container is smoothed.
- 4) When the linkage support structure has reached its rotational limit, the rotational movement of the lead screw extends the linkage and lifts the container into the heater. The bottom plate of the container seals the vacuum chamber. This is illustrated in figure III in sketch 01-02.
- 5) After the heating, the spring keeps the linkage support steady, the stepper motor is rotated clockwise and the linkage lowers the container.
- 6) When the lowest position is achieved, the motor starts to rotate the linkage support which stretches the spring. The motor is rotated 195 degrees and the soil in the container falls out, as in figure IV.
- 7) The motor is rotated counterclockwise and the spring pulls the linkage support back to vertical position.

Analysis

Table B.1 System Characteristics for Proposal I.

Linear Pairs	2
Revolute Pairs	6
Screw Pairs	2
Stepper Motors	1
Servo Motors	1
Power	~2 W
Container Mass to be heated	4.63 g
Container Mass to be weighed	4.63 g
Height	~319mm
Length	~203 mm
Width	~100 mm
Structure Mass	~200 g
Motors and Bearings	~300 g
Electronics Card	~150 g
Overall Mass	~650 g

Problems

1) Container mass is approximately 2.9 times the mass of the sample. This may lead to inaccurate weighing and greater energy consumption during heating. The main reason for high mass is the wide and strong bottom plate, which is used to seal the vacuum chamber.

Solution: Seal the chamber with other parts of the mechanism. The sealing part must be larger than any other part of the container that is to be sealed inside the chamber and it has to be below the container.

Consequence: The weighing procedure must be carried out elsewhere since the sealing surface can't get through the scale which was able to support the container.

2) The container rests on the scale when filling it and measuring the volume. Forces caused by these operations may damage the scale.

Solution 1: Carry out weighing elsewhere.

Solution 2: Carry out volume measurement elsewhere.

Solution 3: Lift linkages a few millimeters:

Consequence: There would be a need for separate motors for linkage extension and linkage support rotation.

3) There is no place for excess soil which may fall on the sealing surface and scale.

Solution 1: Design flexible funnel for excess soil.

Solution 2: Carry out volume measurement elsewhere.

4) In case of linkage support structure jamming the linkage tends to extend which may be hazardous.

Solution 1: Use strong spring.

Consequence: Enlarged power requirement.

Solution 2: Use separate motors for linkage extension and linkage support rotation.

5) When pulling the container out of the heater, friction or jamming cause moment to the linkage support which leads to jamming of the system.

Solution 1: Use strong spring.

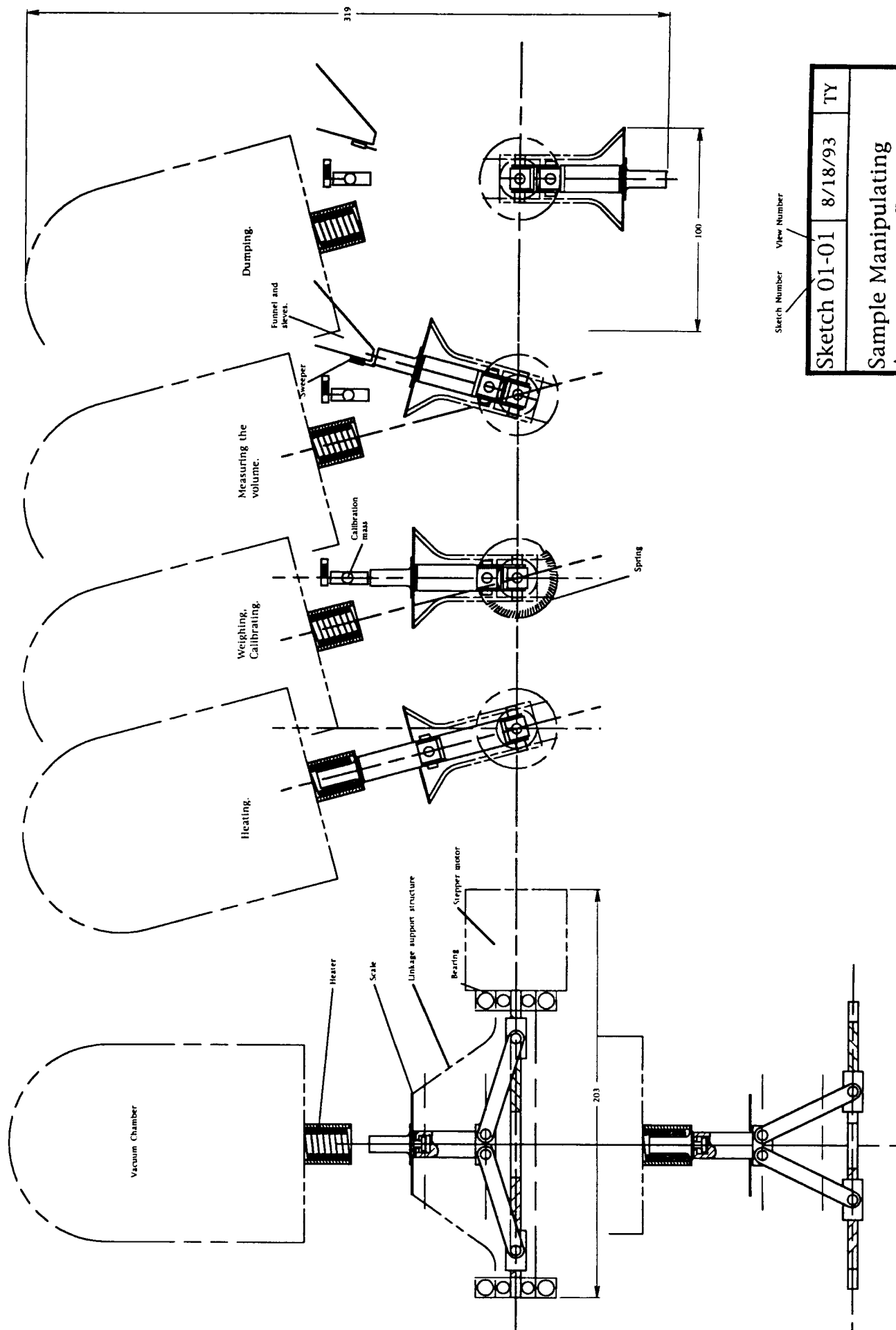
Solution 2: Use separate motors for linkage extension and linkage support rotation.

6) To allow weighing, the container has 1 mm loose in vertical direction. This allows the container to twist and jam in the heater.

Solution: Carry out weighing elsewhere.

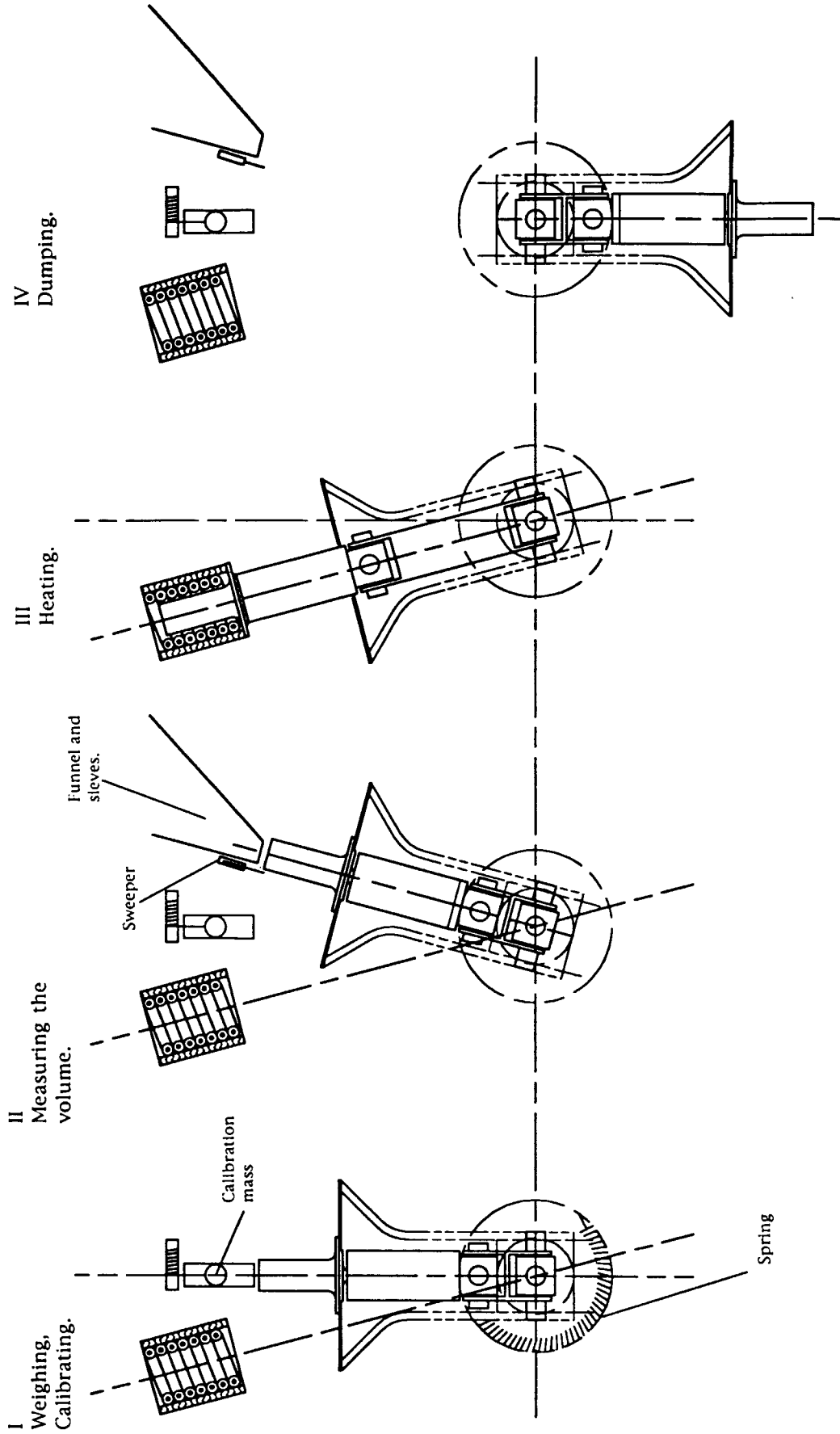
Conclusions

For this kind of mechanism the volume measurement and weighing should be carried out separately from sealing, heating and dumping. By transferring weighing and volume measuring elsewhere problems 1), 2), 3), and 6) are solved with some mass and energy penalty. Solution to problems 4) and 5) is either enlarged controllability with some mass penalty or a risky use of a plain force.

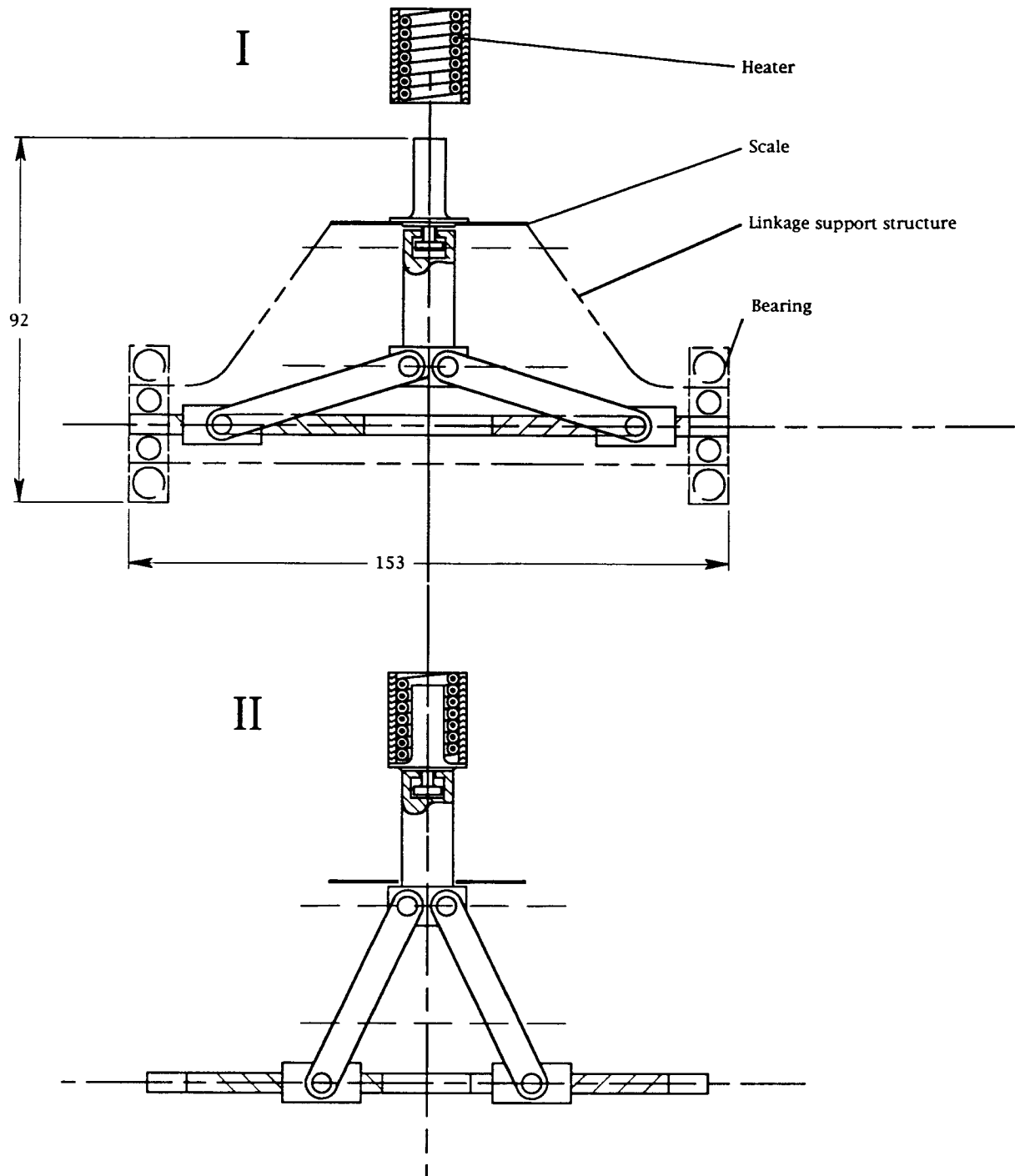


Sketch Number View Number

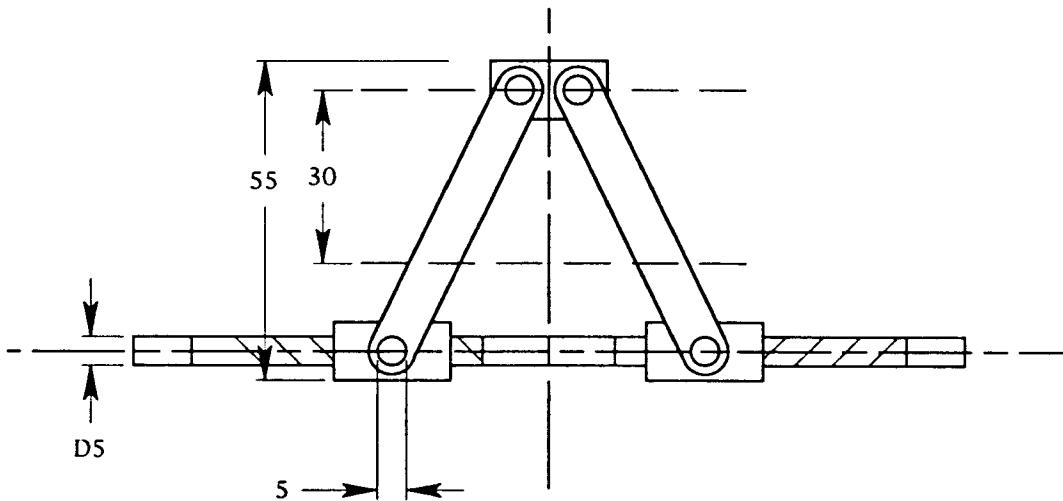
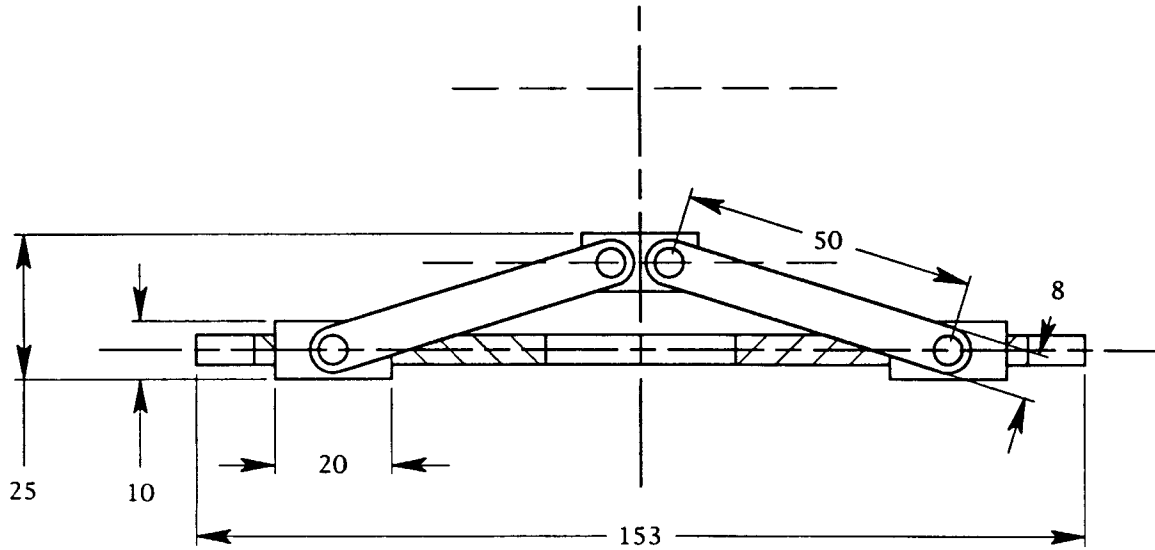
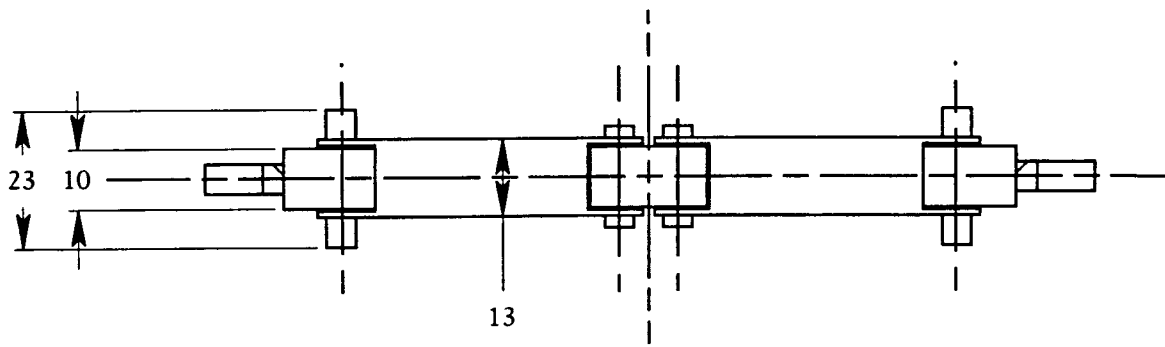
Sketch 01-01	8/18/93	TY
Sample Manipulating Arrangement; Proposal I		



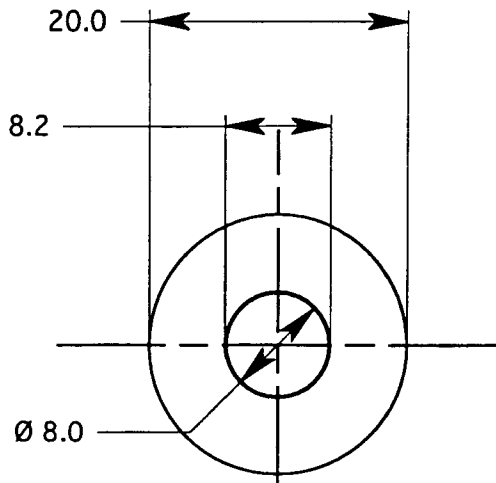
Sketch 01-02	8/18/93	TY
Function of the Sample Manipulating Arrangement; Proposal I		



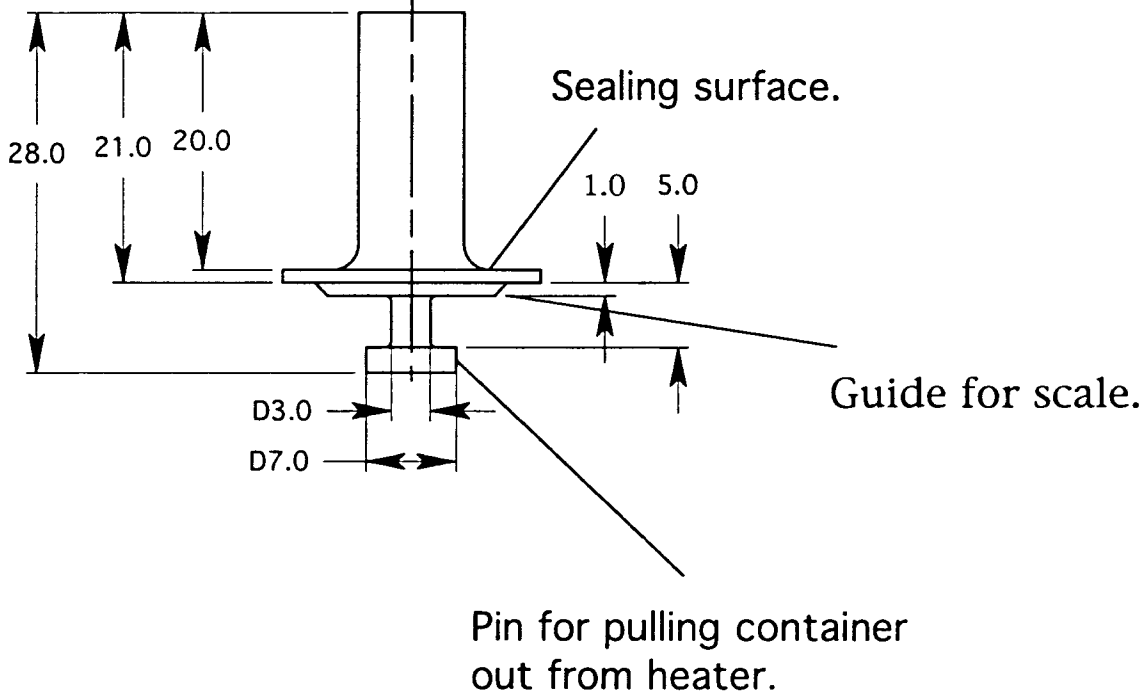
Sketch 02-01	8/18/93	TY
Sample Manipulating Arrangement; Proposal I Lifting Unit		



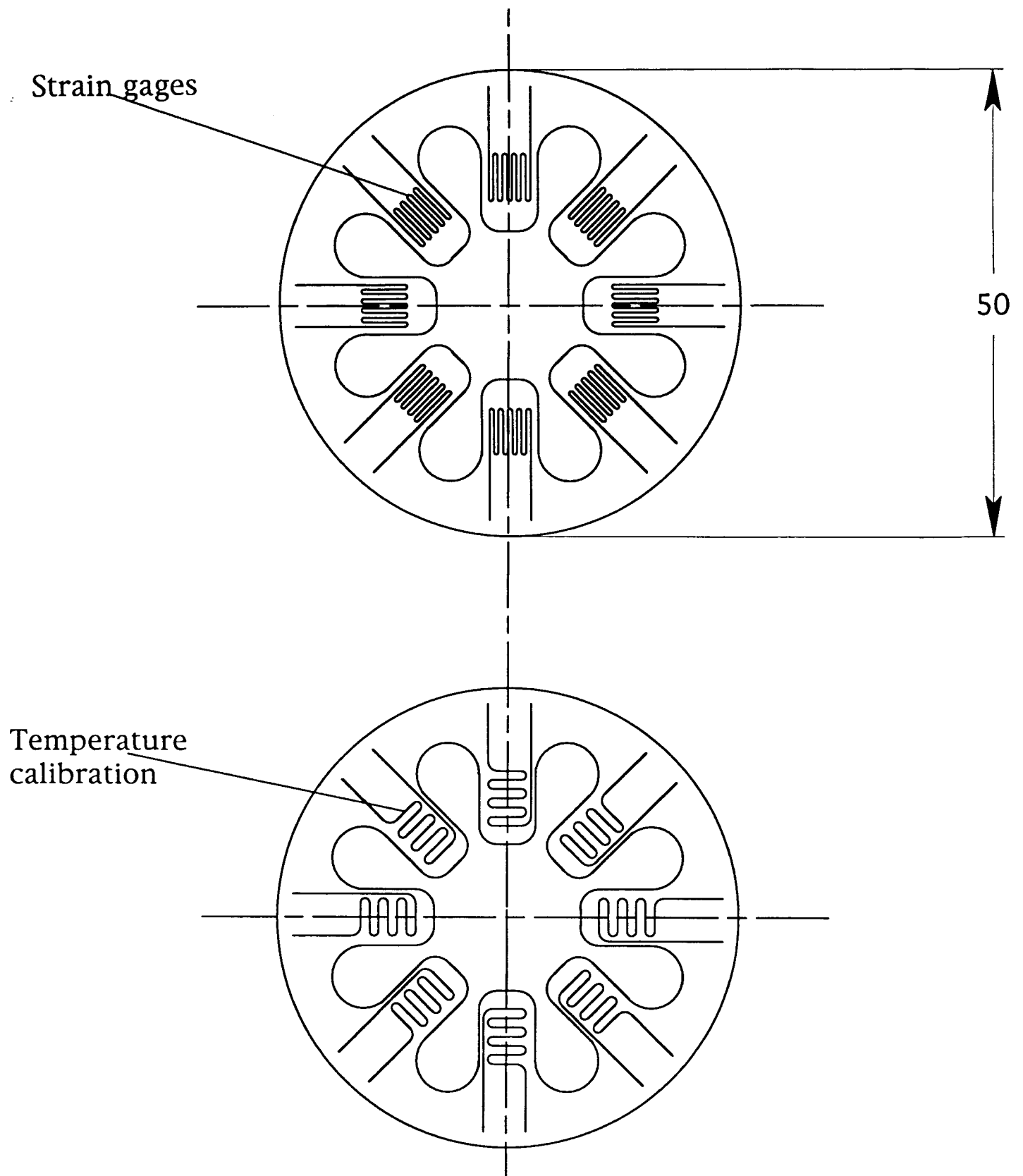
Sketch 03-01	8/18/93	TY
Linkage for the Lifting Unit		



Material volume:
 container walls: 0.051 cm³
 bottom plate: 0.491 cm³
 pin: 0.105 cm³
sum: 0.647 cm³
 material: steel, 7.78 g/cm³
mass: 5.03 g



Sketch 04-01	8/18/93	TY
Sample Container for the Sample Manipulating Arrangement; Proposal I		



Thickness: 0.1 - 0.5 mm
Material: steel
Mass: 5.1 - 25.5 g

Sketch 05-01	8/18/93	TY
Weighing Scale for the Sample Manipulating Arrangement; Proposal I		

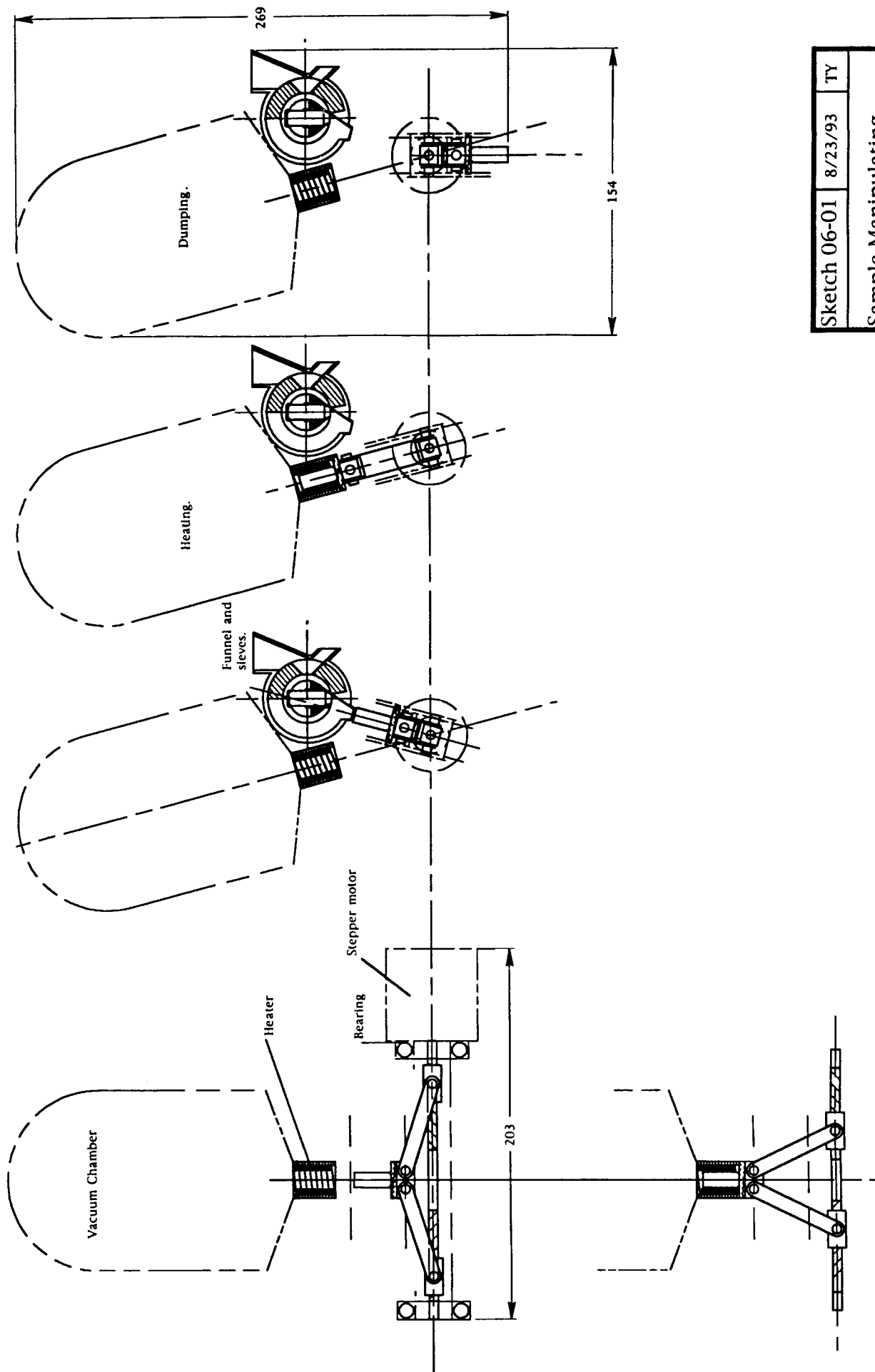
Appendix C:

Sample Manipulating Arrangement; Proposal II

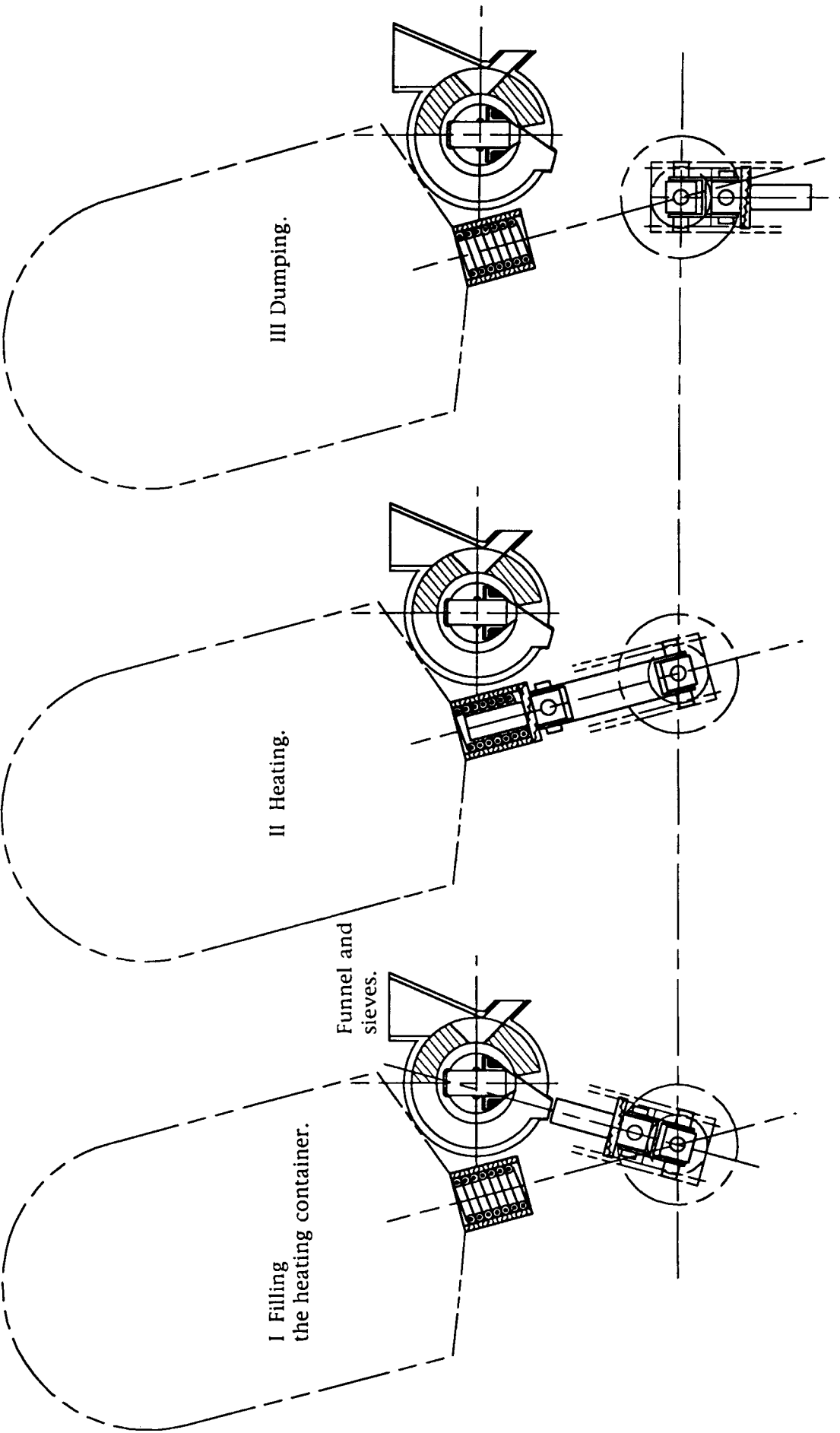
A Parts List for the Measuring Unit

The parts for the measuring unit are illustrated in sketch 08-01.

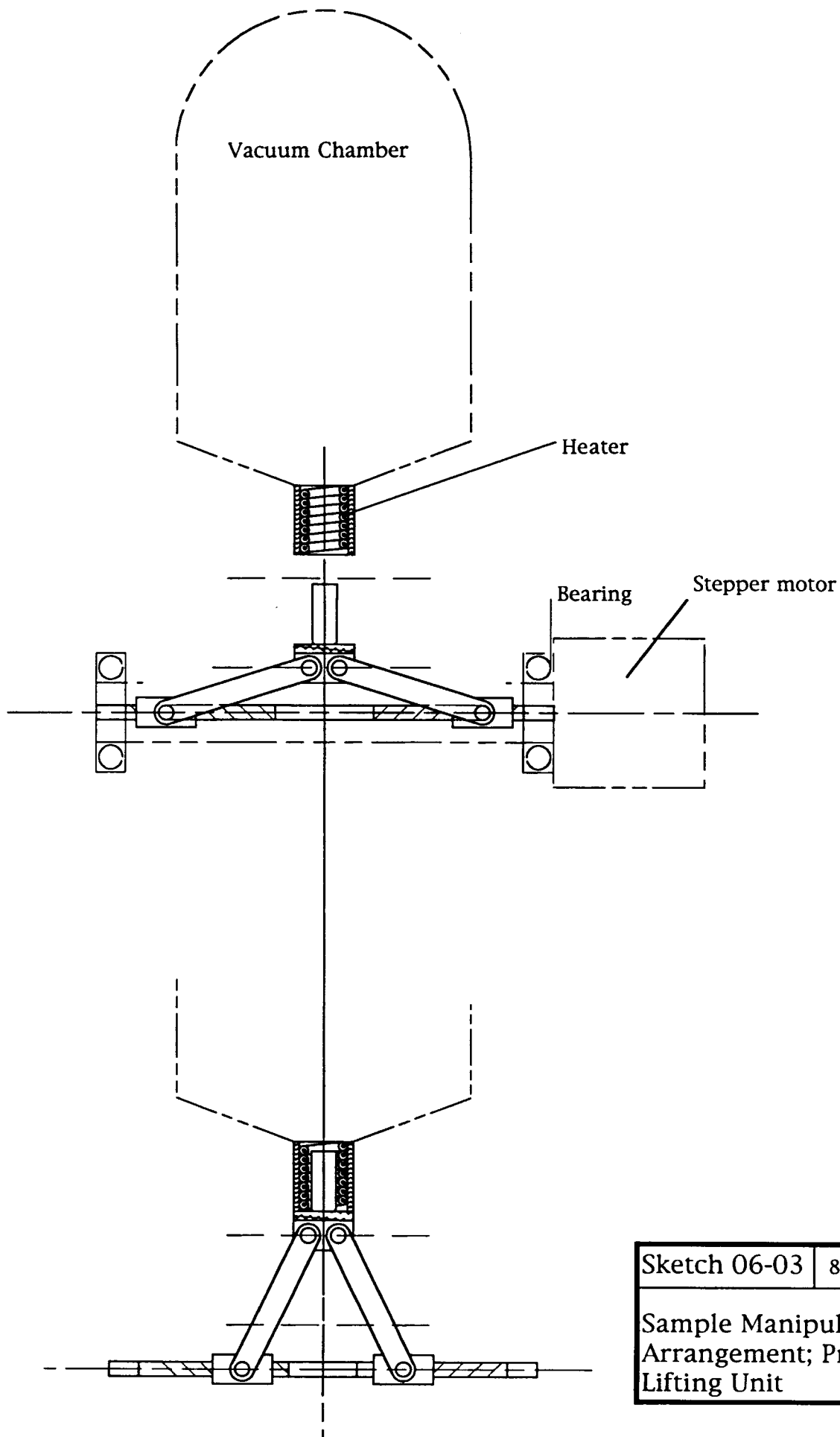
1) Scale	Aluminum, Titanium or BeCu
2) Flipper	Steel or Titanium, outside toothing
3) Slider	Steel or Titanium and soft polymer, inside toothing
4) Pinion	Steel or Titanium
5) Electromagnet	Steel or Cobalt
6) Calibrating weight	Steel
7) Weighing container	Aluminum
8) Pinion bearing	Steel or composite
9) Ball bearing	Steel
10) Stepper motor	
11) Body	Aluminum



Sketch 06-01	8/23/93	TY
Sample Manipulating Arrangement; Proposal II		

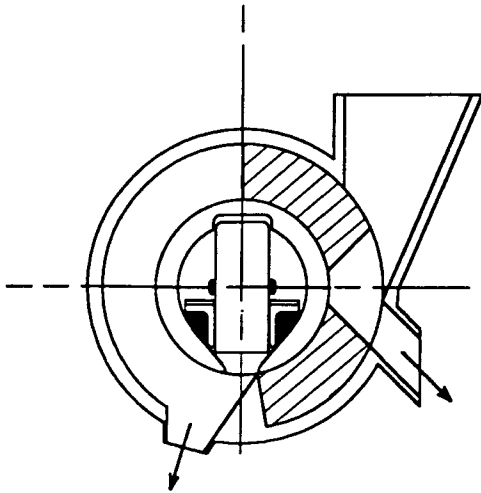


Sketch 06-02	8/23/93	TY
Function of the Lifting Unit; Proposal II		

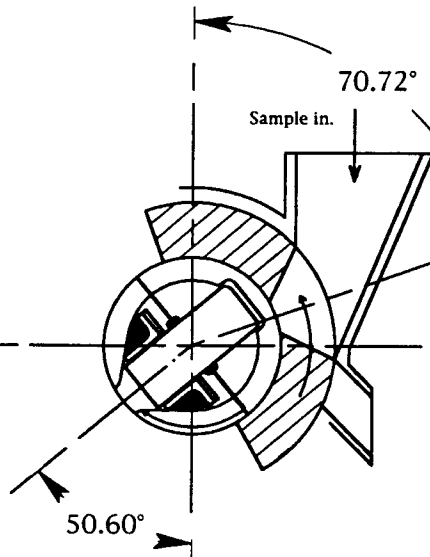


Sketch 06-03	8/23/93	TY
Sample Manipulating Arrangement; Proposal II Lifting Unit		

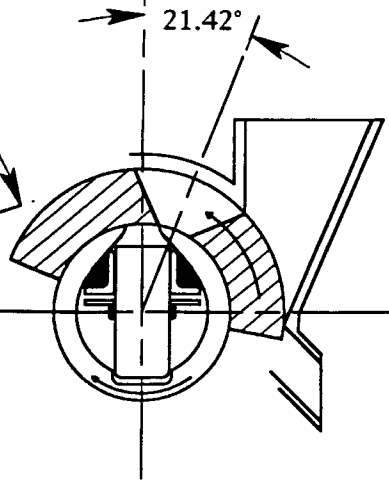
I Emptying and dumping.



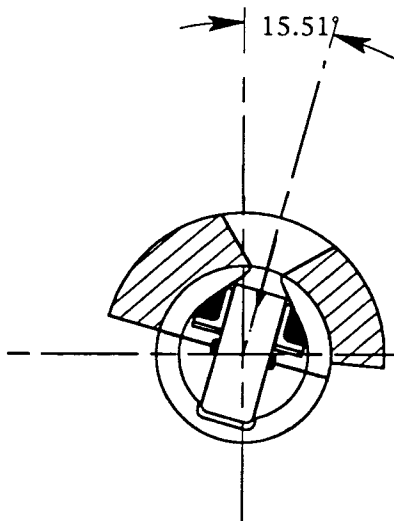
II Receiving sample.



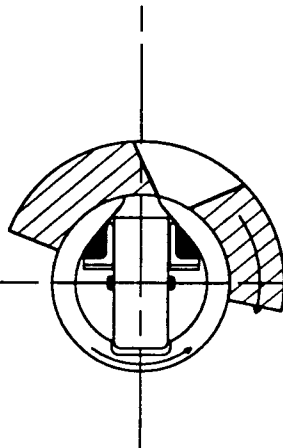
II Measuring the volume and calibrating.



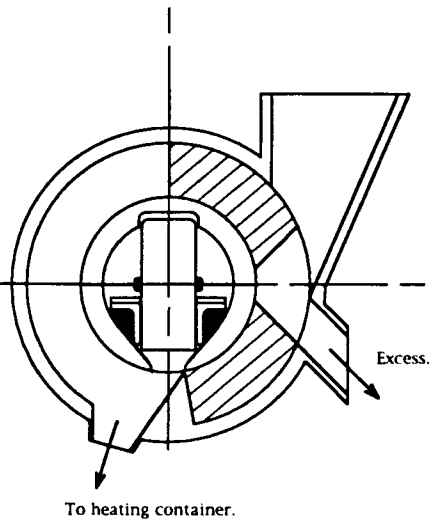
IV Filling the container.



V Weighing the sample.

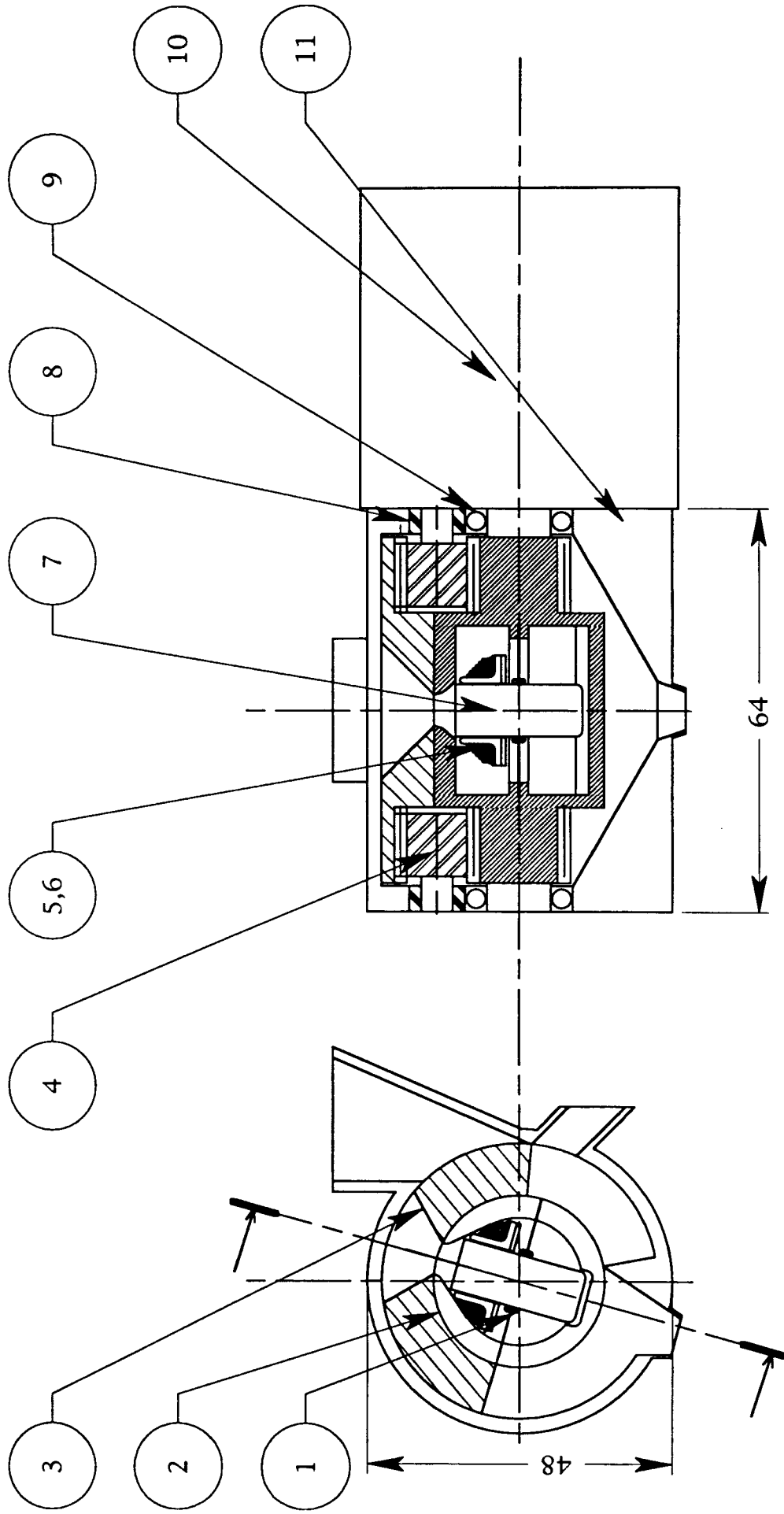


VI Emptying and dumping.

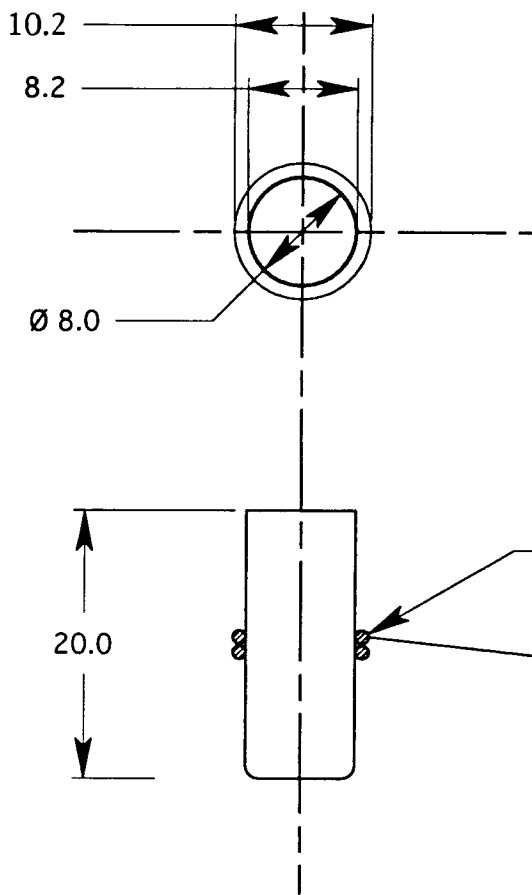


Sketch 07-01	8/23/93	TY
--------------	---------	----

Function of the Measuring Unit; Proposal II
--

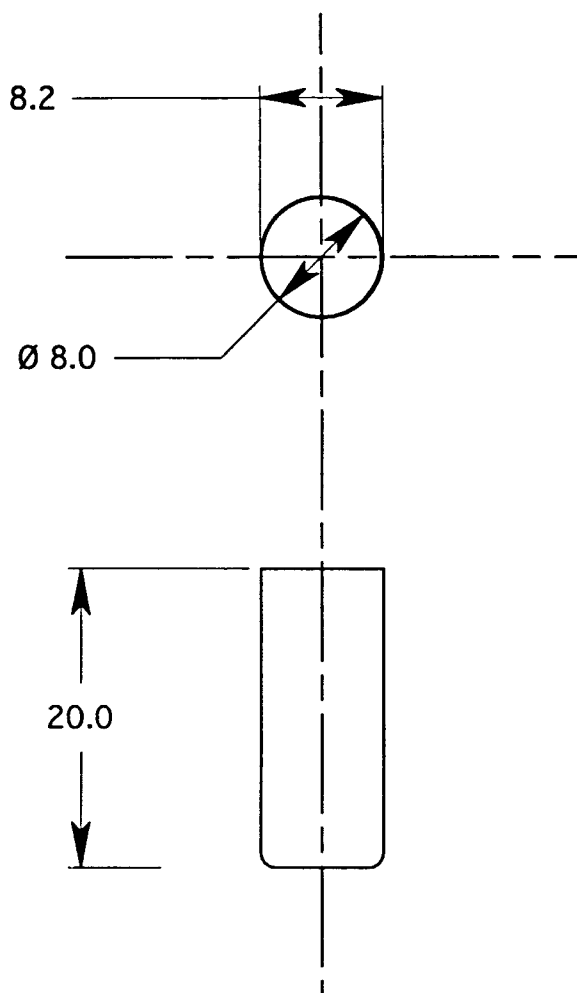


Sketch 08-01	8/23/93	TY
The Measuring Unit; Proposal II		



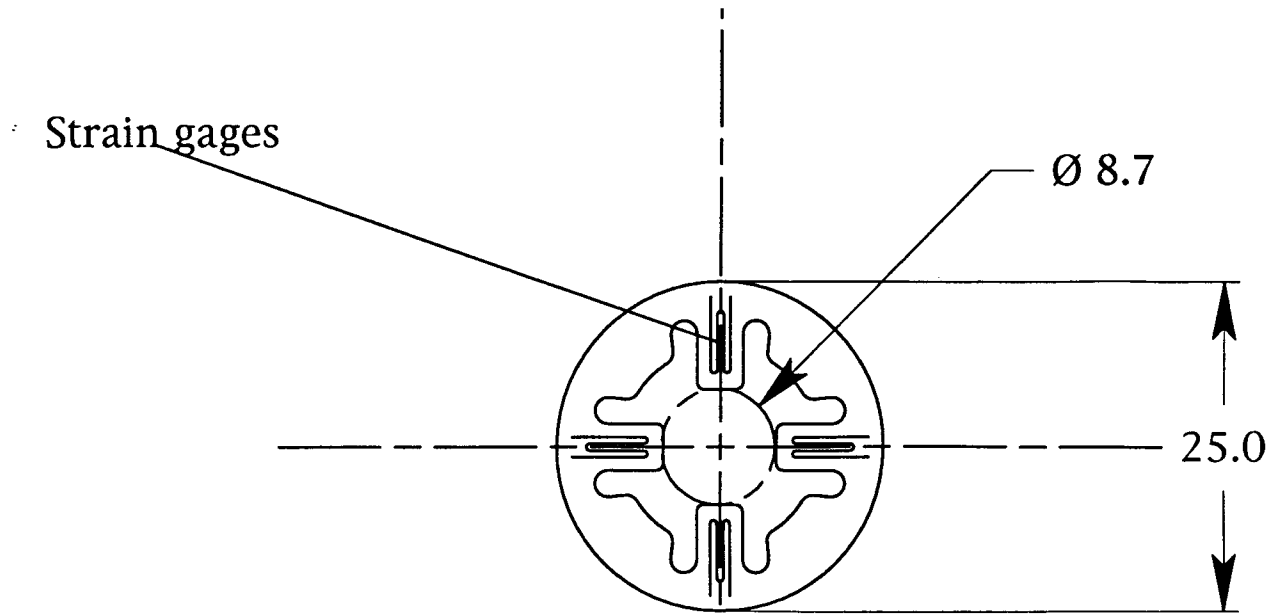
Material volume:
container: 0.0559 cm^3
rings: 0.0454 cm^3
sum: 0.101 cm^3
material: aluminium, 2.70 g/cm^3
mass: 0.27 g

Sketch 09-01	8/23/93	TY
Scaling Container for the Sample Manipulating Arrangement; Proposal II		

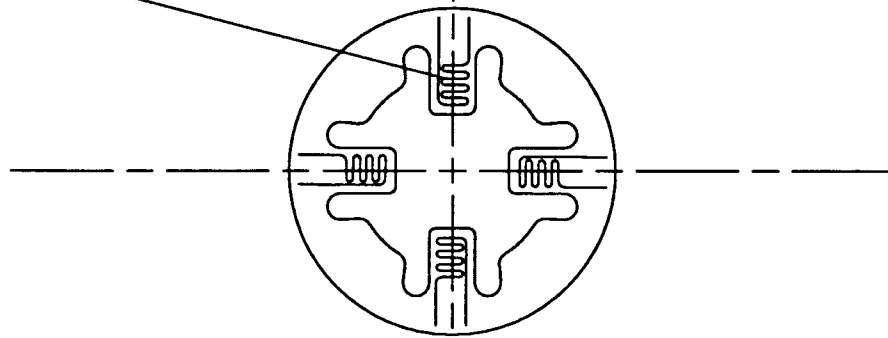


Material volume:
container: 0.0559 cm³
material: steel, 7.78 g/cm³
mass: 0.43 g

Sketch 10-01	8/23/93	TY
Heating Container for the Sample Manipulating Arrangement; Proposal II		



Temperature
calibration



Thickness: 0.1 - 0.5 mm
Material: steel, 7.78 g/cm³
Mass: ~0.34 - 1.70 g

Sketch 11-01	8/23/93	TY
Weighing Scale for the Sample Manipulating Arrangement; Proposal II		

Appendix D:

A Flip Scoop Preliminary Design and System Integration

A Scoop Arm/Obstacle Interaction

When the scoop hits an obstacle it starts to rotate away from the surface. The rate of an angular acceleration depends on surface geometry, arm angle and rover speed during scooping. Low speed with an almost horizontal arm on a smooth surface is an ideal situation. Figure D.1 below illustrates the situation where the scoop hits a buried rock. A nominal moment M of 1.4 Nm presses the scoop against the surface but a force F_t caused by the rock causes the arm to lift off of the surface. Final angular velocity ω depends on the rover speed V_r and arm angle.

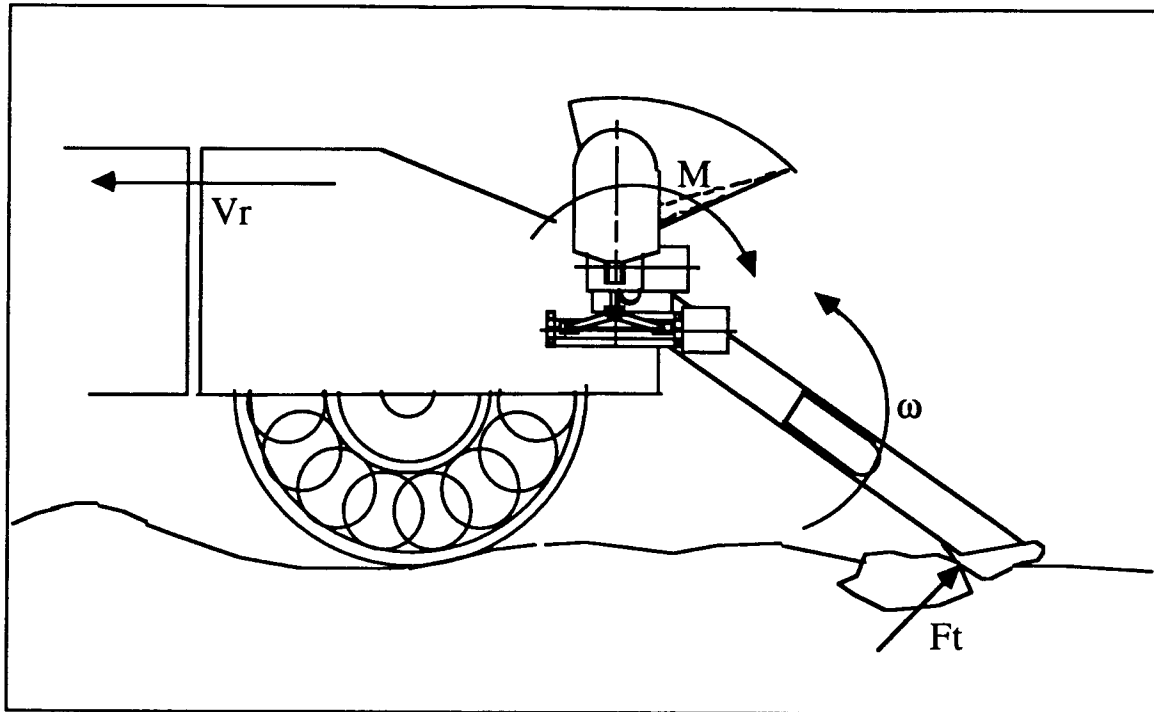


Figure D.1 Arm Interaction with A Buried Rock.

If the rover is roving with speed of 2.5 m/min and the 60 cm long arm is in a 45 degree angle to the surface, the obstacle on the surface makes the arm rotate with an angular velocity of 0.0496 rad/s. See Figure D.2. The velocity decreases as the arm rises.

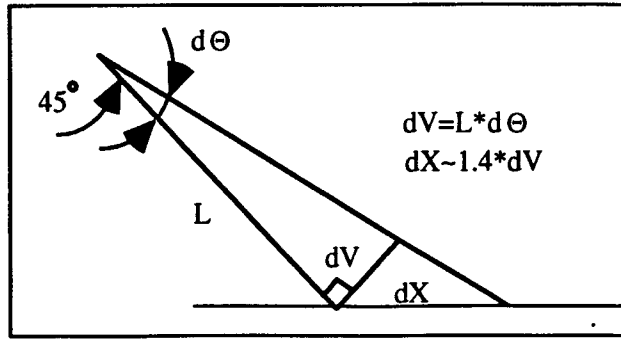


Figure D.2 Geometry of Arm/Obstacle Interaction

Because of the inertia the arm bends before it achieves the needed velocity. Bending increases until the arm velocity is 0.0496 rad/s and after that the energy of the bent arm increases the velocity further. When the arm is straight again, its velocity is higher than required and it bounces off of the obstacle due to its kinetic energy, unless a damper is used. Figure D.3 illustrates the collision. The 1.4 Nm nominal moment and bending due to it are left off for clarity. When using a spring or a slow control loop, (slow in terms of time of collision), the nominal moment stays constant and may be directly added to bending moments due to collision.

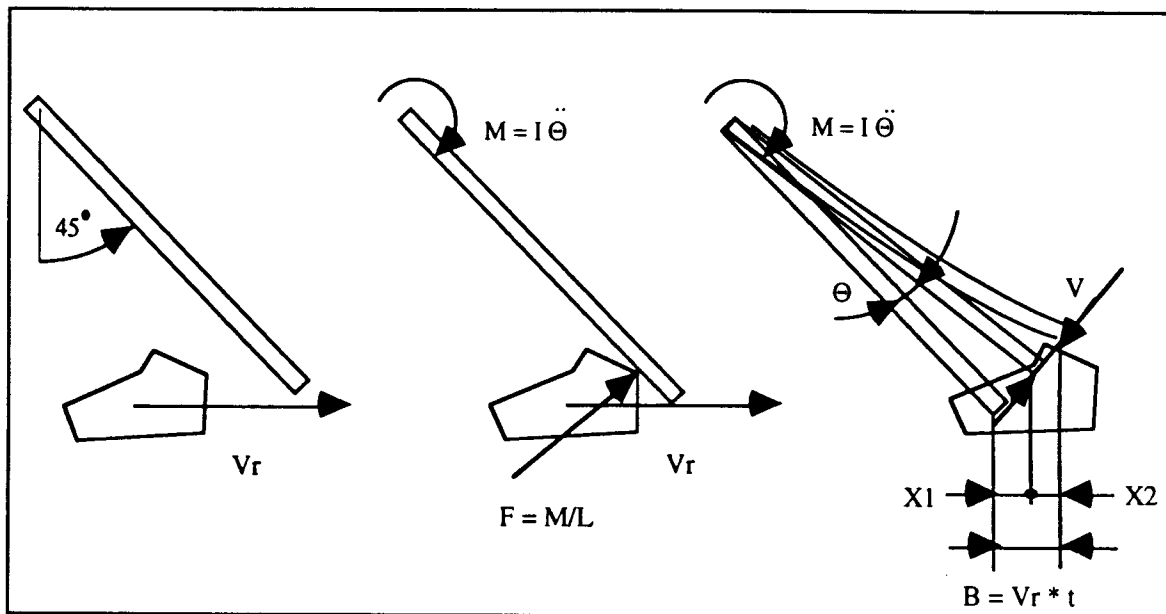


Figure D.3 Scoop Arm Yielding in Collision.

When the arm hits an obstacle, it is exposed to a force F . Inertia I of the arm tries to resist a change in an angular velocity and generates a bending moment M . After time t the rover has moved a distance of B , the arm has rotated an angle Θ causing a horizontal yield $X1$, and has bent a distance of V causing a horizontal yield $X2$. Now the bending V tends to rise the moment in the arm which then accelerates more rapidly and tends to increase $X1$, however, decreases $X2$. There exists also a negative feedback from turning angle Θ to bending V . Figure D.4 presents a mathematical model for the interaction.

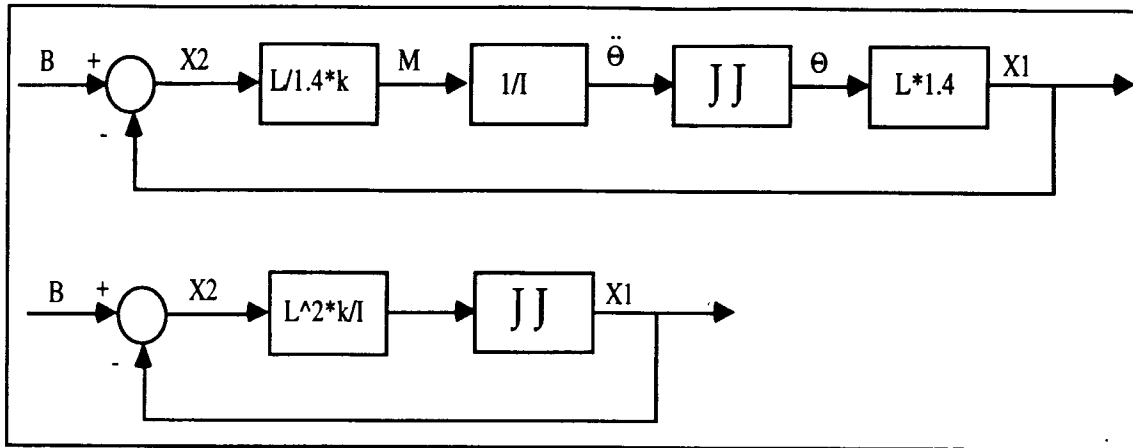


Figure D.4 Mathematical Model for Collision.

A multiplier 1.4 turns a tangential bending V to a horizontal yield $X2$, when the turning angle Θ is small. Error in $X2$ is less than 5% if Θ is less than 2.7 degrees, or $X1$ is less than 19.5 mm. The model is valid until $X1$ exceeds 19.5 mm or the arm bounces off of the obstacle, i.e. $X2 = 0$, whichever happens first. When the rover is roving with speed of 2.5 m/min, or 41.667 mm/s, it causes the total yield B , that is input to the system, to increase at the same rate. That is illustrated in Figure D.4 A 'CCMP' -computer program, version 0.6, (© 1990 by Neil Duffie) the model.

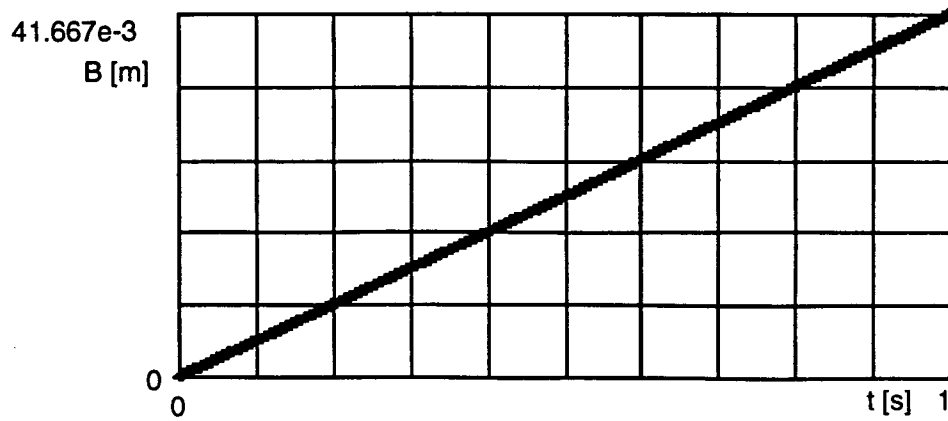


Figure D.5 System Input = Total Yield.

Structure of A Scoop Arm

For solving the model, a hypothetical scoop arm was designed. Figure D.6 below describes the internal structure.

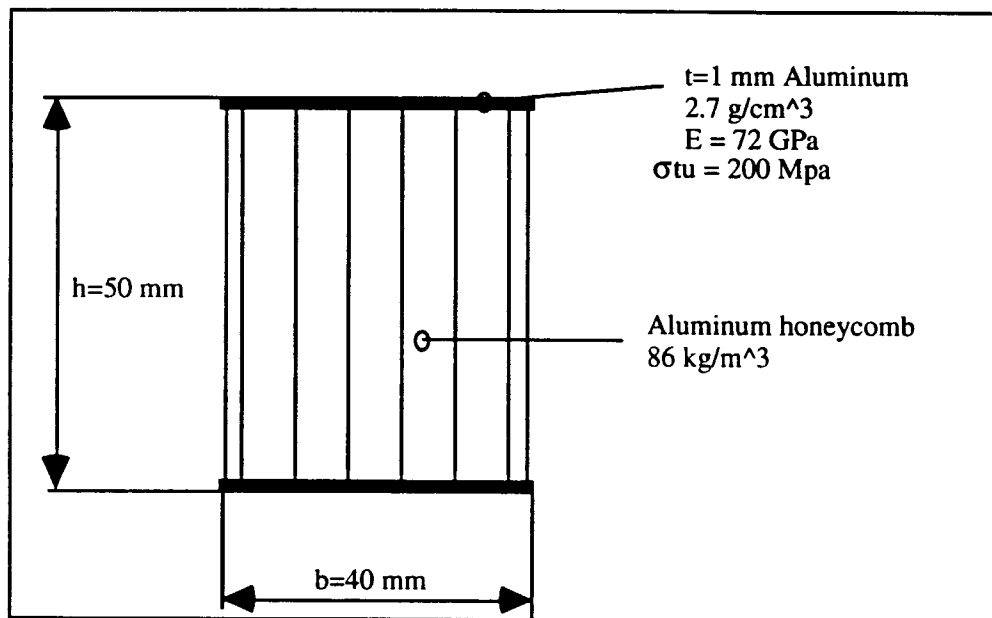


Figure D.6 Scoop Arm Structure.

The mass of the 60 cm long arm is approximately 233 g. Gravitational moment due to scoop mass is $m \cdot L/2 = 0.1$ Nm maximum. Inertia of the arm is $279\,600 \text{ g-cm}^2$, or 0.02796 kg-m^2 , it was calculated the following way:

$$(1) \quad I = \int_0^L r^2 dm = \int_0^L \frac{m}{L} r^2 dr = \frac{mL^2}{3}$$

Moment of inertia is approximately $5\text{e-}8 \text{ m}^4$:

$$(2) \quad I_z \approx 2 \cdot t \cdot b \cdot \left(\frac{h}{2}\right)^2$$

Bending stiffness $k=F/V$ for the 0.6 m long arm is 50 kN/m, when the force is applied to the tip of it.

$$(3) \quad k = \frac{F}{V} = \frac{3EI_z}{L^3}$$

The arm can carry 400 Nm moment, if wrinkling doesn't happen. (However, the wrinkling usually sets limits for loads.)

$$(4) \quad M_{\max} = 2 \cdot tb \cdot \sigma_{tu} \cdot \frac{h}{2}$$

A Scoop Arm Behavior With Different Instrumentation

A. Passive Force Generation

The scooping force is produced by generating a moment on the scoop arm by a spring that is stretched by a stepper motor or a position controlled servo motor. The spring moment is assumed to stay constant during collision. This is valid if the arm doesn't rise very much during the acceleration time or if the spring constant is low. There is no closed loop force or position control for scooping and the total inertia of the system equals to inertia of the arm. Curves in Figure D.7 present the yield due to bending (X2) and due to rotation (X1). The gain $L^2 \cdot k/I$ is 643776.824.

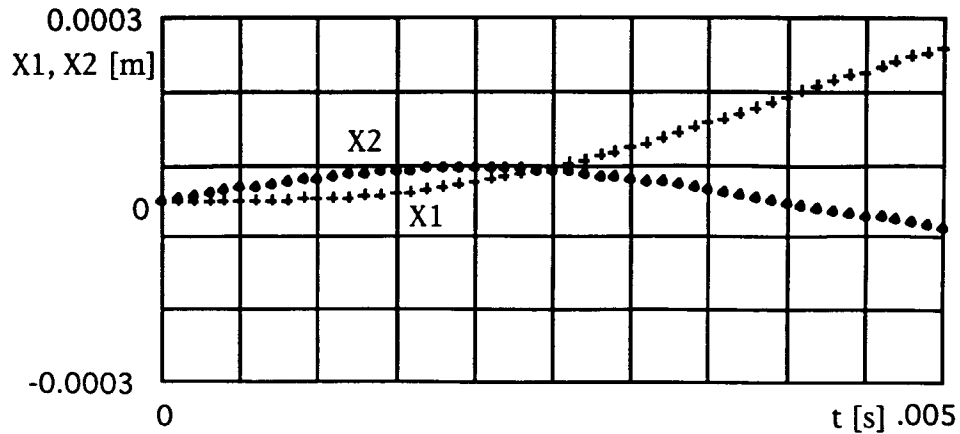


Figure D.7 Time Response Curves; A Spring Stressed System.

Clearly maximum bending takes place at $t=0.002$ s. Computer calculated data below shows, that the maximum yield due to bending is 0.0536 mm, which equals to 0.0383 mm bending and 1.915 Nm maximum moment. This is 1.7 times the nominal moment and lays within acceptable limits. Value of X1 shows, that the model is still valid and a derivative of X1, that is about $(2.9725e-5 - 2.5676e-5)/0.0001 = 0.0405$ m/s, is near to rover velocity, as expected. The moment caused by collision disappears by the time 0.0039 s, when the derivative of X1 is 85.9 mm/s, which is more than twice the rover velocity. Therefore the arm might bounce away from the obstacle with relative speed of 44 mm/s and it possesses $3.8e-5$ J excess energy. That energy equals to work done by 1.4 Nm nominal moment during $8.67e-6$ rads rotation, or 0.0163 mm tangential arm tip motion. However, 1.4 Nm bends the arm 0.047 mm and therefore the arm will not lose touch with the obstacle. Natural friction might be enough to damp oscillations.

Table D.1 System Response Data; A Spring Stressed System.

n	Time	Bn	X2n	X1n
17	1.7000e-3	7.0834e-5	5.2231e-5	1.8603e-5
18	1.8000e-3	7.5001e-5	5.3031e-5	2.1970e-5
19	1.9000e-3	7.9167e-5	5.3491e-5	2.5676e-5
20	2.0000e-3	8.3334e-5	5.3609e-5	2.9725e-5
21	2.1000e-3	8.7501e-5	5.3382e-5	3.4119e-5
22	2.2000e-3	9.1667e-5	5.2810e-5	3.8857e-5
23	2.3000e-3	9.5834e-5	5.1897e-5	4.3937e-5
36	3.6000e-3	1.5000e-4	1.3895e-5	1.3611e-4
37	3.7000e-3	1.5417e-4	9.6005e-6	1.4457e-4
38	3.8000e-3	1.5833e-4	5.2306e-6	1.5310e-4
39	3.9000e-3	1.6250e-4	8.1310e-7	1.6169e-4
40	4.0000e-3	1.6667e-4	-3.6239e-6	1.7029e-4
41	4.1000e-3	1.7083e-4	-8.0519e-6	1.7889e-4
42	4.2000e-3	1.7500e-4	-1.2442e-5	1.8744e-4

After the acceleration period the moment acting on the arm depends only on a scoop angle and a spring constant. Problems may occur when the scoop drops down from the obstacle. Let's assume that the scoop has risen on the 10 cm high rock and drops onto another rock on surface. All of the energy must be absorbed by the scoop without permanent structure damage. 1.4 Nm nominal moment causes 50 rad/s^2 acceleration. With an angle of 45 degrees a vertical height of 10 cm equals approximately 0.23 rads, time to drop is 97 ms and the final velocity is 4.85 rad/s causing the arm energy to be 0.329 J, which is absorbed in 3.627 mm bending causing 181.4 Nm moment. Therefore the maximum force acting on the arm tip is 302.3 N that needs to be directed on only 1.51 mm^2 area in order to avoid breaking the aluminum surface of the scoop. Obviously the arm tip will survive the force peaks in impacts, but the bending moment rises up to 130 times the nominal moment and requires a much stronger structure than needed for sample collection. However, the arm designed earlier is strong enough, even 2.2 times stronger

than needed and therefore it may be made smaller, lighter and less stiff, which leads to a smoother behavior and smaller moments. An optimization should be carried out.

A dropping velocity may be controlled by a tail attached to the scoop, as Figure D.8 below presents. If the maximum moment allowed for the arm is 2.0 Nm, the bending of the arm is 0.067 mm and the energy stored in the structure is 0.11 mJ. This equals the energy of the arm rotating 0.09 rad/s, or 38.4 mm/s vertical speed of the arm tip. Because the rover is moving with speed 41.7 mm/s the angle α must be 95 degrees. Now the tail laying on the rock reduces the dropping speed and the bending moments due to impact against the surface. A 15 cm long tail can handle a 10 cm high rock.

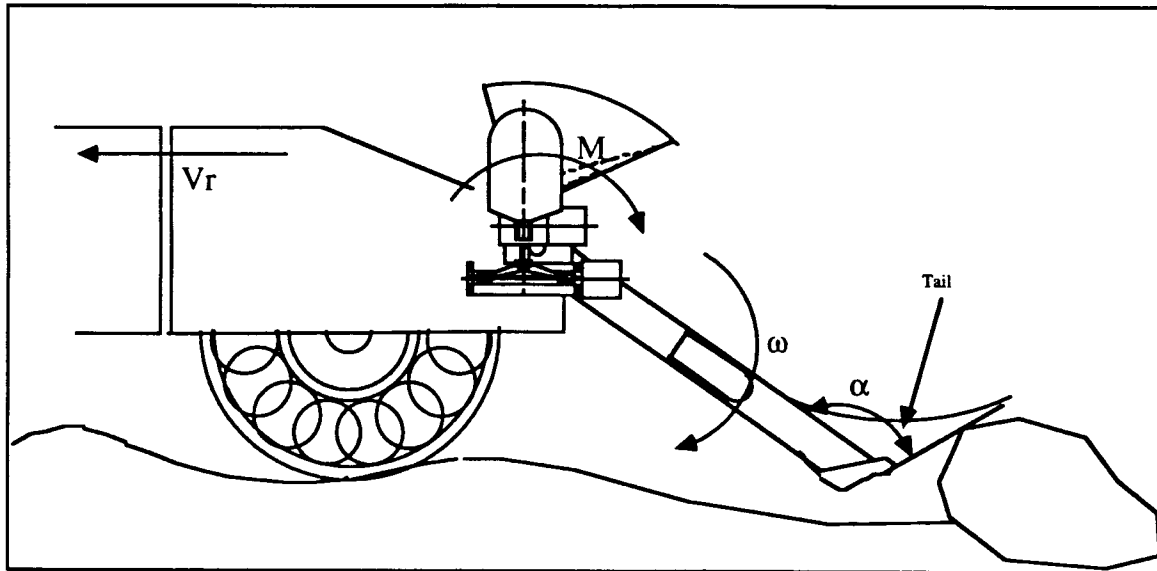


Figure D.8 A Scoop with A Tail

For example, a 2.4 watts 68 grams weighing 7.5 degrees 2-phase stepper motor gives a 0.009 Nm holding moment and therefore requires a gear ratio of 157. An example gearhead weighs 215 grams. When lifting the scoop, torque acting on rotor is $0.1/157 = 0.64$ mNm maximum and stepper velocity will be about 37 rpm causing the arm rotate 222 deg/s. Lifting takes approximately 0.81 seconds that is much faster than needed. Control logic takes power 200-300 mW.

B. Active force control.

Here the force is generated by a closed loop force controller instead of a spring. When a collision occurs, the structure yields quickly by bending and causing an error in force feedback and makes the controller adjust the moment. The arm can't bend forever, it will break if the motor doesn't yield enough. Yielding may happen either due to external bending moments or by a command of controller.

An active force control may also take care of dropping, if the tail presented above is not used. A 1.4 Nm nominal moment causes the system to accelerate 28.3 rad/s^2 , and it takes 20 ms for a 2.4 mm drop, and 128 ms for a 100 mm drop. Clearly the control of dropping is possible. The structure should be designed to stand two or three times nominal moment in collision. The controller should take care of dropping to the surface again.

An example motor weighing 30 g gives 0.0031 Nm continuous moment with 2.4 W input. Gear ratio needed is 451.6 and the rotor inertia is 1.05 g-cm^2 . Total inertia is 2.42 g-cm^2 on rotor axis and 493541 g-cm^2 on arm axis. The gain for the system model 364711.34 and Figure D.9 below presents system behavior when the motor is not used for active force control.

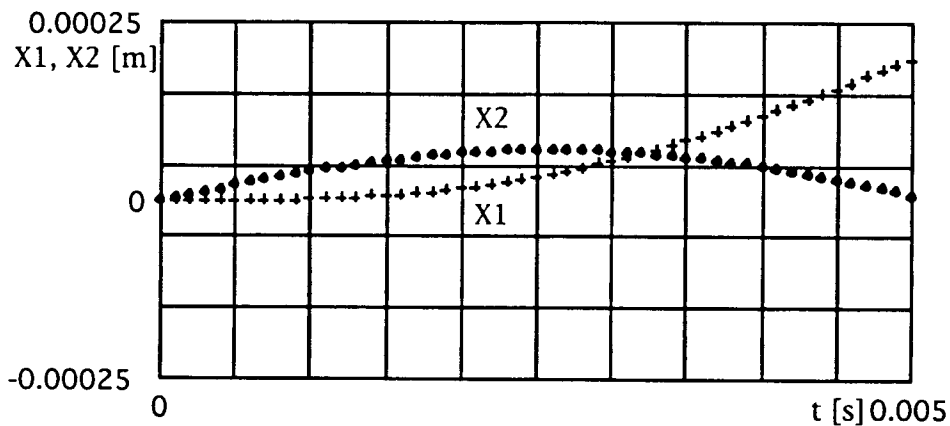


Figure D.9 Time Response Curves; A Motor Operated System.

Table D2. System Response Data; A Motor Operated System.

n	Time	Bn	X2n	X1n
23	2.3000e-3	9.5834e-5	6.9295e-5	2.6539e-5
24	2.4000e-3	1.0000e-4	7.0004e-5	2.9997e-5
25	2.5000e-3	1.0417e-4	7.0458e-5	3.3709e-5
26	2.6000e-3	1.0833e-4	7.0657e-5	3.7678e-5
27	2.7000e-3	1.1250e-4	7.0598e-5	4.1903e-5
28	2.8000e-3	1.1667e-4	7.0281e-5	4.6387e-5
29	2.9000e-3	1.2083e-4	6.9708e-5	5.1127e-5
49	4.9000e-3	2.0417e-4	1.3177e-5	1.9099e-4
50	5.0000e-3	2.0833e-4	8.8810e-6	1.9945e-4
51	5.1000e-3	2.1250e-4	4.5451e-6	2.0796e-4
52	5.2000e-3	2.1667e-4	1.8479e-7	2.1648e-4
53	5.3000e-3	2.2084e-4	-4.1842e-6	2.2502e-4
54	5.4000e-3	2.2500e-4	-8.5459e-6	2.3355e-4
55	5.5000e-3	2.2917e-4	-1.2884e-5	2.4205e-4

Now X2 rises faster and X1 rises slower, and 0.07 mm maximum yield due to bending takes place 2.6 milliseconds after collision causing a 2.52 Nm moment. To be of any use, the control system should reduce the bending significantly in less than 2.6 milliseconds, which requires an extremely fast response. It is obvious, that it is not possible to achieve this fast response. But the arm design presented earlier was not very heavy, and no more than a 100 grams mass saving should be expected. The saving is achieved with the penalty of a much more complex control system, a malfunction of which may lead to severe damage to the arm. Therefore a 100 gram heavier, 'heavy-duty' design is recommended.

A gearhead with ratio 236 weighs 215 grams and stands 4.5 Nm continuous moment, the diameter is 32 mm and total length of the motor package is 90-130 mm depending on the encoder selected. A high gear ratio may cause additional problems in the form of friction, low efficiency and a high motor back-EMF. Therefore a more powerful motor with lower gear ratio is presented. A 7 watts, 169 grams motor gives a 16 mNm moment. A 100:1 gearhead similar to one above is sufficient and available. Total

inertia on arm axis is 467000 g-cm^2 that is less than the example above and therefore the behavior of the system is even better.

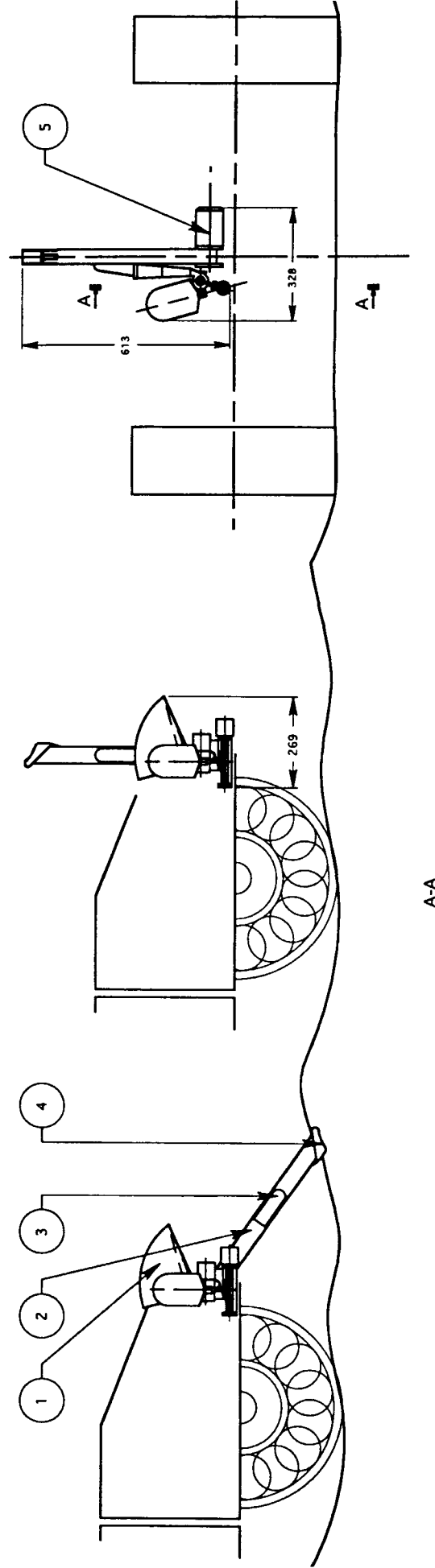
C. Closed loop position control

The above presented an example of a system where the motor doesn't carry out active force control, but generates a constant 1.4 Nm moment. This is the way in which a closed loop position controller functions. Because it was discovered that it is convenient to let the arm structure take care of the collision, the only difference is in the handling of dropping. A position controlled motor can't do anything about it, because it always has to have the 'right position' to generate the needed 1.4 Nm moment. Therefore during dropping the arm accelerates 23.8 rad/s^2 . Maximum speed of the motor is 9500 rpm causing the arm to turn 21.03 rpm or 2.2 rad/s. This is achieved in 0.079 s which equals the time to drop from an obstacle 7.4 cm high. The total energy in movement is then 0.12 J that is absorbed in the 2.19 mm bending of the structure causing 109.3 Nm moment. (Here we assumed that no penetration into the surface occurred, in the case of hitting another rock, for example). Lifting the sample from the surface to rover needs approximately 180 degrees rotation and with maximum speed takes about 1.42 seconds which is faster than needed.

A Parts List for the Flip Scoop

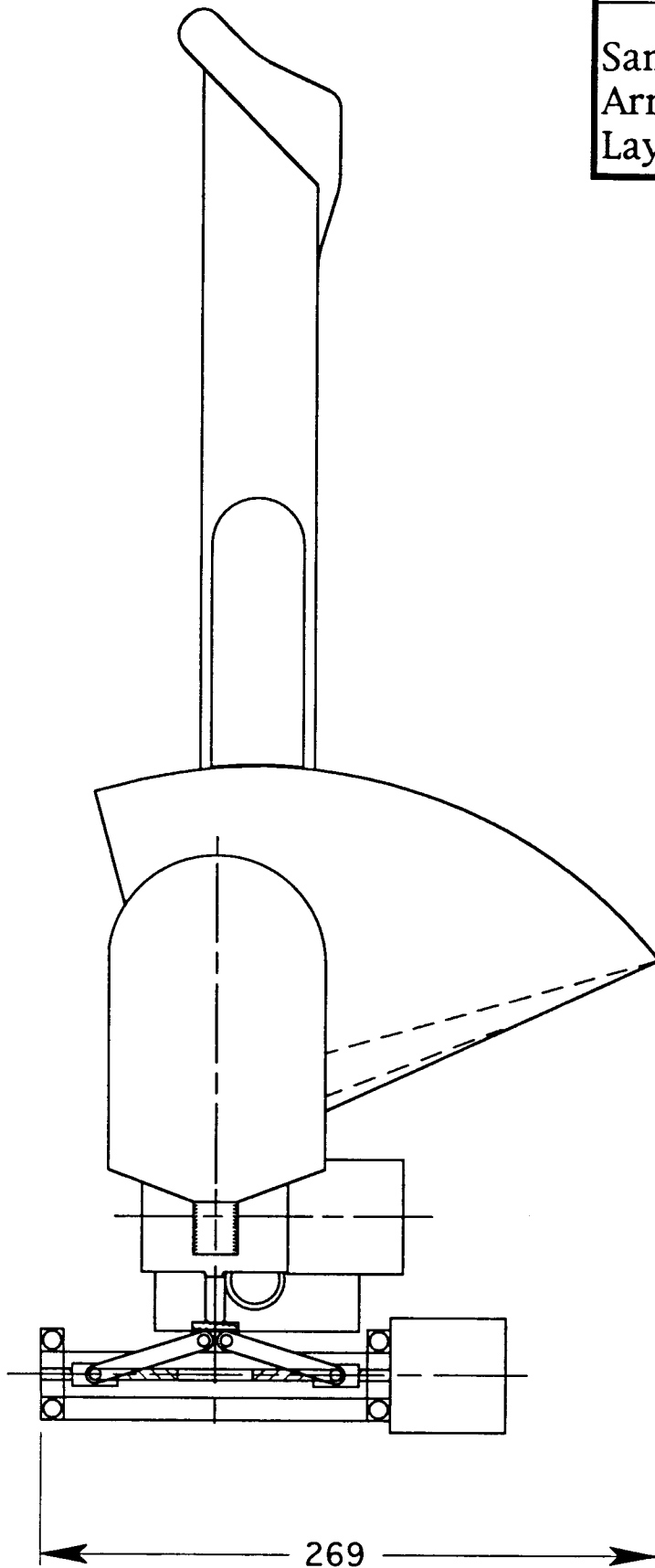
The parts for the Flip Scoop are illustrated in sketches 12-01 and 13-01.

1) Sectorial Funnel	Aluminum or Composite
2) Scoop Arm	Aluminum or Composite
3) Flow-Out Funnel	Aluminum or Composite
4) Slicer	Steel or Titanium
5) Servo/Stepper Motor	
6) Fins	Steel or Titanium
7) Lid	Steel or Composite

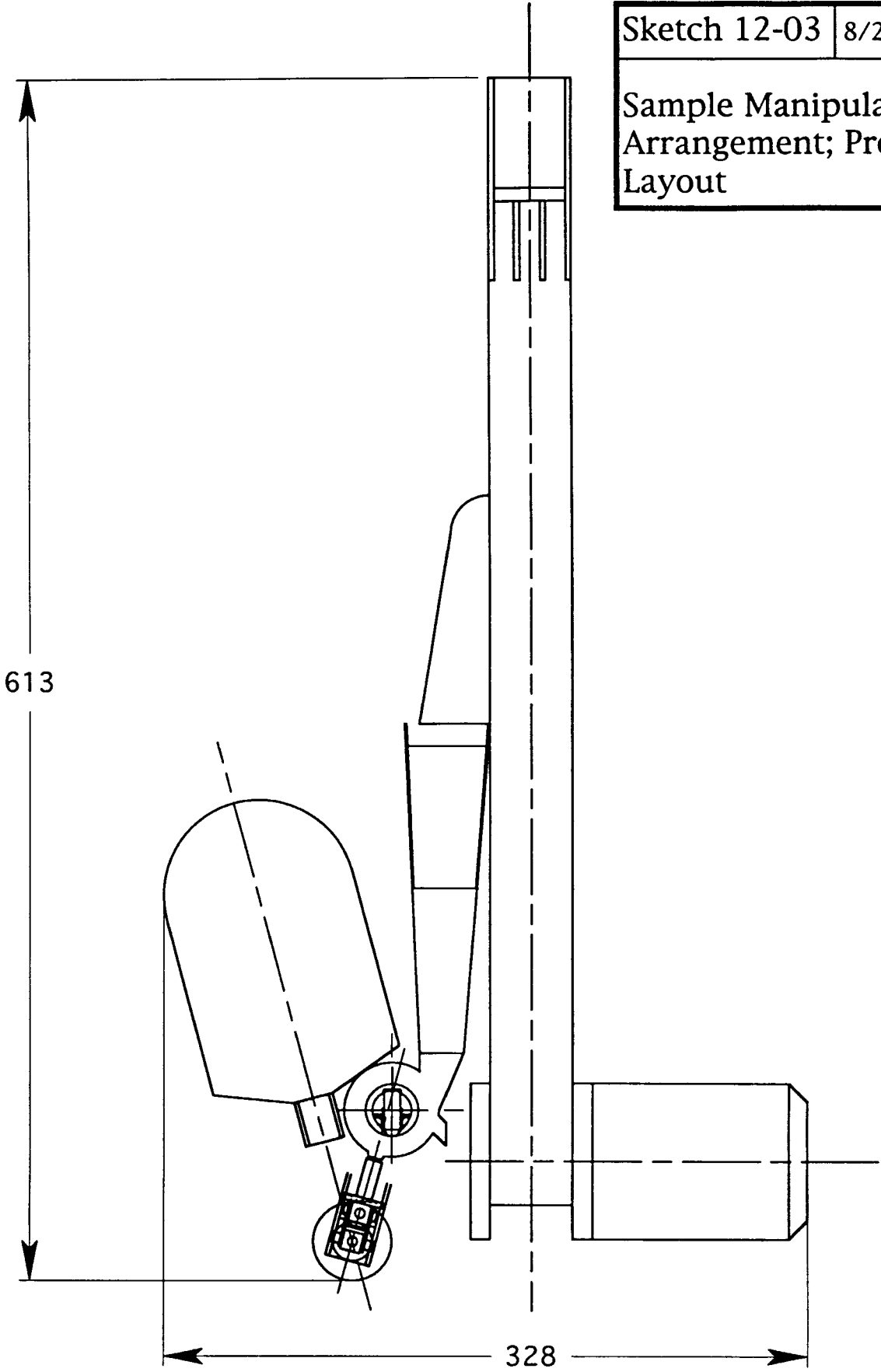


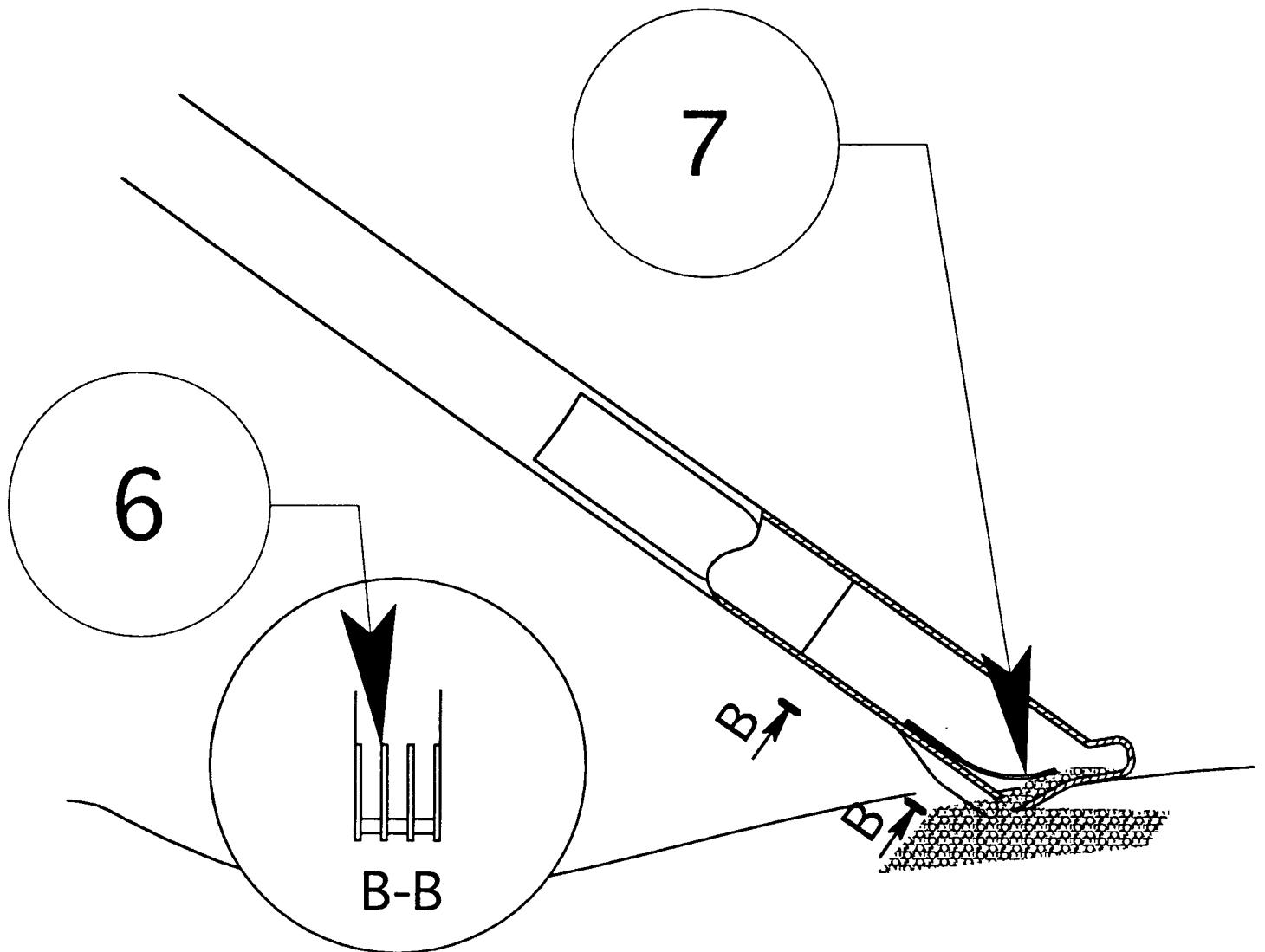
Sketch 12-01	8/23/93	TY
Sample Manipulating Arrangement; Proposal II, Layout		

Sketch 12-02	8/23/93	TY
Sample Manipulating Arrangement; Proposal II, Layout		



Sketch 12-03	8/23/93	TY
Sample Manipulating Arrangement; Proposal II, Layout		





Sketch 13-01	8/23/93	TY
Cutting Soil		

Appendix E:

Sample Manipulating Arrangement; Proposal III

Sample Manipulating Arrangement; Proposal III

The third proposal is based on a rotary sample handling arm that was suggested by Igor Sviatoslavsky. In the previous proposal the regolith sample was moved from one container to another during processing. In this proposal a container holding the sample is moved from station to station. A new kind of lifting unit for taking the container into the heater and sealing the vacuum chamber is presented. The figures below detail the layout of the entire sampling system. Sketches 20-01 and 20-02 show the dimensions and are included at the end of appendix E.

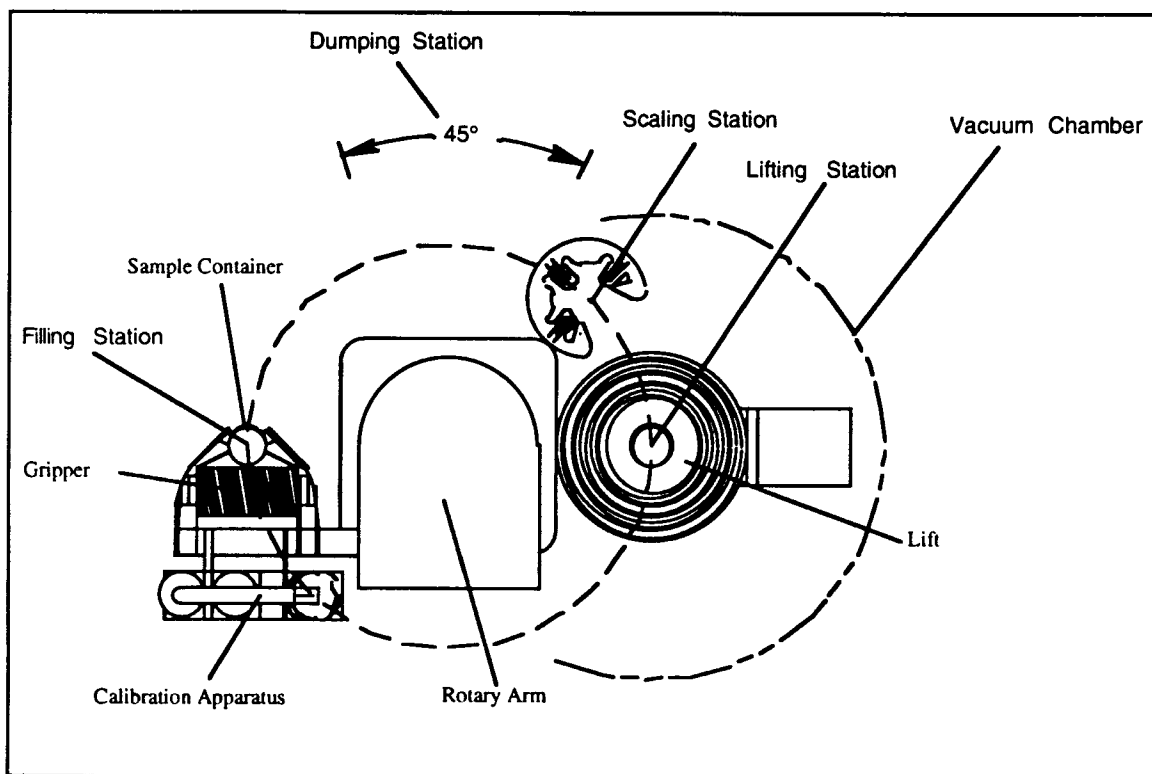


Figure E.1 Sample Manipulating Arrangement; Proposal III, Top View.

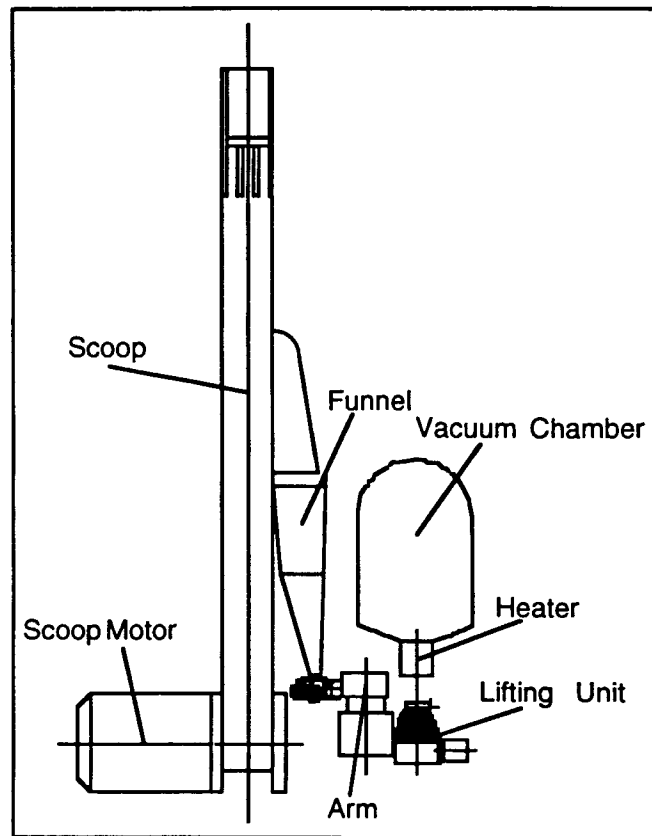


Figure E.2 Sample Manipulating Arrangement; Proposal III, Front View

- 1) As the gripper is holding the container under the funnel the scoop delivers the regolith sample into the funnel. When the arm rotates counterclockwise towards the scaling station, the sweeper in the funnel removes the excess soil from the container, just like in the Proposal I. The gripper and scaling apparatus should be shielded against the falling regolith.
- 2) As the arm passes the lifting station the brushes attached under the calibration apparatus sweep the lift and sealing surfaces clean. When the calibration apparatus is above the scale, the magnet is activated and it lowers the calibration weight onto the scale.

- 3) After the calibration magnet is deactivated, the arm is rotated further until the container sits on the scale. The gripper magnet is deactivated and, if necessary, the arm is rotated farther during the weighing procedure.
- 4) When weighing the is finished the arm moves the container onto the lift and rotates back away from it.
- 5) As the lift motor rotates, the spring lifts the container into the heater and finally seals the vacuum chamber. After analysis, the lift motor rotates in the opposite direction stressing the spring thereby lowering the container.
- 6) The arm transfers the container to the dumping station where either the entire container is dumped or it is emptied by rotating the gripper. This part of procedure will be discussed later.

Gripper

The gripper is illustrated in sketch 15-01. It consists of an electromagnet and gripping arms. The design presented must be activated when carrying the container. However, the energy consumption and robustness to breaks in delivery of electric energy is significantly better if the magnet is activated to drop the container. In that case, even if the magnet fails to work, due to flexible gripper arms, the gripper may grasp and drop the container if the movement of it is limited, for example when it is between the lift and heater. All the other functions may be carried out except the weighing procedure. With some design work even that might be possible, and the magnet might be unnecessary. If the magnet is used, it should be double coiled for redundancy.

Calibration Apparatus

The calibration apparatus is illustrated in sketch 16-01. In the deactivated state the spring is lightly stressed which pulls the calibration mass into the storage hole. The magnet is then activated and the mass is lowered onto the scale.

Rotary Arm

The arm was developed around the stepper motor and gearhead found in the references. The gearhead functions as a vertical axle for the arm. In sketch 14-01 the sliding bearing (part number 6) isolates the rotating arm from the gearhead. A ball bearing may be used, if so preferred. Use of this large gearbox, if any, may not be necessary even a smaller stepper motor might be possible. The arm shaft (number 3) is mounted to arm body (number 7) with ball bearings to allow the gripper (number 5) to rotate when dumping the sample. Dumping takes place when the sequencing rollers (number 10) hit the sequencing disk (number 11) attached to the end of the arm which makes it rotate about 180 degrees. Sequence is illustrates in sketch 14-02. When the arm rotates clockwise, the spiral springs (number 2) pull the gripper back to the right position. The bearings, springs, sequencing rollers and sequencing disk may be left away only if the entire container is dumped instead of only the contents in it.

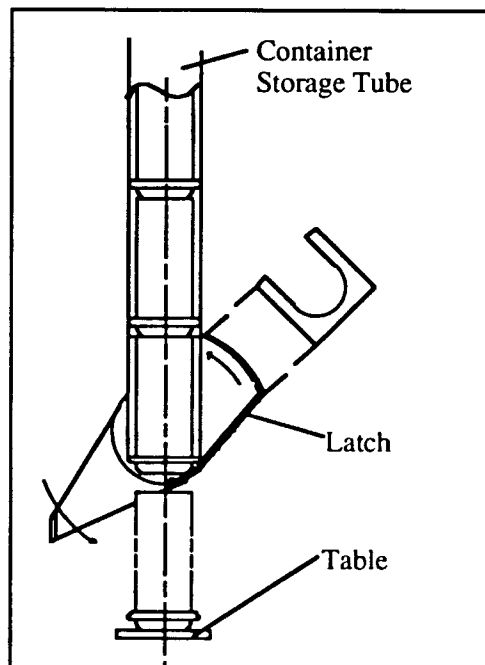


Figure E.3 Container Storage.

Container Storage

Spare containers are needed if dumping is to be carried out by dropping the container. The basic idea of moving a container from station to station involves the need of grasping and loosening the container. Accidentally, the grasping may be unsuccessful and the container will be lost. A possible regolith sintering inside the container calls for dumping the entire container. For these reasons there should be access to spare containers .

The storage system is placed at the other extreme of the arm movement in the dumping area. As the gripper arrives at the storage area, it pushes a latch which releases one container that drops down onto the table for the gripper. Flow of the containers in the tube may be achieved by vibrating it.

A two meter long tube weighs about 100 grams and could store 100 containers. Combining the container storage and rotating gripper appears to be difficult and perhaps a more reliable solution is to dump the entire container and give up the rotating gripper. However, storage for 1000 containers calls for several tubes and a revolver mechanism to switch tubes. The mass of the system is increased by roughly two kilograms. Which solution is better, depends on the reliabilities of the gripper and storage system.

Lifting Unit

Lifting unit presented in sketch 19-01 and Figure E.4 uses a spring to lift the container and seal the chamber, and an electric motor to lower the container.

The motor rotates a reel around which a steel wire is stored. The wire goes around a pulley (number 2) and the end is mounted with an anchor (number 6). This way the force acting on the container base is doubled. Two sets of wires and pulleys are used for redundancy. By replacing the anchor with a rotating wheel and using only one long wire, one end of which is anchored, the force may be quadrupled. Instead of wire and reels, a chain and a sprocket wheel may be used. This may be wise since coiling and uncoiling a wire on the reel stresses it significantly which may cause breaking.

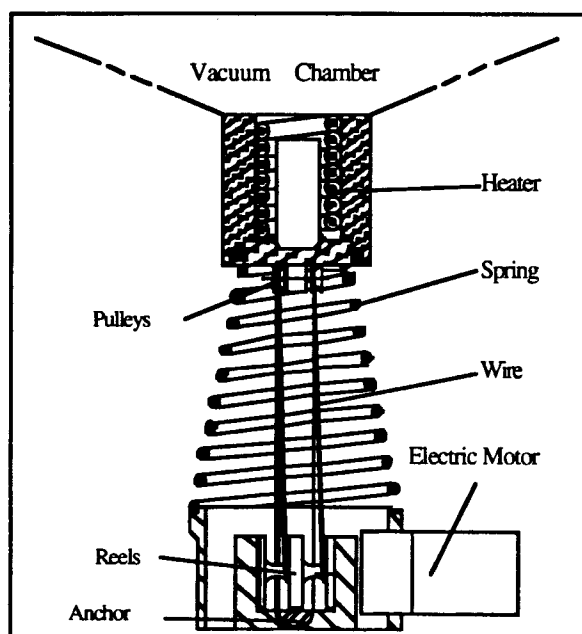


Figure E.4 Lifting Unit.

The sealing takes place when the vertical surfaces of the container base slide against the sealing ring (number 7). The force needed for sealing is expected to fall between 63 N and 630 N. The final value depends on materials and the clearance between surfaces. A troublesome property of this design is that the force needed from the motor is greatest when the processing doesn't need it at all, i.e. when the lift is down. If the sealing force falls near the lower end of the expected values, the small motor and gearhead presented in sketches should be functioning. However, if the force appears to be much larger, a larger motor and gearhead will be required causing roughly 360 grams increase in mass. In this case, the scoop arm motor should be utilized, which may be done by using a clutch or a gearbox. In principle any kind of stroke length and force generation may be achieved by adjusting spring length and spring constant. The overall height will be the limiting factor.

The spring in the sketches appears to be conical because it then provides better horizontal support for the container base. It may not be necessary.

Figure E.5 presents the structure of the heater designed and drawn by Igor Sviatoslavsky. To decrease heat conduction losses from the container, it is supported by long thin steel rods. These rods are too weak to carry the sealing forces and therefore the base plate must be used for that. This calls for a significantly longer stroke from the lift and also requires a longer spring which in turn increases the overall height of the system. The spring itself may also reduce conduction losses but radiation losses may be significant.

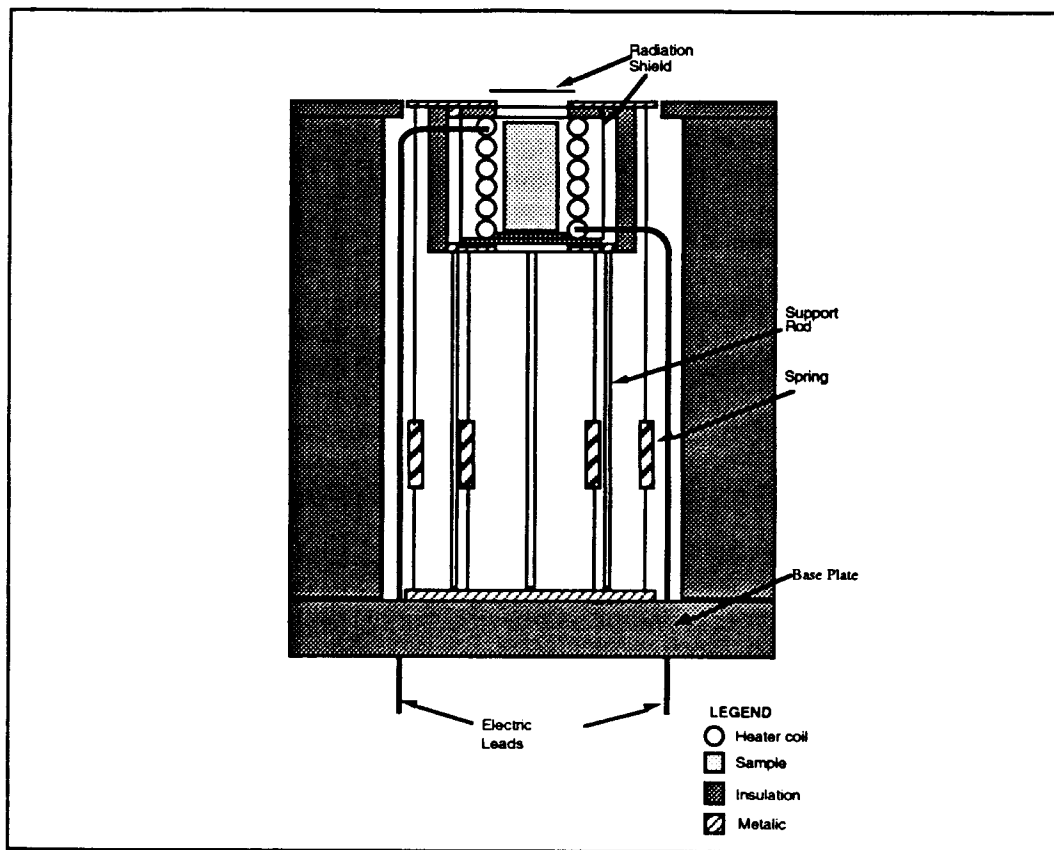


Figure E.5 The Heater.

Analysis

Table E.1 Sampling System Characteristics with Proposal III.

Linear Pairs		-
Revolute Pairs		5
Screw Pairs		-
Stepper Motors		2
Servo Motors (For lift, if required.)		1
Power		2.5 W
Container Mass to be heated	Steel	0.61g
Container Mass to be weighed	Steel	0.61 g
Height (Without a container storage.)		~592mm
Length		~269 mm
Width		~322 mm

Mass estimation for the system is made assuming a very small lift motor (the motor and gearbox weigh only 27 g) for low force, or use of the scoop motor for great force. The rotary motion of the gripper is left off and dumping takes place by dropping the containers. A ten-tube container storage weighing 2 kg is assumed.

The container storage lifts the overall mass far greater than the mass with System Proposal II. If the gripping procedure is reliable enough, the storage may be left off and mass stays 500 grams below the System Proposal II. If the basic idea of Proposal III is preferred to Proposal II, a combination of a rotary dumping gripper and small storage for 100 containers should be analyzed.

Table E.2 Sampling System Mass Budget with Proposal III.

Container Storage	Titanium	1390 g
1000 containers	Steel	610 g
		2000 g
Lifting Unit		
Spring	Steel	23 g
Container Base	Composite	2.5 g
Pulleys + Axles	Steel	2.8 g
Reels	Steel	5 g
Cables	Steel	0.02 g
Body	Aluminum	22 g
Reel Body	Aluminum	27 g

Motor		19 g
Gearhead		8 g
Bearings		20 g
		129.3 g
Calibration Apparatus		
Body	Aluminum	2.2 g
Weight		1.0 g
Spring	Steel	0.2 g
Magnet Core	Steel	6.3 g
Magnet Coil	Copper	3.2 g
		12.9 g
Gripper		
Magnet Core	Steel	9.2 g
Magnet Coil	Copper	3.9 g
Arms	Steel	4.8 g
		17.9 g
Rotary Arm		
Shaft	Titanium	5 g
Body + Sliding Bearing	Al + Comp.	27 g
Stepper Motor		200 g
Gearhead		170 g
		402 g
Scale		1.7 g
Scoop (includes electronics)		1115 g
Interface		1000 g
		4679 g
Marginal 20%		936 g
Overall Mass		5615 g

Problems

1) The basic problem arises when moving the container from one station to another after grasping as the grip may loosen. Accidentally the gripper may hit the container or lose it's grip and drop the container.

Solution 1: Redundancy is increased by having spare containers in storage.

Solution 2: Gripping may be more robust if the container is supported actively or passively at each station and the gripper itself is passive, perhaps spring loaded. This may

happen for example at the lifting station by lifting the container so, that the upper part of it is in the heater and the lower part is in a hole at the container base.

2) The container is not mounted on the lift. During heating it may get stuck inside the heater by welding or because of regolith grains.

Solution 1: Mount the container on the lift with an electromagnet or electromagnet operated clutch.

3) When filling the container, the flow of excess soil must be directed away from mechanics.

Conclusions

The lift presented here is much simpler compared to the previous design, yet its capability to create required sealing force is uncertain. In a final design a combination of the lift and rotary arm from Proposal III and the measuring unit from Proposal II provides a simple and reliable system with little grasping and loosening of the container.

A Parts List for the Rotary Arm

The parts for the Rotary Arm are illustrated in sketch 14-01.

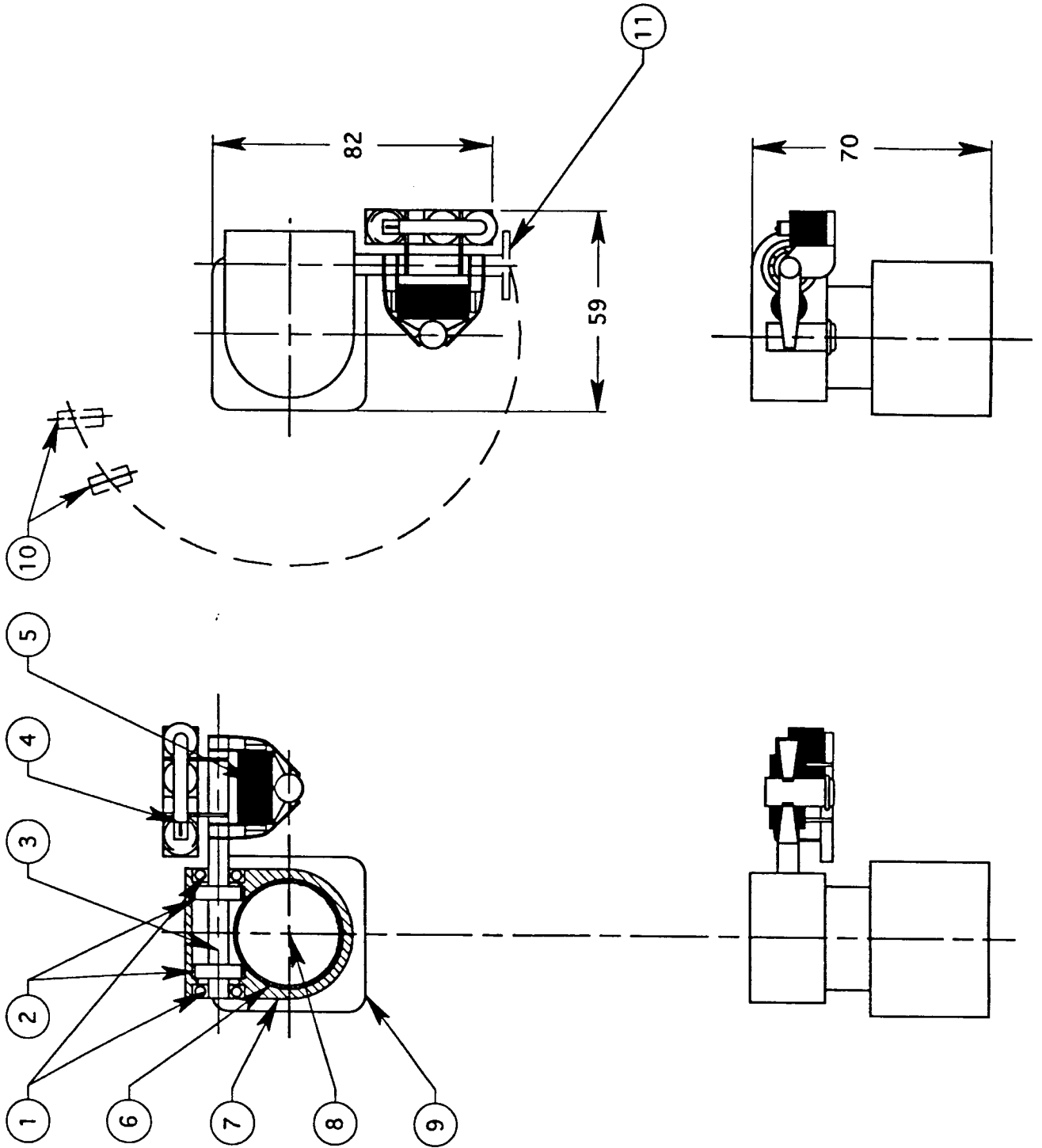
1) Bearings	
2) Springs	Steel
3) Shaft	Titanium
4) Calibration Apparatus	
5) Gripper	
6) Sliding Bearing	Composite
7) Body	Aluminum
8) Gearhead	
9) Stepper Motor	
10) Sequencing Rollers	Steel
11) Sequencing Disk	Steel


A Parts List for the Lift Unit

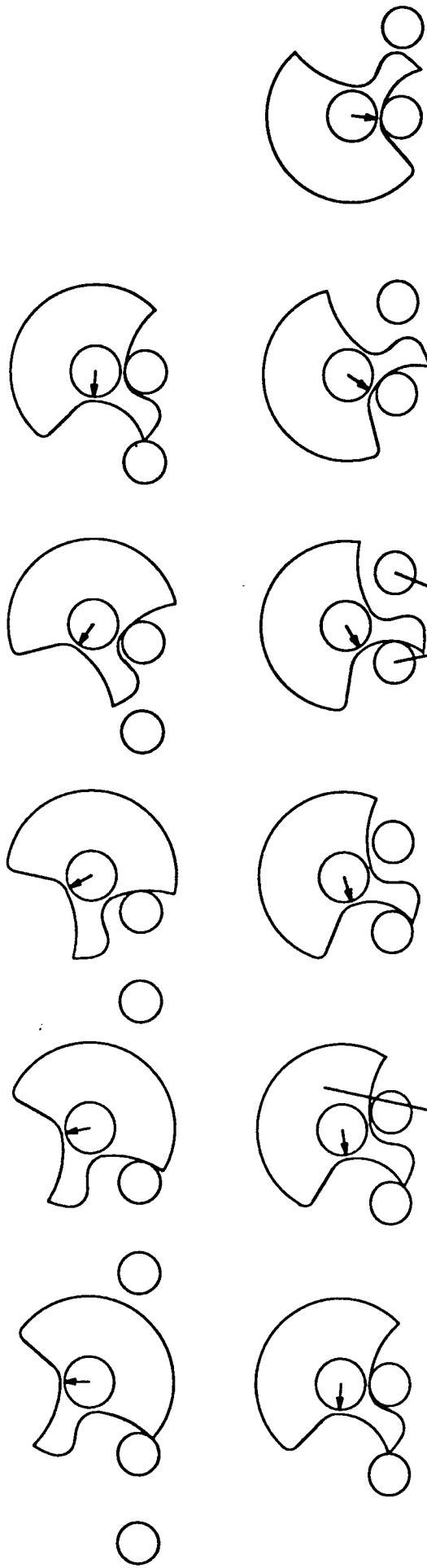
The parts for the Lift Unit are illustrated in sketch 19-01.

1) Container Base	Composite
2) Pulleys	Steel
3) Cable or Chain	Steel
4) Spring	Steel
5) Body	Aluminum
6) Anchor	Aluminum
7) Seal	
8) Reels	Steel
9) Reel Body	Aluminum
10) Motor and Gearhead	

Sketch 14-01	9/24/93	TY
Rotary Arm for the Sample Manipulating Arrangement; Proposal III		



Disk Moves Left


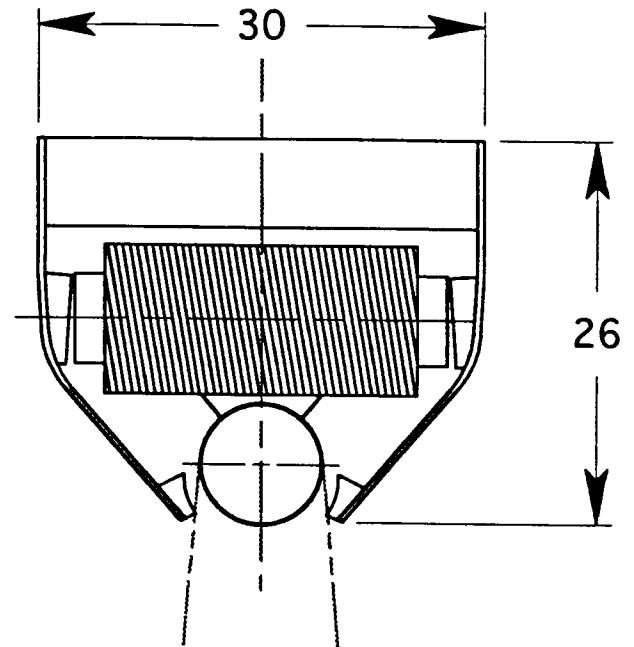
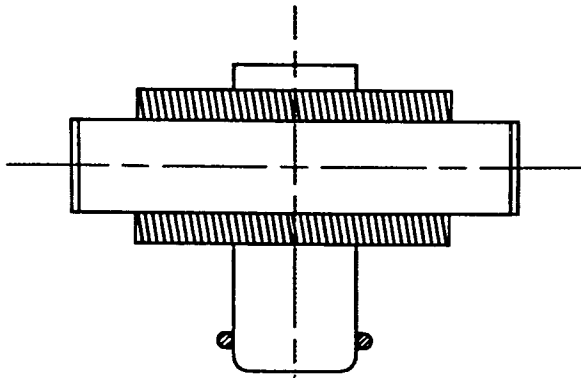


Sequencing Rollers

Sequencing Plate

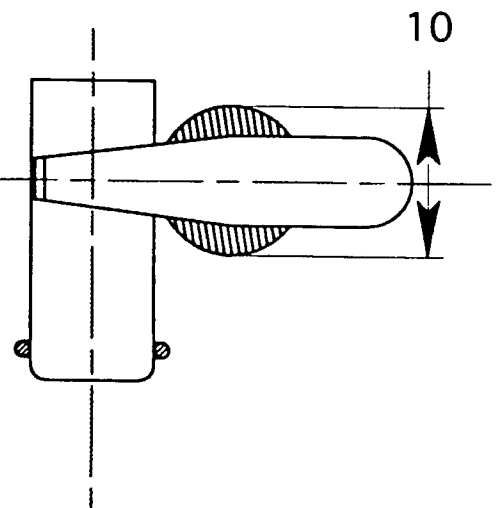
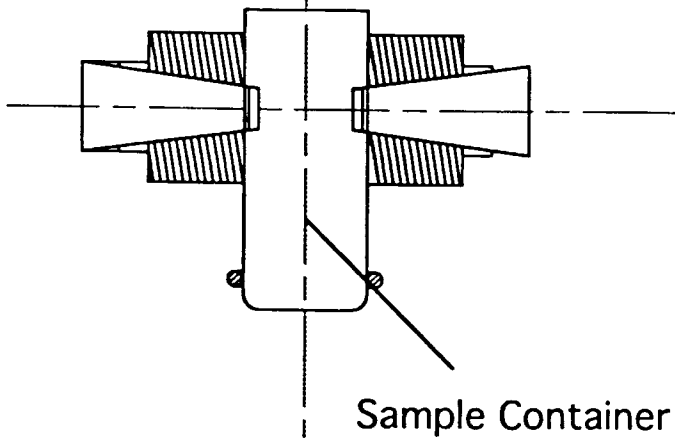
Sketch 14-02	9/24/93	TY
Dumping Sequence for the Sample Manipulating Arrangement; Proposal III		

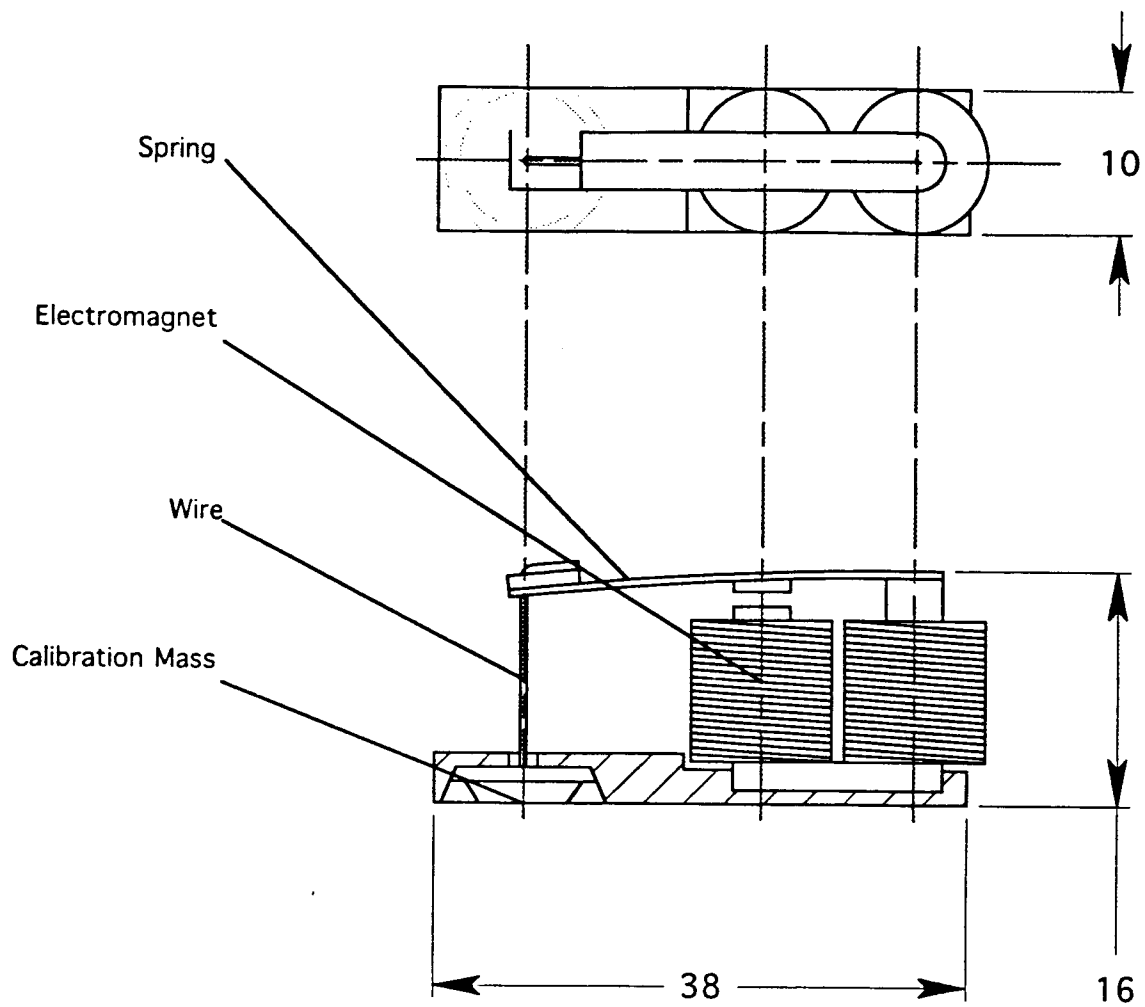
Sketch 15-01	9/24/93	TY
Container Gripper for the Sample Manipulating Arrangement; Proposal III		



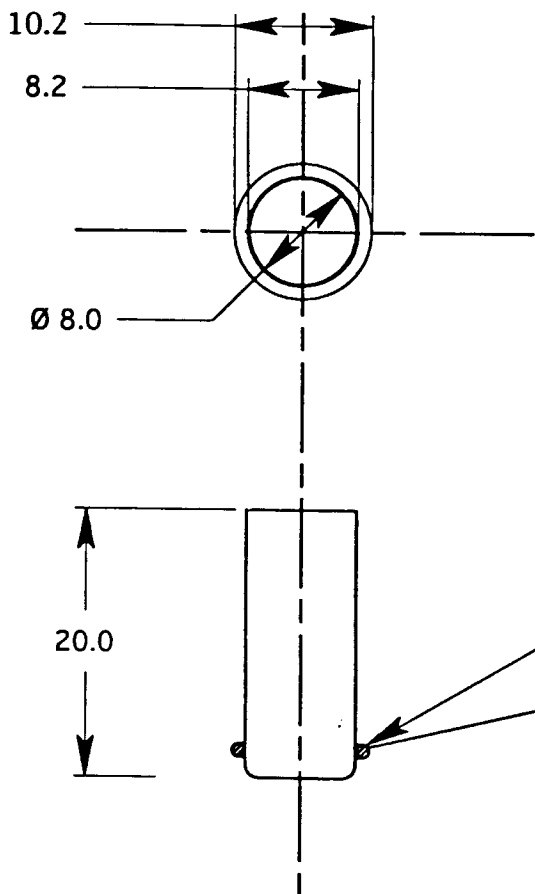
Electromagnet

Gripper



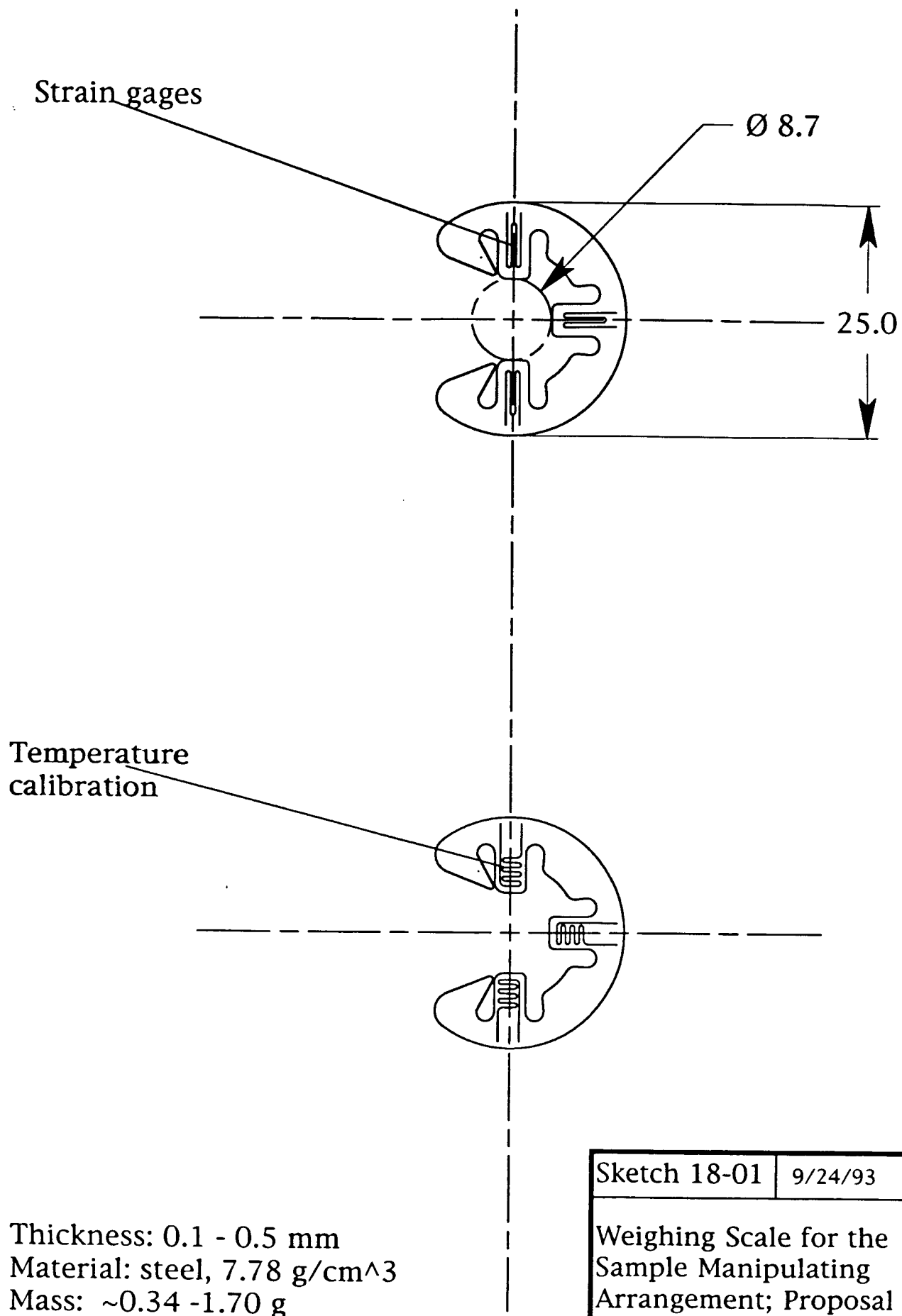


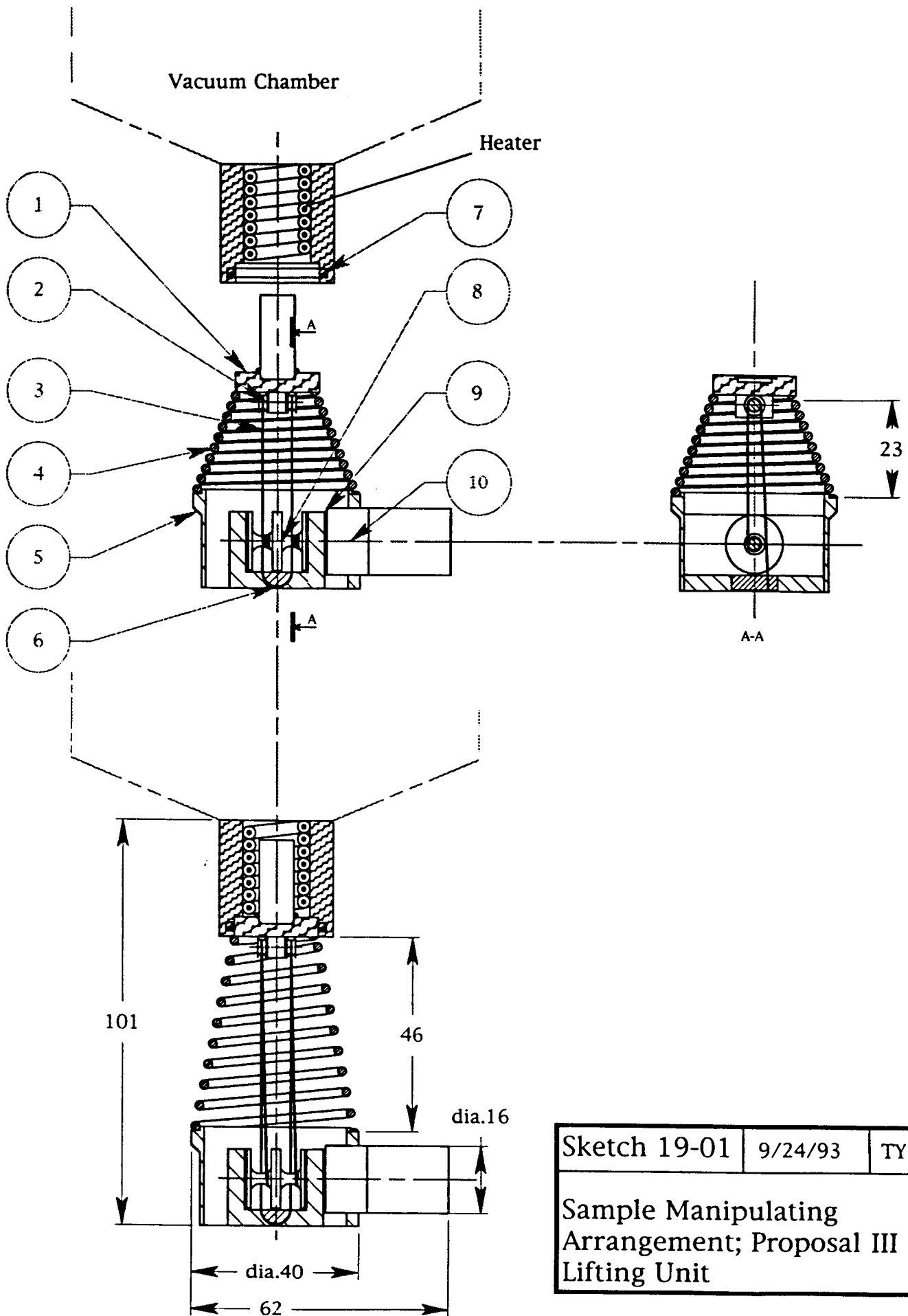
Sketch 16-01	9/24/93	TY
Calibration Lift for the Sample Manipulating Arrangement; Proposal III		



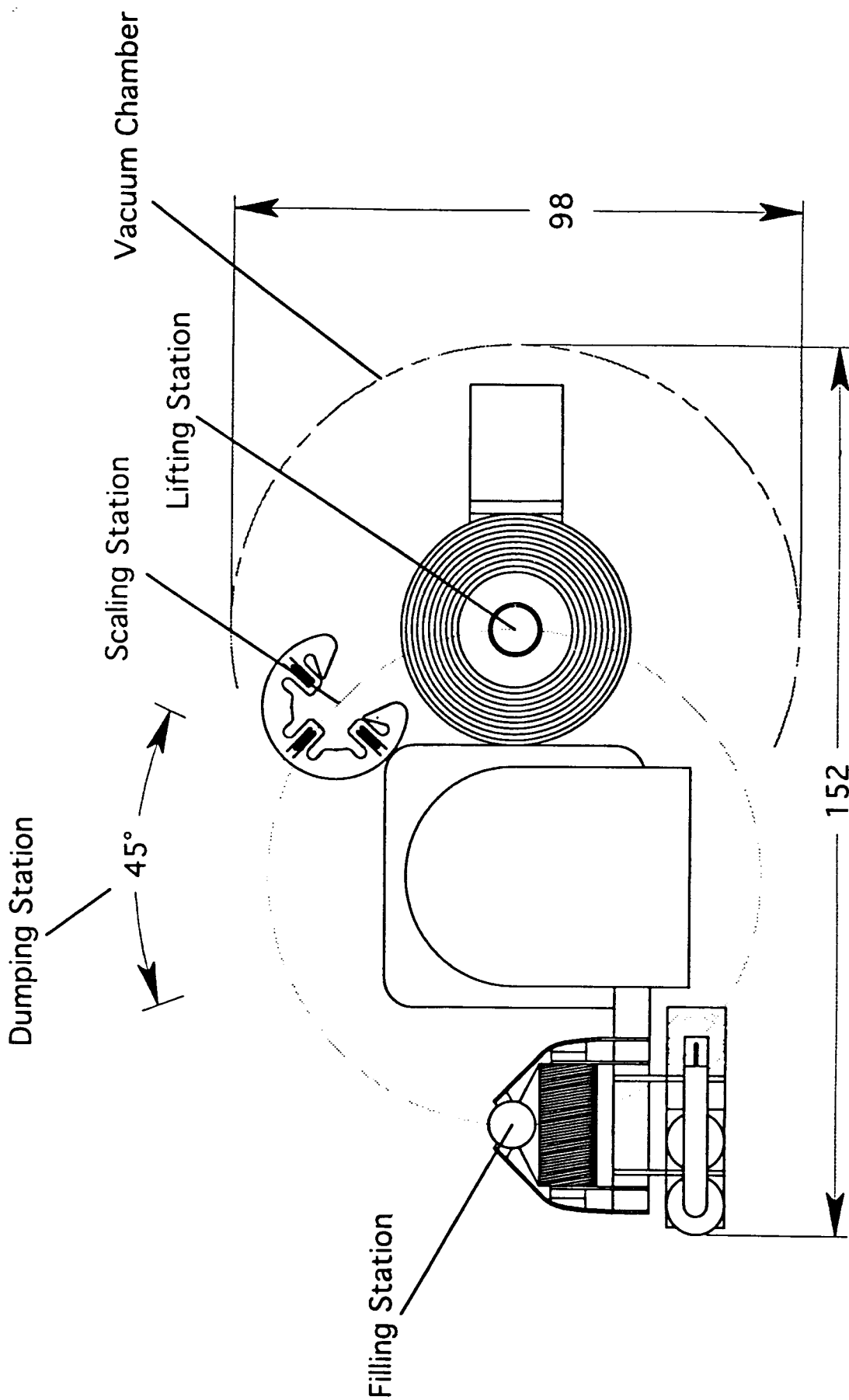
Material volume:
container: 0.0559 cm^3
rings: 0.0227 cm^3
sum: 0.079 cm^3
material: steel, 7.78 g/cm^3
mass: 0.61 g

Sketch 17-01	9/24/93	TY
Sample Container for the Sample Manipulating Arrangement; Proposal III		





Sketch 19-01	9/24/93	TY
Sample Manipulating Arrangement; Proposal III Lifting Unit		



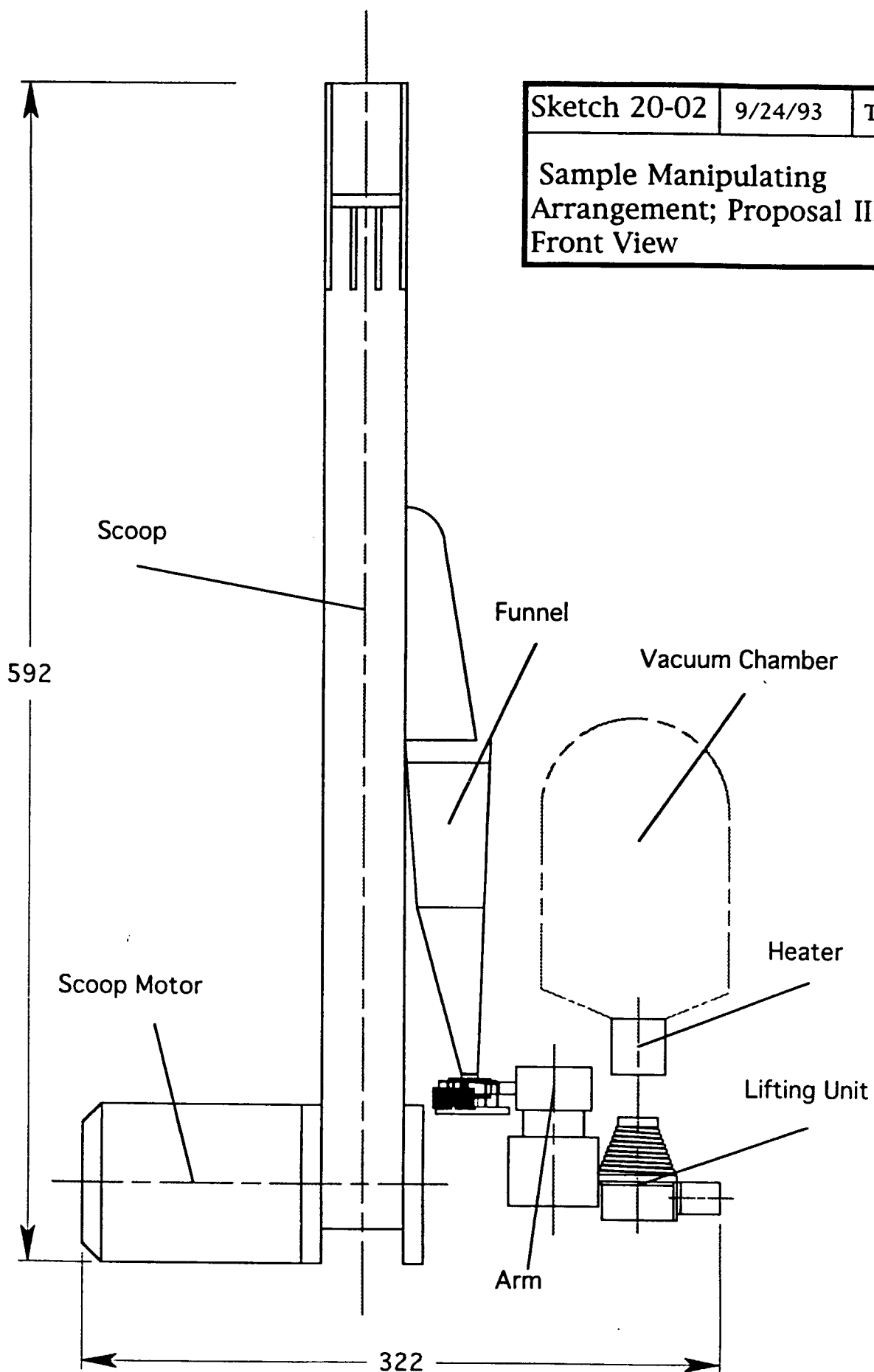
Sketch 20-01	9/24/93	TY
Sample Manipulating Arrangement; Proposal III, Top View		

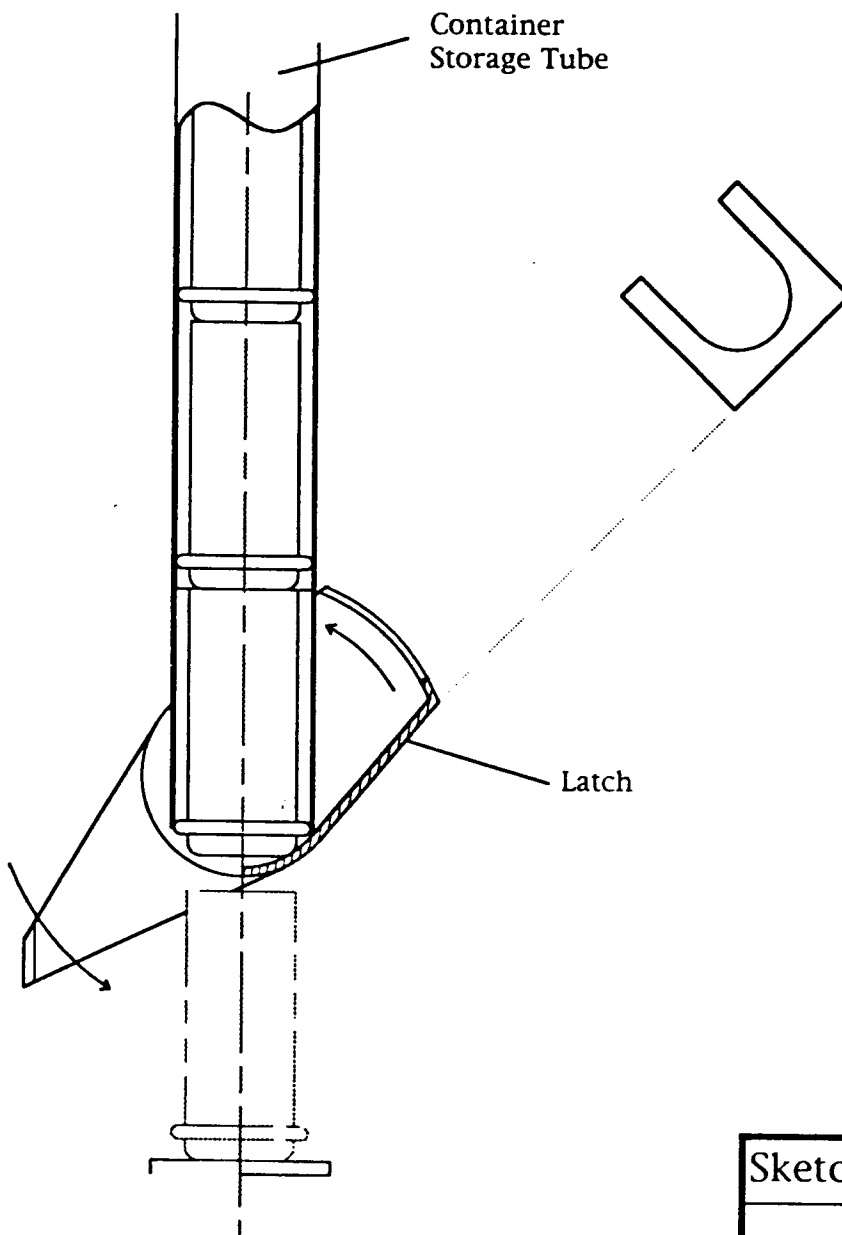
Sketch 20-02

9/24/93

TY

Sample Manipulating
Arrangement; Proposal III,
Front View





Sketch 21-01	9/24/93	TY
Container Storage for the Sample Manipulating Arrangement; Proposal III		